Development of an interplanetary orbital propagator

Supervisors:
G. Kerschen
L. Dell'Elce

Jury member:
G. Rauw

Graduation Studies conducted for obtaining the Master's degree in Aerospace Engineering by Thibault Pichâ

UNIVERSITY OF LIÈGE
FACULTY OF APPLIED SCIENCES
ACADEMIC YEAR 2017-2018

Acknowledgements

My sincere gratitude goes to my supervisors Prof. Gäetan Kerschen and Dr. Lamberto Dell'Elce, and to my jury member Prof. Gregor Rauw. The door to Prof. Kerschen's office was always open. He made me wise comments on the redaction of my thesis and spent precious time answering my questions. Dr. Lamberto Dell'Elce's investment was essential for my daily work. He guided me throughout the thesis and provided me with sound advice on the redaction of my thesis. I am thankful to Prof. Gregor Rauw for its suggestions.

Furthermore, I am grateful to Jean-Louis Simon and Gérard Franscou from the 'Institut de Mécanique Céleste et de Calcul des Ephémérides' (IMCCE, Paris). They provided the data to validate the planetary ephemerides.

Finally, I would like to thank my family who has encouraged me throughout my studies.

Contents

List of Abbreviations

IAU	International Astronomical Union
IOP	Interplanetary orbital propagator
ISS	International Space Station
PMG	Point mass gravity
NASA	National Aeronautics and Space Administration
SOI	Sphere of influence
SRP	Solar radiation pressure
TDB	Barycentric Dynamical time
TT	Terrestrial time
VSOP	Variation séculaire des orbites planétaires.

Introduction

Humanity's interest is to explore the unknown, discover new worlds, find traces of life and understand the creation of our solar system. Interplanetary orbital propagators are developed in that context. They consist of tools allowing us to predict the spacecraft trajectories in our solar system. Propagators are used to support and design real-world missions.

Most of the solar systems consist of one star and the celestial bodies traveling around it. It includes the planets, the moons and the asteroids. There are about tens of billions of solar systems in the Milky Way galaxy [28]. The focus of the thesis is on our solar system. The Sun is the star at the centre of our solar system. Eight planets orbit around it. Mercury is the smallest and the closest planet to the Sun. It is located at 0.4 AU from it. One astronomical unit AU corresponds to 149,597,870 km. Mercury's orbit is represented in purple in Figure 2. It is a highly eccentric orbit compared to other planetary orbits. Venus is the planet situated between Mercury and the Earth. It is located at a distance of 0.7 astronomical unit from the Sun. Venus possesses the most nearly circular orbits. Its eccentricity is very close to 0. The Earth is the third planet from the Sun. The liquid water, the surface temperature and the chemical compounds are key factors allowing life on Earth [28]. Indeed, Earth's oceans cover 70 percent of the planet's surface. The Earth lies at one astronomical unit. The next planet is Mars. It is situated at 1.5 AU from the Sun. Mars houses the largest volcano: Olympus Mons. It is three times higher than Mount Everest [28]. Jupiter is the largest planet in our solar system. Jupiter is 5.2 astronomical units away from the Sun. The second largest planet is Saturn. The main feature of Saturn is to possess spectacular rings. A distance of 9.5 astronomical units separates Saturn and the Sun. The seventh planet from the Sun is Uranus: 19.8 AU. Uranus is the only planet whose equator is almost perpendicular to its orbit around the Sun. The last planet is Neptune. It is located at 30 astronomical units away from the Sun and completes one orbit in 165 years. The scaled sizes of the different planets are represented in Figure 1. The inner planets (Mercury, Venus, Earth, Mars) have a relative small size compared to the four outermost planets (Jupiter, Saturn, Uranus, Neptune). The inner planets are made up of rock and metal. Due to their large size, the outermost planets are called giant planets. They are mainly made up of liquid, ice and gas.

Our solar system does not house only planets. Moons are celestial bodies in orbit around the planets. The giant planets possess a series of moons. A total of 171 moons are observed around these planets [28]. The Earth and Mars only possess one and two moons, respectively. Mercury and Venus do not possess any moons. In addition, five dwarf planets orbit in our solar system. The dwarf planet Pluto is studied in the thesis. It is located farther than Neptune on average. In fact, its orbit has an eccentricity similar to Mercury's orbit. Therefore, Pluto is closer to the Sun than Neptune at its perihelion. The asteroids are mainly located between Mars and Jupiter. There are celestial bodies in orbit around the Sun. Their diameters vary from 10 m to 530 km. The total mass of all the asteroids combined is less than that of Earth's moon [28].

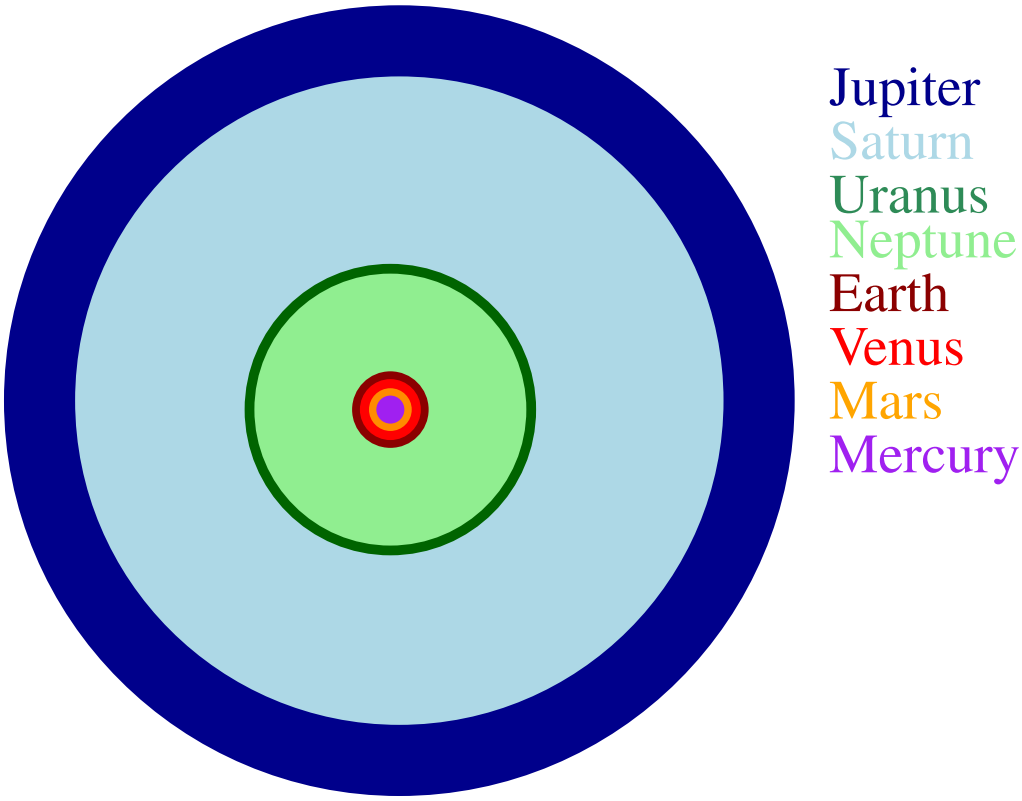

Figure 1: Scaled size of the planets.

The main objective of the thesis is to develop a high-fidelity orbital propagator for interplanetary space missions. It is implemented in the MATLAB environment. The general mission analysis tool GMAT R2017a developed by NASA is used to validate the results. A feature of GMAT is to simulate trajectories in our solar system. It consists of a high-fidelity orbital propagator. GMAT has supported 8 NASA missions and it is used around the world. The propagator developed in this thesis is named IOP.

The functioning of the propagator IOP is described to understand the objectives and the different parts of the thesis. The first 4.5 billion kilometres of our solar system starting from the Sun are represented in Figure 2. Let us start by defining the different elements shown in this figure. The Sun is located at the centre. The eight green points represent the planets. The circles draw the trajectories (orbits) followed by each planet over time. Mercury's orbit departs from a circle due to its eccentricity (≈ 0.2). The planets are trapped by the Sun's gravitational field. As a result, the planets describe 'again and again' the same trajectories over time. The solar system is divided into two regions in the propagator. The first region comprises the gray circles surrounding each planet. They are called spheres of influence and are represented by in Figure 2. The spheres of influence follow the planets in their own motion and admit as centres the planets themselves. The remaining part of our solar system constitutes the second region. This region is much larger than the first one.

The basic principle of the propagator is the following one. The user enters the initial position and velocity of the spacecraft in our solar system at a specified date. It could be any locations in Figure 2. The spacecraft ballistic properties and the duration of the propagation are also specified. IOP should be able to predict the spacecraft trajectory during the interval of time specified by the

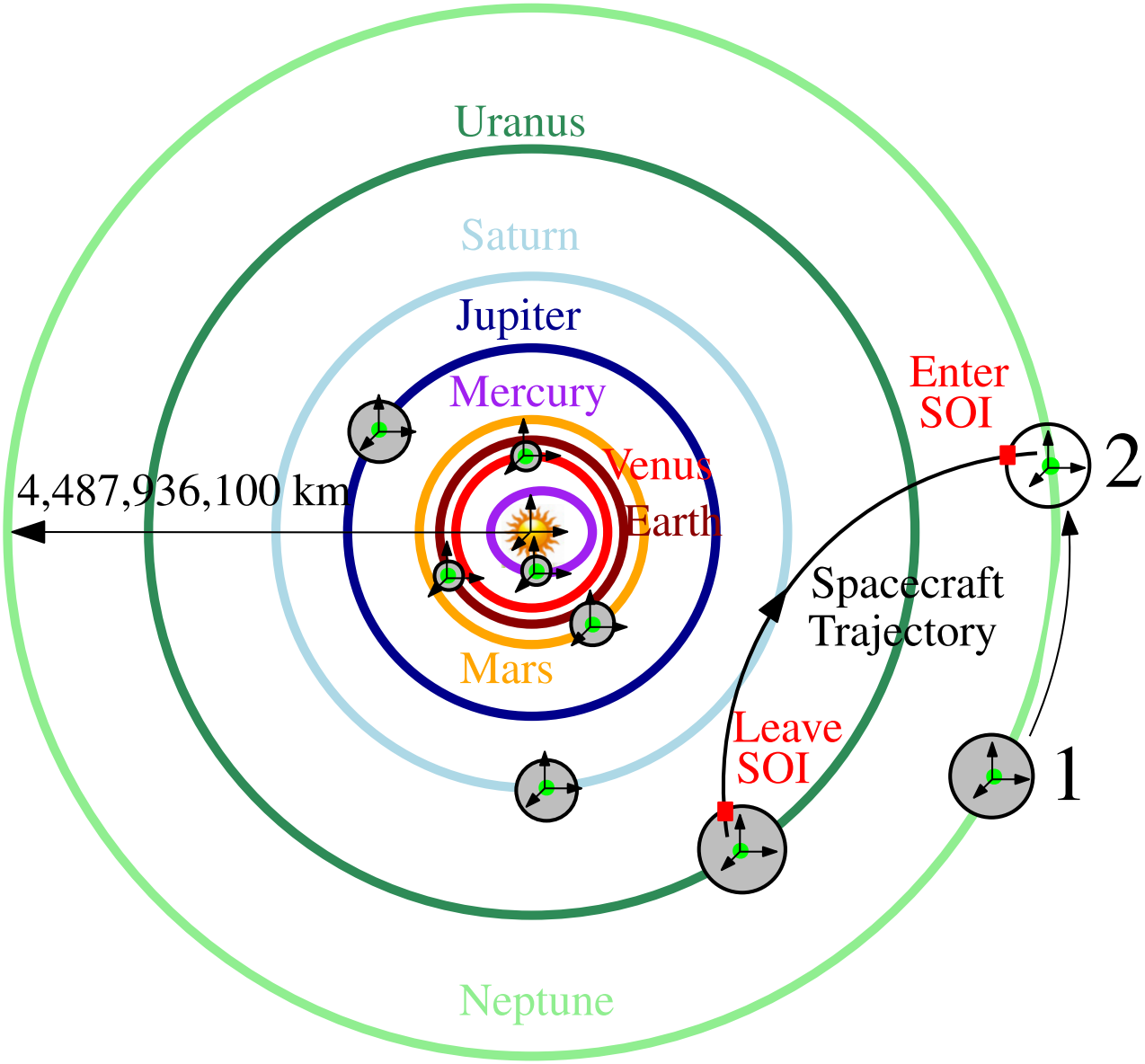

Figure 2: The first 4.5 billion kilometres of our solar system starting from the Sun are represented. The circles draw the trajectories (orbits) followed by each planet over time. Mercury's orbit departs from a circle due to its eccentricity. The eight green points represent the planets. The spheres of influence are represented by gray circles.

user. The motion of the spacecraft is mainly due to the gravitational attractions of the celestial bodies in the solar system.

The first elements to include in the propagator are the coordinate systems. They are needed to describe the spacecraft motion. Nine coordinate systems are included in IOP. They are represented by  in Figure 2. One coordinate system is associated with each planet. The ninth coordinate system is associated with the Sun. If the spacecraft motion happens in one of the eight spheres of influence, the coordinate system associated with the planet at the centre of this sphere of influence is selected. Otherwise, the coordinate system linked to the Sun is used. The second part of Chapter 1

is devoted to the definitions of the coordinate systems. How can the user specify the initial position and velocity? The propagator allows the user to select a coordinate system and to enter 6 orbital elements defining the initial state of the spacecraft. The notion of orbital elements is defined in the first chapter. A propagation consists of the description of the spacecraft trajectory over time. Time systems are also defined to keep track of time and to define the spacecraft departure date. This represents the last topic discussed in the first chapter.

As explained above, the motion of the spacecraft is mainly driven by the gravitational attractions of the celestial bodies. The gravitational attractions acting on the spacecraft depend on the time-varying positions of the celestial bodies. In addition, the planetary positions are needed to define the locations of the spheres of influence. The propagator should be able to locate the celestial bodies and to compute their velocities at each time of the spacecraft propagation. The second chapter focuses on the planetary ephemerides. The semi-analytic VSOP87 planetary theory used to compute the ephemerides is described. Data provided by the authors of the VSOP87 planetary theory are used to validate the results. This method is compared to two other methods to highlight the strengths of this planetary theory. The chapter concludes with the different solutions to improve the ephemerides. Earth's moon and Pluto's ephemerides are developed in the fourth chapter. The asteroids and the other moons described above are not included in the propagator.

An objective of most interplanetary missions is to travel from one planet to another. Traveling in the solar system is not the same as traveling by a car on Earth. On Earth, the towns are fixed. In the solar system, the planets move when the spacecraft goes from one planet to another. It is therefore needed to define a trajectory that intercepts the arrival planet at a chosen date. IOP should be able to compute such trajectories. The user selects the departure and arrival dates as well as the departure and arrival planets. A complementary routine is implemented to provide the user with the initial conditions corresponding to the interplanetary trajectory. This problem is Lambert's problem. It is explained in Chapter 3. The routine is also validated in this chapter. An example of interplanetary trajectory is shown in Figure 2. The spacecraft starts within the sphere of influence of Uranus. Chapter 3 also deals with the meaning of a sphere of influence and the limits of the gray circles in Figure 2. The aim is to reach Neptune. Neptune is located at the point denoted 1 in Figure 2 at the beginning of the propagation. At the end, Neptune is situated at the point denoted 2. The red rectangles define two specific instants of the propagation. The first rectangle is the location where the spacecraft leaves Uranus's sphere of influence. The second rectangle defines the moment where the spacecraft enters Neptune's sphere of influence. The propagator should be able to detect these particular moments. These two topics are also discussed in Chapter 3.

Propagation entails numerical integration of the spacecraft equations of motion. These equations are not identical within and outside the spheres of influence. Three cases are considered. First, the user selects initial conditions and the duration so that the spacecraft is located within a sphere of influence during all its propagation. For example, it is the case of a nearly closed orbit around a given planet. The second case is opposed to the first one. The spacecraft is located outside the spheres of influence during all its propagation. Only a unique numerical integration is needed in the first two cases. The propagation stops when the current time exceeds the duration specified by the user. The third case includes a spacecraft entering and leaving different spheres of influence. Lambert's trajectory described above illustrates this case. A first numerical integration is performed until the spacecraft reaches Uranus's sphere of influence. Chapter 4 describes the contributions acting on the spacecraft trajectory within a sphere of influence and provides the associated equations

of motion. Then, a second integration is performed until the spacecraft enters Neptune's sphere of influence. Chapter 4 also describes the contributions acting on the spacecraft trajectory outside spheres of influence and provides the associated equations of motion. Specifically, contributions coming from the primary gravitational attractions, non-sphericity of the attractors, solar radiation pressure, planetary eclipse models and point mass gravity attractions should be taken into account within and outside the spheres of influence. The thesis focuses on the physical understanding and the validation with GMAT of each of these contribution models. Emphasis is put on the accuracy of the results and the different ways to improve them. The last part of the fourth chapter explains the contributions that are not taken into account in IOP. In Chapter 5 the main algorithm behind IOP is explained and the choices of the numerical parameters and solvers are discussed. The thesis ends with the application of the propagator to the Cassini-Huygens mission. This mission started from the Earth and spent 13 years orbiting Saturn. IOP is used to recreate its trajectory and its corresponding velocity in the coordinate system centred on the Sun. A particular emphasis is put on the flyby manoeuvres.

Chapter 1

Time and coordinate systems

Time and coordinate systems are needed to describe spacecraft trajectories in our solar system. They are specifically used to define the positions and velocities of celestial bodies and spacecraft at a given time. The chapter is divided into three sections. The first section presents the time systems. The second section introduces the coordinate systems used throughout the report. The chapter concludes with the definition of the orbital elements.

1.1 Time systems

Time is used in the thesis to compute ephemerides and to integrate the spacecraft equations of motion. There are four main time scales in astrodynamics: sidereal time, solar time, dynamical time and atomic time. Figure 1.1 shows the differences between the four time scales. The times are obtained by following the paths showed in this figure. Red crosses indicate that the associated time scales are not used in the propagator.

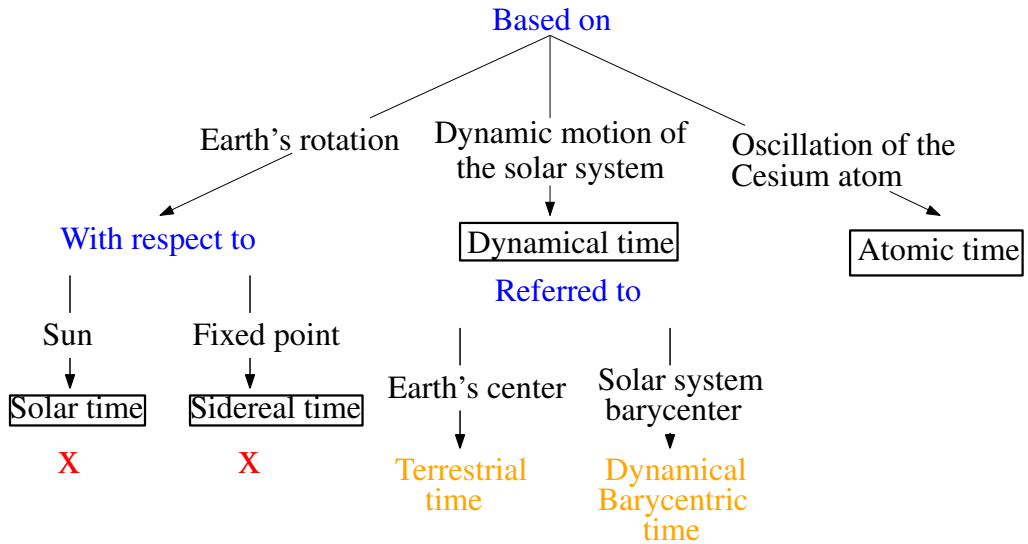

Figure 1.1: Time scales are inside the black rectangles. The figure shows the paths to follow to obtain the different times. Red crosses indicate that the corresponding time scales are not used in the propagator.

Sidereal time is the first time scale. It is based on Earth's rotation with respect to a fixed point. According to Vallado [24], sidereal time is defined as the time between transits of the stars over a particular meridian. The solar time scale is also based on Earth's rotation. The difference comes from the fact that the rotation is related to a fictitious Sun in uniform motion around the Earth. According to Vallado [24], the solar time is defined as the interval between successive transits of the fictitious Sun over a particular meridian. For example, it is used in GMAT to determine Earth's orientation at a given epoch. The time scales related to the Earth's rotation are not employed in the thesis.

Atomic time scale accurately defines the second. It is based on the specific quantum transition of electrons in a Cesium atom [24]. The transition causes the emission of photons of a known frequency that we can count [24]. A number of 9,192,631,770 oscillations of the Cesium nuclide 133Ce defines the duration of one second [17]. It is suitable to integrate the equations of motion in Chapter 4.

Dynamical time is the last time scale. It is based on the dynamic motion of the solar system and takes into account the relativistic effects [18]. Dynamical time is the independent variable in the dynamic theory and ephemerides [18]. Therefore, they are the most suitable time systems to compute the ephemerides at a given time. The terrestrial time TT and the Barycentric Dynamical time TDB consist of the two dynamical time of interest. TT is related to the Earth's centre whereas TDB is linked to the barycenter of the solar system. A transcendental equation must be solved to convert terrestrial time in Barycentric Dynamical time [18]. TDB is the time appearing in the VSOP planetary theories used in the following chapter. However, the Barycentric Dynamical time can be safely replaced by the terrestrial time as shown in this chapter.

The departure date in terrestrial time is entered in IOP at the beginning of a propagation. The Gregorian date format is selected: $(Year, Month, Day, Hour, Minute, Second)$. It begins at Christian era. Gregorian date format is not practical for computer calculations. The departure date is transformed in Julian date JD [24]

$$\begin{aligned} JD &= 367(Year) - Int\left\{\frac{7\{Year + Int(\frac{Month+9}{12})\}}{4}\right\} + Int(\frac{275Month}{9}) \\ &\quad + Day + 1,721,013.5 + \frac{\frac{Second}{60} + minute}{60} + Hour}{24}, \end{aligned} \tag{1.1}$$

where Int denotes real truncation. The relationship is valid between 1 March 1900 and 28 February 2100. Julian date represents the number of days elapsed since the epoch 1 January 4713 12:00:00 BC TT. An epoch must be chosen to compute ephemerides and to define inertial coordinate systems in the following section. It defines the starting point from which one starts to count. The J2000 epoch is used as a reference epoch in IOP. It occurred on 1 January 2000 12:00:00 TT. As a result, 2,451,545 corresponding to the Julian date on 1 January 2000 at noon is subtracted from the Julian date to compute ephemerides. This operation shifts the epoch from 1 January 4713 12:00:00 BC TT to 1 January 2000 12:00:00 TT.

1.2 Coordinate systems

Nine coordinate systems are used to describe the motion of spacecraft in the propagator. The inertial coordinate systems proposed in GMAT [18] are selected. An inertial coordinate system has

neither translational nor rotational acceleration relative to a fixed point [24]. The nine coordinate systems proposed in GMAT have their z-axis aligned with the spin axes of the planets and the Sun. However, these coordinate systems are not output systems of the VSOP planetary theories defined in Simon and al. [20]. Therefore, the Sun inertial coordinate system proposed in GMAT is replaced by the heliocentric inertial coordinate system defined in section 1.2.2. In fact, all the coordinate systems presented in this section are pseudoinertial and right-handed. The right-handed characteristic is a choice. The only constraint is to be consistent with this choice throughout the report. It is used to perform change of coordinate systems in section 3.2. As proposed in GMAT [18], the coordinate systems are assumed sufficiently inertial to neglect the pseudoinertial characteristic. The pseudoinertial characteristic comes from the fact that the centres of the coordinate systems do not move at constant speed. Indeed, the planets describe elliptic trajectories around the Sun. Therefore, a correction should be added.

The coordinate systems are realized with respect to a reference frame. 'A reference frame consists of a set of identifiable points in the sky along with their coordinates, which serves as the practical realization of a reference system' [13]. The J2000 inertial frame is chosen. It consists of a frame relative to the stars Catalogue FK5. There is an inertial frame relative to quasars called International Celestial Reference Frame. This frame is the best approximation of an inertial coordinate system. The origin of the corresponding coordinate system is located at the barycenter of the solar system. However, transformation between coordinate systems and ephemerides are given in the J2000 inertial frame in GMAT [18] and in Simon and al. [20].

The section is divided into three parts. First, the Earth and Sun inertial coordinate systems are defined. These coordinate systems play central roles in IOP. The third part introduces the inertial coordinate systems associated with the other planets.

1.2.1 Earth inertial coordinate system $\{E_1, E_2, E_3\}$

A coordinate system is defined by specifying its origin and the orientation of its three axes. The origin of the Earth inertial coordinate system denoted EarthJ2000 is the Earth's centre. It is represented in Figure 1.2. The reference direction E_1 is the Vernal equinox. It is defined as the intersection between the ecliptic plane and the equatorial plane of the Earth at the J2000 epoch in the direction where the Sun crosses the equatorial plane moving from southern to the northern hemisphere [24]. The ecliptic plane is defined in the following coordinate system. The equatorial plane is the plane perpendicular to the rotation axis of the Earth. The E_3-axis is parallel to the spin axis at the J2000 epoch and positive toward the North. The E_2-axis completes the right-handed coordinate system.

This coordinate system has two functions. First, it is used to integrate the spacecraft equations of motion in the sphere of influence (SOI) of the Earth. The meaning of sphere of influence is specified in Chapter 3. EarthJ2000 is also employed as an intermediate coordinate system in section 3.2 to perform change of coordinate systems. Indeed, the orientation of the axes of the other planetocentric coordinate systems (section 1.2.3) are defined with respect to the axes of EarthJ2000. Change of coordinate systems implies to translate the origin from one planet/Sun to another planet/Sun. Therefore, it is introduced in Chapter 3 after ephemerides are introduced in Chapter 2.

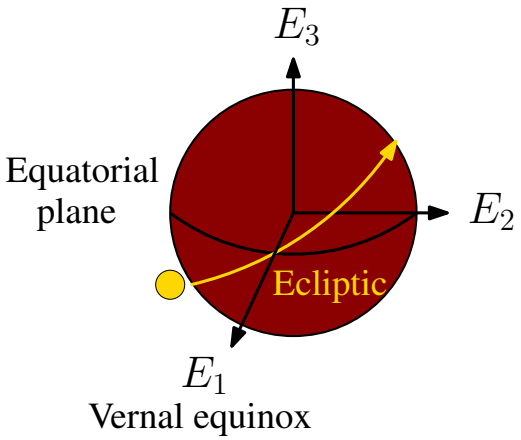

Figure 1.2: Earth inertial coordinate system. The dark-red sphere represents the Earth. The yellow line represents the path of the Sun. It illustrates the crossing of the Sun from southern to the northern hemisphere. $\{E_1, E_2, E_3\}$ are the axes of the Earth inertial coordinate system.

1.2.2 Heliocentric inertial coordinate system $\{X, Y, Z\}$

The heliocentric coordinate system is an inertial coordinate system associated with the Sun. It uses the mean orbit of the Earth (free of periodic variations) around the Sun at the J2000 epoch as reference plane. This plane is called ecliptic plane. The X-axis is the Vernal equinox as in the previous coordinate system. The Z-axis is the normal to the ecliptic plane. It is referred to as the North pole of the ecliptic. The Y-axis completes the right-handed coordinate system. The origin is located at the centre of the Sun. The axes of the heliocentric coordinate system differ from the axes of EarthJ2000 by a rotation about the Vernal equinox as shown in section 3.2.

The heliocentric coordinate system also has two functions. First, it is used to integrate the spacecraft equations of motion outside the spheres of influence[1]. In addition, the planetary theories, used to compute planetary ephemerides in the following chapter, provide the positions and velocities of planets in this coordinate system. This choice is driven by the small inclinations of planets' orbital planes with respect to the ecliptic plane.

1.2.3 Planetocentric inertial coordinate systems $\{I, J, K\}$

The inertial coordinate systems associated with the Earth and the Sun have been defined. Additional inertial coordinate systems are used to integrate the spacecraft equations of motion in the SOI of the seven remaining planets. They are defined as follows. The origin is located at the centre of the considered planet. The I-axis is the intersection between the body equator and the E_1E_2 plane of the Earth inertial coordinate system at the J2000 epoch. The K-axis is the spin axis direction at the J2000 epoch. The J-axis completes the right-handed coordinate system.

As explained in section 1.2.1, the orientation of the axes of the other planetocentric coordinate systems are defined with respect to the axes of EarthJ2000. Two angular coordinates are needed to define the direction of a spin axis. The right ascension α_0 and declination δ_0 of the spin axis direction

[1]Outside the spheres of influence means outside the planetary spheres of influence in the thesis. It corresponds to the second region defined in the introduction. It also means that the spacecraft is located within the sphere of influence of the Sun.

of the seven planets with respect to the Earth inertial coordinate system at the J2000 epoch are given in Table 1.1. They are provided by the International Astronomical Union (IAU). Right ascension is measured positive to the east in the plane of the equator from the Vernal equinox direction [24]. The declination is measured northward from the Earth's equator to the spin location [24]. The negative declination of the Uranus' spin axis implies that it is located south to the Earth's equator.

Planets	α_0 (deg)	δ_0 (deg)
Mercury	281.01	61.45
Venus	272.76	67.16
Mars	317.68143	52.88650
Jupiter	268.05	64.49
Saturn	40.589	83.537
Uranus	257.311	-15.175
Neptune	299.36	43.46

Table 1.1: Spin axis directions at the J2000 epoch. α_0 and δ_0 are the right ascension and declination of the spin axis with respect to the axes of EarthJ2000.

1.3 Orbital elements

The Cartesian positions and velocities of a spacecraft are not suitable to get insight into the shape and the characteristics of the associated orbit. Orbital elements are introduced in that context. More specifically, six orbital elements are needed to describe the state of a given body (planets or spacecraft). The description in terms of orbital elements can be used with each coordinate system defined in the previous section.

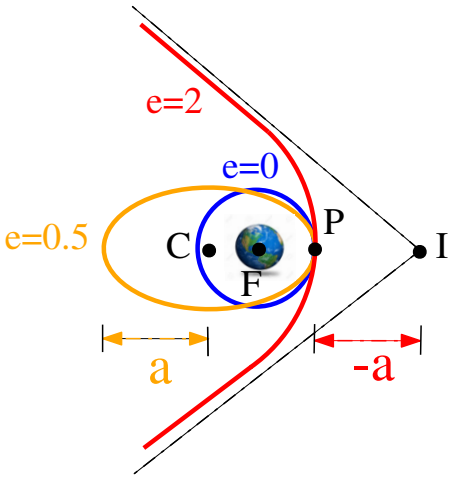

Figure 1.3: Type of orbits. The parabola is not represented.

The eccentricity e [-] indicates the shape of the orbit. It is never negative. There are four types of orbit. The eccentricity is equal to 0 for a circle, smaller than 1 for an ellipse, is equal to 1 for a parabola and higher than 1 for a hyperbola. The corresponding shapes are represented in Figure 1.3.

The semi-major axis a [km] describes the size of conics. It is positive for both the circle and the ellipses, infinite for a parabola and negative for a hyperbola [24]. Each conic has two foci. For the ellipse, the center C in Figure 1.3 is defined as the mean distance between the foci. The semi-major axis for an ellipse is the distance between C and the extremities denoted a in this figure. The point P is called the periapsis. It represents the point where the spacecraft comes the closest from the celestial body lying at the occupied focus F. In fact, the eccentricity e is the norm of the vector **e** pointing to periapsis. The distance between I and P defines the minus of the hyperbola semi-major axis $-a$. The point I is the intersection between the two asymptotes of the hyperbola.

The inclination i [deg], the right ascension of the ascending node or longitude of the ascending node Ω [deg] and the argument of periapsis ω [deg] define the orientation of the orbit with respect to the reference plane. These angles are represented in Figure 1.4. The inclination is measured from the unit vector **z** to the angular momentum $\mathbf{h} = \mathbf{r} \times \mathbf{v}$ [24]. **r** and **v** denote respectively the position and velocity vectors. It varies from 0° to 180°. The intersection between the reference plane and the orbital plane is called the line of nodes. **N** stands for the vector along the line of nodes pointing in the direction of the ascending node. It represents the location where the spacecraft/planet crosses the reference plane from south to north (blue). The longitude of the ascending node is the angle measured positively in the reference plane from the reference direction to the location of the ascending node [24]. "Positively" means counterclockwise in the right-handed coordinate system convention. Ω varies from 0° to 360°. The argument of periapsis locates the closest point to the orbit. It is measured positively from **N** in the direction of the satellite's motion.

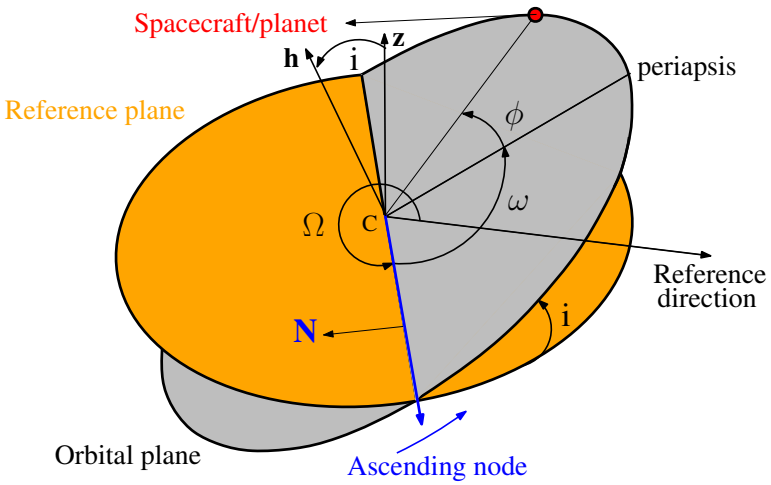

Figure 1.4: Orbital elements. The figure is inspired by [26].

The true anomaly ϕ locates the spacecraft/celestial body in the orbital plane and is the angular displacement measured from periapsis to the position vector along the direction of motion [24]. It varies from 0° and 360° for both circle and ellipse. It is comprised between -180° and 180° for a parabola. For the hyperbola, the true anomaly is limited by [24]

$$-180° + \arccos\frac{1}{e} < \phi < 180° + \arccos\frac{1}{e}. \tag{1.2}$$

Additional orbital elements are introduced in the special case of planetary ephemerides. All the planetary orbits are elliptic orbits around the Sun lying at one of the foci (Kepler's first law). The

first angle is the eccentric anomaly E shown in Figure 1.5. A circle of radius a is drawn around the ellipse. Its center is located in C defined previously. The eccentric anomaly is related to the true anomaly. It defines the planet's position in its orbital plane.

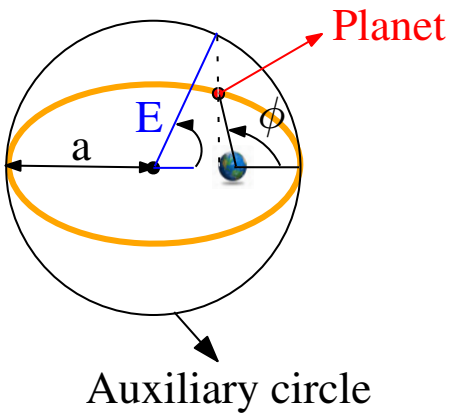

Figure 1.5: Eccentric anomaly.

The second angle M is the mean anomaly. It does not represent a physical element like E. It corresponds to a uniform angular motion on a circle of radius a [24]. It is related to time.

The inclinations of the planets' orbital planes with respect to the ecliptic plane are small. As a result, the right ascensions of the ascending node can be poorly defined. The longitude of perihelion $\bar{\omega}$ is introduced to remove the ambiguity. It is the location of the perihelion measured Eastward from the reference direction [24]

$$\bar{\omega} = \omega + \Omega \tag{1.3}$$

The planetary orbits have also small eccentricities. The mean longitude L is introduced in the case of circular ecliptic orbit. It is computed by [24]

$$L = \bar{\omega} + M. \tag{1.4}$$

Chapter 2

Ephemerides

Planetary ephemerides constitute a milestone of an interplanetary orbital propagator. It will be shown in Chapter 4 that the accuracy of the perturbation models is directly linked to the accuracy of planetary ephemerides. In addition, the positions and velocities of the planets are also used in the change of coordinate systems discussed in the following chapter.

Three methods are implemented to compute planetary ephemerides. They are described to understand the improvements linked to the contributions taken into account in the VSOP87 planetary theory. The most basic method describes the motion of a planet considering that the Sun and the selected planet as the only celestial bodies in our solar system. This represents the two-body approximation. Then, semi-analytic methods based on numerical integration of planetary equations of motion are implemented to improve the results. Nowadays, most accurate numerical integration is provided by NASA Jet Propulsion Laboratory. They are referred to as Development Ephemeris DE-NUMBER, where NUMBER gives the version of the integrated ephemeris. The integration methods are both believed to be sufficiently complete and accurate [22]. The integrated ephemerides are only differentiated through quality, quantity and coverage in time of the observational data included in the numerical integration. The higher the quality, quantity and coverage in time of the observational data are, the higher the accuracy of the numerical integration is.

The semi-analytic methods implemented are based on the Development Ephemeris DE200. In addition to the two-body approximation, semi-analytic methods take into account the mutual interactions between the considered planet and the other celestial bodies (planets and asteroids). The VSOP82 planetary theory is the first semi-analytic method. It takes into account the secular perturbations of the other celestial bodies on the considered planet. Secular perturbations are non-oscillatory perturbations. It means that their effects stay 'forever'. Secular perturbations are opposed to periodic perturbations. Periodic perturbations are repeated in time, and the average of these perturbations over one period is equal to zero. However, these periodic perturbations affect significantly the planets which are located farther from the Sun (Jupiter to Neptune). The semi-analytic planetary theory VSOP87 takes into account both secular and periodic perturbations.

The Development Ephemeris DE405 is one of the most used Development Ephemerides. There are only few improvements (some kilometres [8]) between the development ephemeris DE405 and the newest Development Ephemeris. Therefore, DE405 is used to assess the accuracy of the results. The accuracy is measured as the distance between the predicted position/velocity of planets and the

position/velocity computed with the integrated ephemeris DE405 [1]. It is given by

$$d = \|\mathbf{x}_{\text{predicted}} - \mathbf{x}_{\text{DE405}}\|, \tag{2.1}$$

where $\|\|$ denotes the norm of a vector and $\mathbf{x}$ $[3 \times 1]$ stands for the position or the velocity depending on the case. The higher the distance is the higher the error is.

The chapter is divided into four sections. The first section explains the procedure used to compute the positions and velocities of planets at a given date. The validation of the three methods is performed in the second section. The third section focuses on the results and the comparison between the different methods. The chapter concludes with the possible improvements.

2.1 Procedure

The objective is to compute the planetary orbital elements $(a, e, i, \Omega, \omega, E)$ at the given date. A conversion can be applied thereafter to obtain the corresponding position and velocity vectors. The procedure followed by the three methods is represented in Figure 2.1.

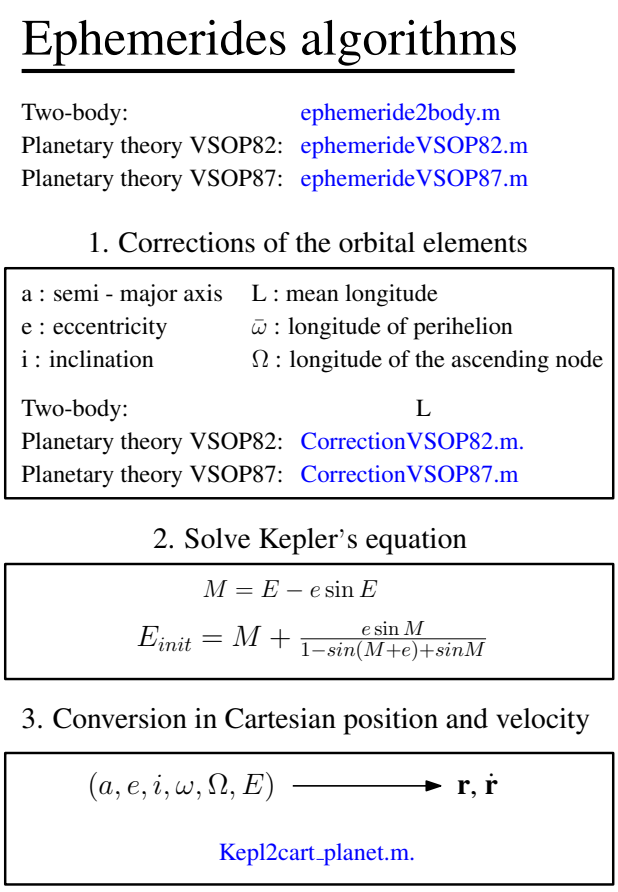

Figure 2.1: Description of the algorithms to compute ephemerides.

[1] The data come from CNES website: `http://vo.imcce.fr/webservices/miriade/?forms`. The parameters are as follows. Reference centre: heliocenter, planetary theory: DE405, Reference plane: ecliptic, Type of coordinate: Cartesian, Type of ephemeris: MeanJ2000.

The starting point of the three methods are six orbital elements of the considered planet in the heliocentric coordinate system at the J2000 epoch: semi-major axis a [km], eccentricity e [-], inclination with respect to the ecliptic plane i [deg] , the mean longitude L_0 [deg], longitude of perihelion $\bar{\omega}$ [deg] and longitude of the ascending node relative to the Vernal equinox Ω [deg].

Planetary ephemerides are evaluated in three steps. The first step is to correct the orbital elements in function of the given date. Only the mean longitude L changes in time in the two-body approximation [19]

$$L = L_0 + n(JD - 2451545), \tag{2.2}$$

where n [deg/day] stands for the mean angular rate of change of the planet in orbit [24] and JD stands for the given Julian date. In the case of the semi-analytic methods, each of the J2000 orbital elements is corrected with [20], [24]

$$OE = oe_0 + oe_1 T_{\text{TBD}} + oe_2 T_{\text{TBD}}^2 + oe_3 T_{\text{TBD}}^3, \tag{2.3}$$

where oe_0 corresponds to the orbital element at the J2000 epoch. The remaining part is the correcting part in which T_{TBD} represents the number of Julian thousands years elapsed from J2000 in Barycentric Dynamical time. The mean coefficients oe_0 to oe_3 are fitted from the Development Ephemeris DE200 to represent at best the impact of the secular perturbations of the other celestial bodies on the motion of the considered planet. Periodic corrections given in terms of Poison series are added to the secular corrections given in Equation 2.3 in the case of the VSOP87 planetary theory. The two other steps are identical in the three methods.

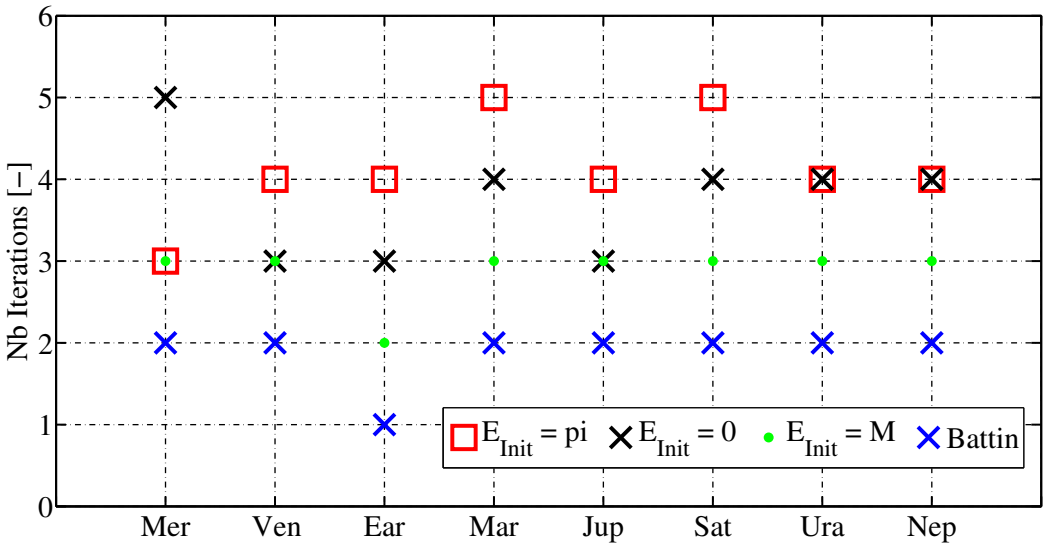

Figure 2.2: Convergence of the Newton-Raphson algorithm in function of the initial guess.

Once the orbital elements are known, the mean anomaly $M = L - \bar{\omega}$ and the argument of perihelion $\omega = \bar{\omega} - \Omega$ are computed. The second step is to solve the transcendental Kepler's equation for elliptic orbits to extract the eccentric anomaly E. Kepler's equation allows us to determine the relation of the time (M) and angular displacement (E) [24]. The solution of a transcendental

equation cannot be given in a finite number of terms but it is unique. Newton-Raphson algorithm is chosen to solve the transcendental equation. The tolerance of 10^{-8} proposed in Vallado [24] is selected. The last parameter to select is the initial guess of the iterative algorithm. Four classical initial guesses are given in Battin [2], Montenbruck [17] and Vallado [24]: 0, π, M and $M + \frac{e \sin M}{1-sin(M+e)+sinM}$. The last one comes from Battin. The initial guess influences the convergence speed. The following test case is proposed. The date is on 1 January 2000 12:00:00 TT. Newton-Raphson's algorithm is solved using each of the initial guess for the eight planets. Figure 2.2 shows the number of iterations needed to converge. The initial guess proposed by Battin leads to the fastest convergence of the Newton-Raphson algorithm. Two iterations are needed on average to converge. At this stage, the orbital elements $(a, e, i, \Omega, \omega, E)$ at the given date are known. A conversion is applied to obtain the Cartesian position and velocity vectors in the heliocentric coordinate system.

2.2 Validation

The two-body and the VSOP82 planetary theory routines have been validated with numerical examples provided in Curtis [6] and Vallado [24]. Data provided by authors of VSOP87 planetary theory are used to validate the results.

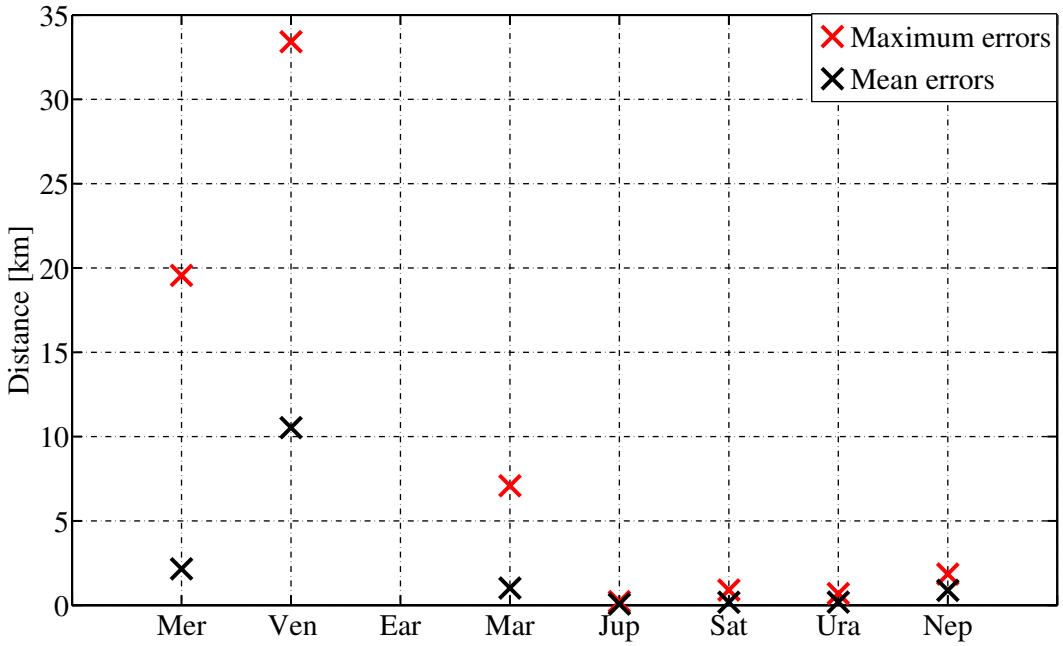

Figure 2.3: Difference between data provided by the authors of the VSOP87 planetary theory and IOP for all planets apart from the Earth. The 77 values are generated in a Fortran code. The difference is measured in kilometres.

The positions of the planets in the heliocentric coordinate system for 77 dates have been provided. The distance between these positions and the positions computed by IOP are evaluated using

Equation 2.1. The mean and the maximum of these distances for each planet are shown in Figure 2.3. The mean error represents $2\times10^{-6}\%$ of the planetary semi-major axes. The maximum peak of errors arises for Venus. It represents $3\times10^{-5}\%$ of its semi-major axis. The origins of these small differences come from numerical errors.

Earth periodic perturbations are not given in the VSOP87 planetary theory. Only the perturbations of the Earth-Moon barycenter are provided. Therefore, it will not bring any improvements to the Earth. VSOP82 is used to compute the ephemerides of this planet.

2.3 Results

Table 2.1 contains the averages of the errors computed on the 5th, 10th, 15th, 20th, 25th of each month for the years 1960-1970-1980-1990-2000-2010. For each of these dates, the distances between the positions computed with the three methods and DE405 are computed with Equation 2.1. It means that each of the 23 mean errors shown in Table 2.1 is the average of 360 distances.

The results for the two-body approximation are given in the first column in Table 2.1. The two-body approximation can be used as a first approximation of planetary ephemerides. The errors for the inner planets (Mercury to Mars) represent 0.02 % of their semi-major axis which corresponds to a mean error of 27,838 km. This error increases to 0.73 % (22,449,556 km) for the outer planets.

Planets	*Error between positions TwoBody-DE405* (km)	*Error between positions VSOP82-DE405* (km)	*Error between positions VSOP87-DE405* (km)
Mercury	9,974	1,592	281
Venus	7,261	5,479	903
Earth	19,434	13,196	/
Mars	74,682	50,703	4,782
Jupiter	1,240,540	1,225,997	63,502
Saturn	6,722,816	6,644,242	189,192
Uranus	38,842,630	38,912,324	567,825
Neptune	42,992,237	42,911,557	153,717

Table 2.1: Comparison between the two-body method, VSOP82 and VSOP87 planetary theories. The values are averaged of the distances with DE405 computed on the 5th, 10th, 15th, 20th, 25th of each month for the years 1960-1970-1980-1990-2000-2010.

The second column in Table 2.1 contains the averages of the distances between the VSOP82 planetary theory and DE405. The results are improved compared to the two-body method for the inner planets (Mercury to Mars). The errors represent 0.01% of the semi-major axes of the four inner planets (Two-body: 0.02%). In contrast, VSOP82 does not improve the results of the outer planets. It comes from the fact that the secular perturbations are not sufficient to compute accurate ephemerides of the outer planets. The periodic perturbations play a preponderant role in their motion.

The averages of the distances computed with the VSOP87 planetary theory are given in the third column in Table 2.1. The columns of this table highlight the improvements linked to the different

methods. The errors represent respectively 0.003% and 0.01% of the semi-major axes of the inner planets and of the outer planets. The mean error of the outer planets is 226,701 km instead of 22 million kilometres found with the VSOP82 planetary theory. The improvements to the inner planets are smaller. The mean error is 17,742 km in the VSOP82 planetary theory, whereas the mean error is 4,723 km in the VSOP87 planetary theory. In summary, the periodic corrections improve the results of one order of magnitude for the inner planets and of two orders of magnitude for the outer planets.

Why are the errors on the outer planets higher than the errors on the inner planets? The planetary formulations VSOP82 and VSOP87 come from the Development Ephemeris DE200. The accuracy of VSOP82 and VSOP87 results directly from the observational data integrated in DE200. DE200 shows significant positional errors during the present epoch for all the four outermost planets (Jupiter to Neptune) [22]. Indeed, ephemerides of outer planets mainly rely on optical observations whereas inner planets are observed with satellite ranging.

It has to be stressed that the time used to correct the orbital elements in the VSOP82 and VSOP87 planetary theories is the Barycentric Dynamical time (Equation 2.3). However, a transcendental equation must be solved to compute the Barycentric Dynamical time exactly. Therefore, it is replaced by the terrestrial time TT to decrease the computational time. The terrestrial time shows a difference of maximum of 0.002 s with respect to the Barycentric Dynamical time. The difference in the results is negligible. For Mercury and Saturn (year 1990), the difference between the distance with terrestrial and Barycentric Dynamical time are respectively 28 and 8 metres.

Planets	*Error between positions VSOP87-DE405* (km)	*Standard deviation* VSOP87-DE405 (km)	*Minimum* VSOP87-DE405 (km)	*Maximum* VSOP87-DE405 (km)
Mercury	281	157	34	891
Venus	903	494	87	2,481
Earth	13,196	4504	1,141	29,309
Mars	4,782	2,724	629	15,867
Jupiter	63,502	7,625	38,592	162,234
Saturn	189,192	17,741	24,189	442,744
Uranus	567,825	11,608	126,679	883,981
Neptune	153,717	3,864	11,062	270,678

Table 2.2: Overview of the results obtained with the VSOP87 planetary theory. The first column contains the mean errors between VSOP87 and DE405 computed over the years 1960-1970-1980-1990 -2000-2010. The second column provides the standard deviations. The third and the fourth columns provide the minimum and maximum distances obtained for each planet over the years 1960-1970-1980-1990-2000-2010.

The averages of the errors highlight the general trend. They are suitable to compare the three methods. However, the errors committed on planetary ephemerides can be close or not to the mean values depending on the date. A statistical analysis is performed. The minimum and maximum of errors as well as the dispersion of the errors around the mean value are computed. The dispersion is

given by the standard deviation

$$std = \sqrt{\frac{1}{n}\sum_{i=1}^{n}(x_i - \bar{x})^2}, \tag{2.4}$$

where n [-] is the number of samples (360), x_i [km] is the value of the ith distance and $\bar{x}$ [km] is the mean distance. The standard deviations are given in the second column in Table 2.2. The third and fourth columns contain the minimum and maximum values of the errors over the six years. A distinction can also be made between the standard deviation of the inner and outer planets. For the inner planets, the standard deviation is high compared to the mean values. It is opposed to the outer planets. The distances tend to be close to the mean values. For the inner and outer planets, the minimum and maximum can be quite far from the mean value. The semi-analytic methods try to represent at best the ephemerides of the planets. For some specific dates, the predictions could be in large errors or very close to the real planetary positions.

	Error between velocities VSOP82-DE405 (m/s)	*Error between velocities VSOP87-DE405* (m/s)	*Mean orbital velocities* (km/s)
Mercury	1.36	0.4	48
Venus	1.27	0.8	35
Earth	12.62	/	30
Mars	5.30	1.8	24
Jupiter	24.02	11	13
Saturn	39.37	16	10
Uranus	93.16	16	7
Neptune	56.48	13	5

Table 2.3: Comparison between the VSOP82 and VSOP87 planetary theories. The first two columns contain the means of the distances between VSOP82/VSOP87 and DE405 over the years 1960-1970-1980-1990-2000-2010. The third column contains the mean planetary orbital velocities.

Up to now, only positions of the planets have been discussed. The VSOP87 planetary theory also improves the results in terms of velocities as shown in the first and second columns in Table 2.3. The mean planetary orbital velocities are given in the third column of this table. The mean orbital velocities decrease when the distance between the planets and the Sun increases. The eccentricities of the orbits around the Sun are close to 0. Therefore, the velocities can be approximated by the expression of velocities for circular orbits given by

$$v = \sqrt{\frac{\mu}{R}}, \tag{2.5}$$

where μ [km^3/s^2] stands for the gravitational parameter and R [km] represents the radius of the orbit of the considered planet assumed to be a circular orbit. The velocity decreases when the radius of the orbit increases. Therefore, the velocity is smaller for Neptune (outer planet) than for Mercury (inner planet). The errors on velocities are higher in magnitude for the outer planets than the errors for the inner planets. It means that the errors are maximum for the outer planets and minimum for the inner planets. Indeed, it is more detrimental to have a large error on a small mean orbital velocity (outer

planets) than a large error on a larger mean velocity (inner planets). For example, Neptune has an error of $2 \times 10^{-3}\%$ on its mean orbital velocity. It is opposed to Mercury. Its error is $8 \times 10^{-6}\%$. The accuracy obtained with the VSOP87 planetary is sufficient to build an accurate interplanetary orbital propagator. The statistical analysis performed for the positions in Table 2.2 is also made for the velocities. The results are given in Appendix B.1.

2.4 Possible improvements

The planetary formulations VSOP82 and VSOP87 come from the Development Ephemeris DE200. A semi-analytic method based on the most advanced Development Ephemeris DE405 could be implemented to improve the results. DE405 uses very-long-baseline interferometry (relative to quasars) in contrast to DE200 which uses stars. This semi-analytic method is called VSOP2000. However, it is not yet available online. The solution is from 10 to 100 times more precise than the previous semi-analytic methods VSOP82 and VSOP87 according to BRETAGNON and al. [16]. In addition, VSOP2000 takes perturbations by 300 asteroids into account. The best solution to compute planetary ephemerides is to couple the propagator with tabulated data computed by numerical integration. The propagator interpolates the data to obtain ephemerides at the desired date.

Ephemerides developed in this chapter are valid for the interval 1800-2050. It has to be stressed that ephemerides for 1000-3000 can be obtained by adding few corrections. However, these corrections degrade the precision over the interval 1800-2050. In addition, the routine given in Vallado [24] (Equation 1.1) to compute the Julian date is only valid in the interval 1900-2100. Considering these constraints the ephemerides are therefore valid in the interval 1900-2500. The extension can be implemented by modifying the routine that computes the Julian date and by including the additional corrections. They are given in Simon and al. [20].

The importance of accurate planetary ephemerides will be highlighted in the following chapters. Even if the VSOP87 planetary theory is not the most advanced planetary theory, IOP is able to model the trajectories of spacecraft with a high degree of confidence. The only exception occurs during change of coordinate systems as shown in section 3.2

Chapter 3

Spheres of influence

A sphere of influence for a central body is an imaginary sphere within which the gravity of an object is primary responsible for the spacecraft's motion [24]. The central bodies are the planets and the Sun in IOP. Their impacts are referred to as the primary attractions. The chapter focuses on the planetary spheres of influence. The origins of the spheres are the centres of the planets. Their radii are much larger than the equatorial radii of their associated planets.

Two main objectives are pursued in introducing the concept of a sphere of influence. First, the motion of the spacecraft in the solar system is driven by the primary attractions and perturbations coming from the eight planets, the Moon, the dwarf planet Pluto and the Sun. The user selects the perturbations it wishes to include in the propagator. However, some of these perturbations impact to a negligible extent the spacecraft trajectories depending on their positions in the solar system. The concept of a sphere of influence allows the propagator to determine the locations where these perturbations should be turned off. It means that the terms corresponding to these perturbations are added or removed from the equations of motion. For example, even if the user activates the J_2 perturbation, its impact is negligible outside the SOI. It can be turned off outside the SOI to reduce the computational time. The same reasoning can be performed for the eclipse models. In addition, the concept of a sphere of influence allows the propagator to determine in which coordinate system it is the most convenient to express the motion of the spacecraft. A coordinate system linked to the central body is suitable to describe the motion of the spacecraft. It means that a coordinate system linked to a planet is chosen within a sphere of influence. The heliocentric coordinate system, which is the coordinate system associated with the Sun, is chosen for the motion of spacecraft outside the spheres of influence. These coordinate systems are compatible with the equations of motion proposed in Curtis [6] and Vallado [24]. Using the concept of SOI is a choice. There are other techniques to develop an interplanetary orbital propagator. For example, GMAT integrates all the equations of motion in the Earth inertial coordinate system.

The chapter is divided into four sections. The first section focuses on the properties of the spheres of influence. The motion of the spacecraft is expressed in a planetocentric coordinate system within a sphere of influence and in a heliocentric coordinate system outside the spheres of influence. A change of coordinate system is therefore needed when the spacecraft crosses a sphere of influence. The second section is devoted to this topic. The third and fourth sections focus on the practical implementation of crossing a sphere of influence. More specifically, the third section defines the condition to detect when a spacecraft leaves a sphere of influence, whereas the fourth section defines the condition to detect when a spacecraft enters a sphere of influence.

3.1 Properties

Laplace defined the sphere of influence for a given planet as the surface where the magnitude of the specific forces acting on the spacecraft satisfy [12]

$$\frac{P_{\mathrm{p}}}{A_{\mathrm{s}}} = \frac{P_{\mathrm{s}}}{A_{\mathrm{p}}}, \tag{3.1}$$

where P_{p} stands for the third-body perturbation due to the planet, A_{s} stands for the primary gravitational attraction due to the Sun, P_{s} stands the third-body perturbation due to the Sun and A_{p} stands for the primary gravitational attraction due to the planet. The surface corresponding to this relation can be approximated by a sphere. Its radius is given by

$$R_{\mathrm{SOI}}^{\mathrm{P}} \approx \left(\frac{m_{\mathrm{p}}}{m_{\mathrm{s}}}\right)^{2/5} \sqrt{x_{\mathrm{p}}^2 + y_{\mathrm{p}}^2 + z_{\mathrm{p}}^2}, \tag{3.2}$$

where m_{p} [kg] stands for the mass of the planet, m_{s} [kg] stands for the mass of the Sun and $(x_{\mathrm{p}}, y_{\mathrm{p}}, z_{\mathrm{p}})$ stands for the Cartesian position of the considered planet in the heliocentric coordinate system. This relation is valid if the mass of the planet is much smaller than the mass of the Sun. In fact, the mass of the Sun represents 99.8% of the total mass of the celestial bodies in our solar system [28]. The Cartesian position $(x_{\mathrm{p}}, y_{\mathrm{p}}, z_{\mathrm{p}})$ is computed with the VSOP87 planetary theory.

Planets	*Mean* (km)	*Mass* (m_{Earth})	*a* (AU)
Mercury	1.13×10^5	0.05	0.4
Venus	6.17×10^5	0.81	0.7
Earth	9.24×10^5	1	1
Mars	5.79×10^5	0.11	1.5
Jupiter	4.83×10^7	318	5.2
Saturn	5.47×10^7	95	9.5
Uranus	5.17×10^7	14	19.8
Neptune	8.67×10^7	17	30

Table 3.1: The first column provides the averages of the radii of the planetary SOI. The second and third columns provide the values of the two parameters driven the size of the spheres of influence.

The concept of SOI is used in the patched-conic methods (Battin [2], Curtis [6]). The radii of the spheres of influence are assumed constant. Battin and Curtis assume that the orbits of the planets around the Sun are circular orbits due to their small eccentricities (given in the second column in Table 3.2). The square root in Equation 3.2 is considered to be equal to the mean radius of the planetary orbit around the Sun. In fact, the positions of the planets change in time. Therefore, the radii of the SOI also depend on time. Knowing the positions of the planets at any date gives flexibility to the propagator. The radii of SOI for the eight planets are computed over one orbit of these planets around the Sun. The averages of the radii are provided in the first column in Table 3.1. The two key parameters in Equation 3.2 are the distance separating the Sun from the considered planet and the planetary mass. Indeed, the sphere of influence consists of the region where the impact

of the planet on the spacecraft trajectory exceeds the impact of the Sun. The farther the planet is from the Sun the higher the radius of the sphere of influence is. Indeed, the primary attraction of the Sun decreases as the square of the distance. The outer planets are more massive and further from the Sun than the inner planets as can be seen in the third and fourth columns in Table 3.1. The masses are expressed on Earth masses and the semi-major axes are expressed in astronomical units. As a result, the radii of the sphere of influence for the outer planets (order of 10^7 km) are larger than those of the inner planets (order of 10^5 km).

Planets	*Standard deviation/Mean* (%)	*Eccentricities* (-)
Mercury	14	0.206
Mars	7	0.094
Saturn	4	0.056
Jupiter	3	0.049
Uranus	3	0.046
Earth	1.2	0.017
Neptune	0.6	0.011
Venus	0.5	0.007

Table 3.2: The first column provides the percentages of the standard deviations with respect to the mean radii of the spheres of influence. The second column provides the main parameter driven the standard deviations.

One can wonder about the need to use time-varying radii of the spheres of influence. This choice is driven by the computation of the standard deviations for the different radii of the SOI. The values are given in the first column in Table 3.2. The standard deviation represents up to 14% of the mean radius of Mercury. In fact, Mercury has the highest eccentricity which means the highest deviation from a perfect circular orbit. There is a direct relationship between the standard deviations and the eccentricities of the orbits as can be seen by comparing columns 1 and 2 in Table 3.2.

Planets	*mean (SOI) /a* (%)	SOI *radius* (body radii)
Mercury	0.2	46
Venus	0.6	101
Earth	0.6	145
Mars	0.3	171
Jupiter	6.2	675
Saturn	3.8	907
Uranus	1.8	2025
Neptune	1.9	3434

Table 3.3: The first column provides the percentages of the mean radii of the SOI compared to the semi-major axes. The second column provides the radii of the spheres of influence in planet radii.

The radii of the planetary spheres of influence are very large compared to their equatorial radii which mean view from the planets (second column in Table 3.3). In contrast, the radii of the spheres

of influence are very small at the scale of the solar system. The results are provided in the first column in Table 3.3. The radius of Jupiter's sphere of influence, which consists of the most massive planet, only represents 6% of its semi-major axis. The radii of the SOI are proportional to $\left(\frac{m_p}{m_s}\right)^{2/5}$ and therefore very small. As a result, an interplanetary spacecraft traveling from one planet to another spends most of its time outside the SOI.

3.2 Transformation between heliocentric and planetocentric coordinate systems

The planetocentric inertial coordinate systems defined in section 1.2.1 and in section 1.2.3 are suitable to describe the motion of spacecraft within the spheres of influence, whereas the heliocentric inertial coordinate system defined in section 1.2.2 is chosen to describe the motion of spacecraft outside the spheres of influence. A change of coordinate system is therefore needed when the spacecraft leaves or enters a sphere of influence. The case when a spacecraft enters a sphere of influence is considered. The other case is the reverse process of the one described below.

The starting point is the position and velocity of the spacecraft in the heliocentric inertial coordinate system at the SOI of a given planet denoted $\mathbf{r}^{\odot}_{\odot \mathrm{S}}$ and $\dot{\mathbf{r}}^{\odot}_{\odot \mathrm{S}}$. The symbols $\odot$ and S are respectively used for the Sun and the spacecraft. The subscript $\odot$ S means that the vector goes from the Sun's centre to the spacecraft's centre. The superscript refers to the orientation of the axes of the inertial coordinate system. The superscript $\odot$ denotes the orientation of the heliocentric inertial coordinate system axes in the considered case.

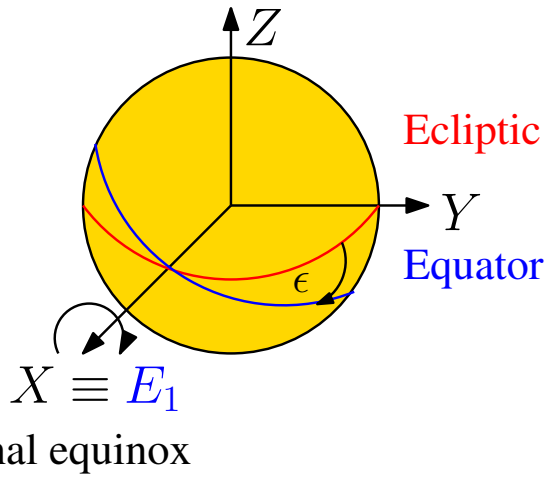

Figure 3.1: Rotation through an amplitude ϵ about the Vernal equinox to rotate the axes of the heliocentric coordinate system to the axes of the Earth coordinate system.

The International Astronomical Union provides the orientation of the axes of the planetocentric inertial coordinate systems with respect to the orientation of the axes of the Earth inertial coordinate system. They have been provided in section 1.2.3. The first transformation is therefore to rotate the axes of the heliocentric inertial coordinate system to the orientation of the EarthJ2000 axes. The origin of this new coordinate system is the Sun as in the heliocentric coordinate system. This is represented in Figure 3.1. Both coordinate systems share the Vernal equinox as reference

direction. A clockwise rotation about the Vernal equinox $\mathbf{R}_1(-\epsilon)$ is therefore performed, where $\epsilon = 23.439291111°$ represents the obliquity of the ecliptic with respect to the Earth's equator at J2000 epoch. Euler angles are chosen to relate coordinate systems. The Euler rotations $\mathbf{R}_1(\theta)$ and $\mathbf{R}_3(\theta)$ are respectively rotations about the x-axis and about the z-axis through an amplitude θ

$$\mathrm{R}_1(\theta) = \begin{bmatrix} 1 & 0 & 0 \\ 0 & \cos\theta & \sin\theta \\ 0 & -\sin\theta & \cos\theta \end{bmatrix}$$

$$\mathrm{R}_3(\theta) = \begin{bmatrix} cos\theta & \sin\theta & 0 \\ -\sin\theta & \cos\theta & 0 \\ 0 & 0 & 1 \end{bmatrix}$$

The coordinate systems used are all right-handed coordinate systems. The minus sign in front of ϵ comes from the fact that a clockwise rotation has a negative sign in this convention. This transformation and the following transformations are between inertial coordinate systems. Therefore, the same treatment can be applied to the positions and the velocities. No additional corrections are needed for the velocity as in the case of rotating coordinate systems. It should be recalled that the coordinate systems are pseudoinertial. An additional correction should be added. The corrections are neglected as proposed in GMAT [18]. The position and velocity vectors become

$$\mathbf{r}^{\mathrm{E}}_{\odot\,\mathrm{S}} = \mathbf{R}_1(-\epsilon)\mathbf{r}^{\odot}_{\odot\,\mathrm{S}} \tag{3.3}$$

$$\dot{\mathbf{r}}^{\mathrm{E}}_{\odot\,\mathrm{S}} = \mathbf{R}_1(-\epsilon)\dot{\mathbf{r}}^{\odot}_{\odot\,\mathrm{S}}, \tag{3.4}$$

where the superscript E means that the axes are those of the Earth inertial coordinate system. The second step is to translate the origin from the Sun's centre to the planet's centre. This operation is represented in Figure 3.2 for the position.

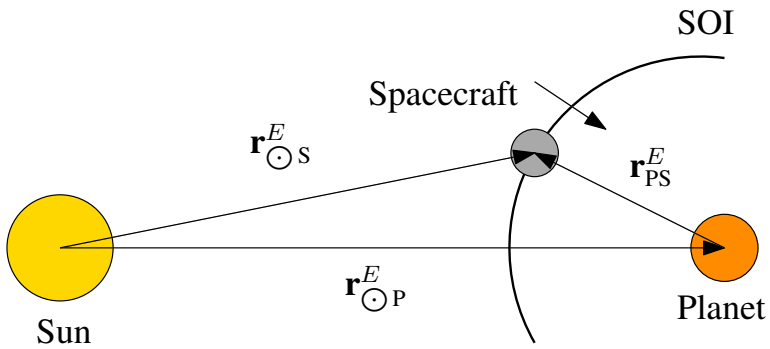

Figure 3.2: This figure represents the translation of the origin from the Sun's centre to the planet's centre. After the translation, the position of the spacecraft view from the planet $\mathbf{r}^{\mathrm{E}}_{\mathrm{PS}}$ is obtained. The superscript E means that the axes are those of the Earth inertial coordinate system.

The following relationships are deduced from this figure

$$\mathbf{r}^{\mathrm{E}}_{\mathrm{PS}} = \mathbf{r}^{\mathrm{E}}_{\odot\,\mathrm{S}} - \mathbf{r}^{\mathrm{E}}_{\odot\,\mathrm{P}} \tag{3.5}$$

$$\dot{\mathbf{r}}^{\mathrm{E}}_{\mathrm{PS}} = \dot{\mathbf{r}}^{\mathrm{E}}_{\odot\,\mathrm{S}} - \dot{\mathbf{r}}^{\mathrm{E}}_{\odot\,\mathrm{P}}. \tag{3.6}$$

The position and velocity of the target planet with respect to the Sun in the heliocentric inertial coordinate system $\mathbf{r}^{\odot}_{\odot\mathrm{P}}$ and $\dot{\mathbf{r}}^{\odot}_{\odot\mathrm{P}}$ are computed with the VSOP87 planetary theory developed in Chapter 2. The translation of the origin requires these position and velocity vectors to be expressed in a coordinate system whose axes are aligned with the Earth inertial coordinate system axes. The transformations 3.3 and 3.4 are therefore applied to obtain $\mathbf{r}^{\mathrm{E}}_{\odot\mathrm{P}}$ and $\dot{\mathbf{r}}^{\mathrm{E}}_{\odot\mathrm{P}}$. At this stage, the coordinate system is centred on the target planet and the axes are those of the Earth inertial coordinate system. The final transformation rotates these axes on the planetocentric inertial axes with the values provided by IAU. It consists of a combination of two rotations. This is represented in Figure 3.3. The first one is a counterclockwise rotation about the E_3-axis through an angle $\Omega = 90° + \alpha_0$ to rotate the Vernal equinox to the planetocentric I-axis, where Ω is the longitude of the planetocentric I-axis with respect to the Vernal equinox E_1 at J2000 epoch. The second rotation is also a counterclockwise rotation about the I-axis through an angle $90 - \delta_0$ to rotate the normal of the Earth's equator at J2000 E_3 to the K-axis of the planetocentric inertial coordinate system. α_0 and δ_0 are the right ascension and declination of the spin axis of the targeted planet with respect to the Earth inertial axes.

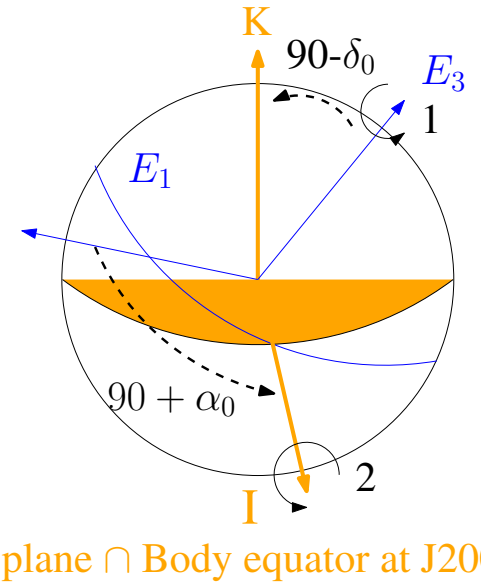

Figure 3.3: Transformation between the Earth and the planetocentric inertial coordinate system axes. E_1 and E_3 are the axes in the Earth's inertial coordinate system at J2000. E_1 represents the Vernal equinox and E_3 represents the normal to Earth's equator at the J2000 epoch. I and k are the axes of the planetocentric inertial coordinate system. The numbers 1 and 2 give the order of the rotations and the associated axes. The figure is inspired by [18].

The mathematical translation of this procedure is as follows [18]

$$\mathbf{r}^{\mathrm{P}}_{\mathrm{PS}} = \mathbf{R}_1(90° - \delta_0)\mathbf{R}_3(90° + \alpha_0)\mathbf{r}^{\mathrm{E}}_{\mathrm{PS}} \tag{3.7}$$

$$\dot{\mathbf{r}}^{\mathrm{P}}_{\mathrm{PS}} = \mathbf{R}_1(90° - \delta_0)\mathbf{R}_3(90° + \alpha_0)\dot{\mathbf{r}}^{\mathrm{E}}_{\mathrm{PS}}. \tag{3.8}$$

The transformation between heliocentric and planetocentric inertial coordinate systems is performed each time the spacecraft crosses a sphere of influence. The end of this section assesses the

accuracy of the procedure and validates the change between inertial coordinate systems. The General Mission Analysis Tool GMAT developed by NASA provides, at the end of a propagation, the final position and velocity of the spacecraft in the inertial coordinate systems of the eight planets and the Sun. Starting from the position and the velocity vectors in the heliocentric inertial coordinate system on 6 January 2000 12:00:00 TT, the change of coordinate systems are applied. The results are compared to the positions and velocities given by GMAT. The distance between the positions and velocities computed with IOP and GMAT are evaluated, as for planetary ephemerides, with

$$d_{\text{Pos}} = \|\mathbf{r}_{\text{IOP}} - \mathbf{r}_{\text{GMAT}}\| \tag{3.9}$$

$$d_{\text{Vel}} = \|\dot{\mathbf{r}}_{\text{IOP}} - \dot{\mathbf{r}}_{\text{GMAT}}\|. \tag{3.10}$$

The change of coordinate systems defined above consists of three steps. A distance of 10^{-3} m and 10^{-10} m/s are respectively found for the distance between positions and velocities in the two steps involving rotations. Indeed, new positions and velocities are obtained after a rotation. Therefore, Equation 3.9 and Equation 3.10 can be applied to compute the distances between positions and velocities obtained with IOP and GMAT. The small differences are due to numerical errors. The positions and velocities of the planets are computed with the VSOP87 planetary theory during the translation of the origin between the Sun's centre and planets' centre. This introduces an error directly linked to the error on the ephemerides. The errors in the translations are given in Table 3.4. These values are close to the errors obtained between VSOP87 planetary theory and DE405 on 6 January 2000 12:00:00 TT. It has to be stressed that, at the specific chosen date, the error on the velocity of Saturn is close to its maximum in Appendix B.1 (26 m/s), whereas the error on the position of Neptune is close to its minimum in Table 2.2 (11,062 km). In contrast, the error on the position of Mercury is close to its mean value in this table (281 km). As a result, an error is added each time the spacecraft enters or leaves a sphere of influence. This highlights the importance to develop accurate ephemerides. If the ephemerides of the eight planets are extracted from the CNES website with the DE405 planetary theory at the chosen date, a maximum difference of 6 km is found. To sum up, the way to minimize the errors on the change of coordinate system is to couple the propagator with an integrated ephemeris as carried out in GMAT.

Planets	*Errors between positions* (km)	*Errors between velocities* (m/s)
Mercury	278	0.05
Venus	233	1.16
Earth	9,010	12
Mars	6,507	1.64
Jupiter	93,085	16
Saturn	291,741	25
Uranus	126,864	19
Neptune	14,075	12

Table 3.4: Errors in the change of coordinate systems: translation operation. The distances between the positions obtained with IOP and GMAT are provided in the first column. The second column contains the distances between velocities.

3.3 Leave a sphere of influence

Consider a spacecraft on an orbit escaping a given planet. The aim of this section is to define a condition allowing the propagator to detect when the spacecraft crosses the sphere of influence from inside to outside. At this moment, the change between planetocentric and heliocentric inertial coordinate systems is performed. The events are used to detect this condition. An event consists of writing a function. This function is evaluated at each time of the integration and the integration stops when the value of the specified function changes of sign. In the case of a spacecraft leaving a sphere of influence, the function can be expressed as

$$value = \sqrt{x^2 + y^2 + z^2} - R_{\text{SOI}}^{\text{P}}, \tag{3.11}$$

where (x,y,z) stands for the position of the spacecraft in the planetocentric inertial coordinate system and $R_{\text{SOI}}^{\text{P}}$ stands for the radius of the sphere of influence computed with Equation 3.2. The representation of a spacecraft on an orbit leaving a sphere of influence is represented in Figure 3.4. At the beginning of the propagation, the spacecraft is located close to the planet so that $\sqrt{x^2 + y^2 + z^2} < R_{\text{SOI}}^{\text{P}}$ and the value is negative. The norm of the position increases during the propagation due to the fact that the spacecraft goes away from the planet. The blue line representing the surface of the sphere of influence in Figure 3.4 moves slightly during the propagation depending on the position of the considered planet with respect to the Sun. Indeed, the radius of the sphere of influence changes in time. Condition 3.11 is evaluated at each time of the integration and the integration stops when the value becomes positive or equal to 0. $\sqrt{x^2 + y^2 + z^2} - R_{\text{SOI}}^{\text{P}} = 0$ represents the equation of a sphere centred on the planet and with a radius equal to the radius of the sphere of influence at the specific date. A change of coordinate between the planetocentric inertial coordinate system of the planet the spacecraft is leaving and the heliocentric inertial coordinate system is performed at the end of the integration. These new position and velocity vectors are used as initial conditions to integrate the spacecraft equations of motion in the heliocentric inertial coordinate system.

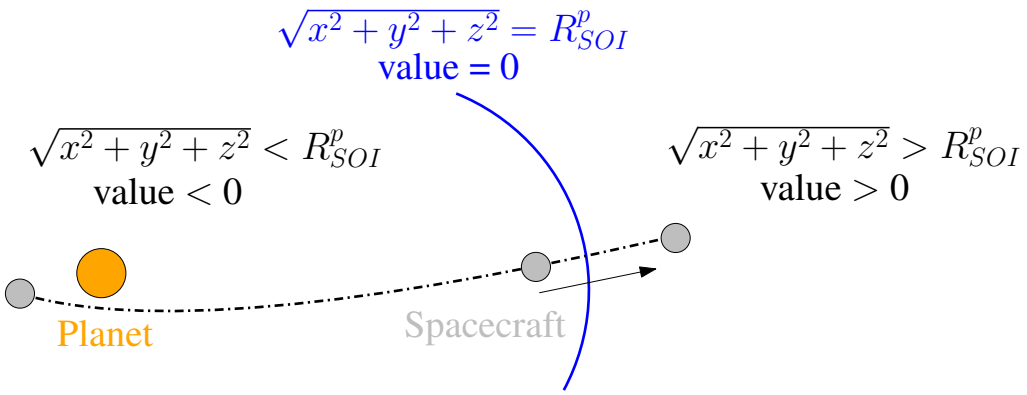

Figure 3.4: Illustration of the condition: leave a sphere of influence.

3.4 Enter a sphere of influence

The problem differs in the case of a spacecraft entering a sphere of influence. The spacecraft is located outside the spheres of influence of the eight planets and could possibly enter any spheres of

influence. Entering a sphere of influence occurs when

$$value = \sqrt{(x - x_{\mathrm{p}})^2 + (y - y_{\mathrm{p}})^2 + (z - z_{\mathrm{p}})^2} - R^{\mathrm{P}}_{\mathrm{SOI}} \tag{3.12}$$

becomes negative where (x_{p},y_{p},z_{p}) is the position of the planet in the heliocentric inertial coordinate system at the current date and (x,y,z) is the position of the spacecraft in the heliocentric inertial coordinate system. At each time of the integration, Condition 3.12 is evaluated for the eight planets of the solar system until a detection of an event occurs. $\sqrt{(x - x_{\mathrm{p}})^2 + (y - y_{\mathrm{p}})^2 + (z - z_{\mathrm{p}})^2} - R^{\mathrm{P}}_{\mathrm{SOI}} = 0$ represents the equation of a sphere centred on the planet's centre and with a radius $R^{\mathrm{P}}_{\mathrm{SOI}}$. At this stage, a change of coordinate is performed between the heliocentric inertial coordinate system and the planetocentric inertial coordinate system of which the spacecraft is entering the sphere of influence. Validations are needed to evaluate if the propagator is able to detect a spacecraft leaving or entering a sphere of influence. For the condition 'leave a sphere of influence', the spacecraft is put on an escape orbits and one checks if the propagator detects the event correctly. This procedure is repeated for each planet. A rendezvous with a specific planet has to be implemented to test the condition: enter a sphere of influence. Given the position of the departure planet at a specific date and the position of a target planet at the arrival date, a routine is implemented to compute the corresponding spacecraft trajectory. A routine is implemented to intercept a chosen planet at a specified date. The event does not know the planet chosen and should be able to detect the crossing of the SOI of the target planet. This problem is Lambert's problem.

3.4.1 Lambert's problem

Lambert's problem is addressed in this section. Given two position vectors $\mathbf{r}_1$ and $\mathbf{r}_2$, and the transfer time between these two positions t_T, Lambert's problem allows the propagator to compute the orbit connecting the two positions vectors as well as the initial and final velocity vectors. The unknown quantities are represented in blue in Figure 3.5. In the thesis, Lambert's problem is used to test the condition: enter a sphere of influence, design interplanetary trajectories to study the perturbations in the following chapter and to recreate the Cassini-Huygens mission in Chapter 5.

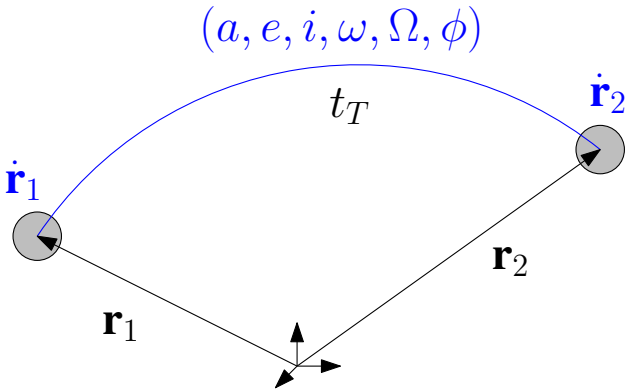

Figure 3.5: Inputs (black) and unknown quantities (blue) of Lambert's problem.

Only the primary attractions of the central bodies are considered in Lambert's problem. Universal variables are used to solve this problem. Universal variables are defined in Curtis [6] and in Vallado [24]. These variables are not specific to the shape of a given orbit. It enables us to develop a general algorithm valid for all types of transfer orbits (ellipse, hyperbola,...). The procedure followed

has been proposed by Bate, Mueller and White (1971). It is provided in Curtis [6]. The procedure uses a Newton-Raphson iterative algorithm. The algorithm has been validated with numerical examples given in Curtis [6] for both types of orbit (ellipse, hyperbola). In fact, there are plenty of algorithms to solve Lambert's problem. The method implemented in IOP is compared to three classical algorithms to assess the accuracy of the selected method: Lambert's minimum-energy, Gauss's solution and Universal-variable algorithm proposed by Battin [2]. The following test case proposed in Vallado [24] is considered. The spacecraft orbits the Earth. The two positions vectors are: $\mathbf{r}_1$ = 15,945.34 $\mathbf{E}_1$ and $\mathbf{r}_2$ = 12,214.83899 $\mathbf{E}_1$ + 10,249.46731 $\mathbf{E}_2$. The transfer time is 76 min. The aim is to compare the values of the initial and final velocities found with the different methods. The results are provided in Table 3.5. The method proposed by Battin retrieves the "exact solution". The term exact solution should be defined. It consists of the Lambert's universal method defined in Vallado [24]. This method uses a bisection technique instead of a Newton-Raphson algorithm. The solution obtained after 25 iterations is assumed to be the exact solution. A slight difference appears between the exact solution and IOP. The two other methods exhibit higher gap with the exact solution. The accuracy of the algorithm is sufficient to design interplanetary trajectories and to test the condition: enter a sphere of influence.

Methods	*Velocities*	$\mathbf{E}_1$-component (km/s)	$\mathbf{E}_2$-component (km/s)	$\mathbf{E}_3$-component (km/s)
Exact	V_1	2.058913	2.915965	0
Battin	V_1	2.058913	2.915965	0
IOP	V_1	2.058913	2.915964	0
Gauss's original	V_1	2.058925	2.915956	0
Minimum-energy	V_1	2.047409	2.924003	0
Exact	V_2	-3.451565	0.910315	0
Battin	V_2	-3.451565	0.910315	0
IOP	V_2	-3.451565	0.910314	0
Gauss's original	V_2	-3.451569	0.910301	0
Minimum-energy	V_2	-3.447919	0.923867	0

Table 3.5: Comparison between IOP and three algorithms: Lambert minimum-energy, Gauss's solution and Universal-variable algorithms proposed by Battin. The differences between IOP and the exact solution are highlighted in blue.

3.4.2 Three-dimensional patched conic method

The three-dimensional patched conic method considers that the spacecraft starts at the centre of the departure planet in the heliocentric inertial coordinate system. It means that the portion of the trajectory within the sphere of influence of the departure planet is replaced by a trajectory in the heliocentric inertial coordinate system. As seen in section 3.1, the spheres of influence are points on the scale of the solar system. Therefore, the part within the spheres of influence can be safely replaced by a heliocentric path for long propagation outside the spheres of influence. The spacecraft joins the arrival planet in a transfer time t_{transfer}. The three elements needed to design a trajectory with Lambert's problem are gathered. The initial position is the departure planet at the time t_{init}, the transfer time is t_{T} and the final position is the arrival planet at the time t = t_{init} + t_{T}.

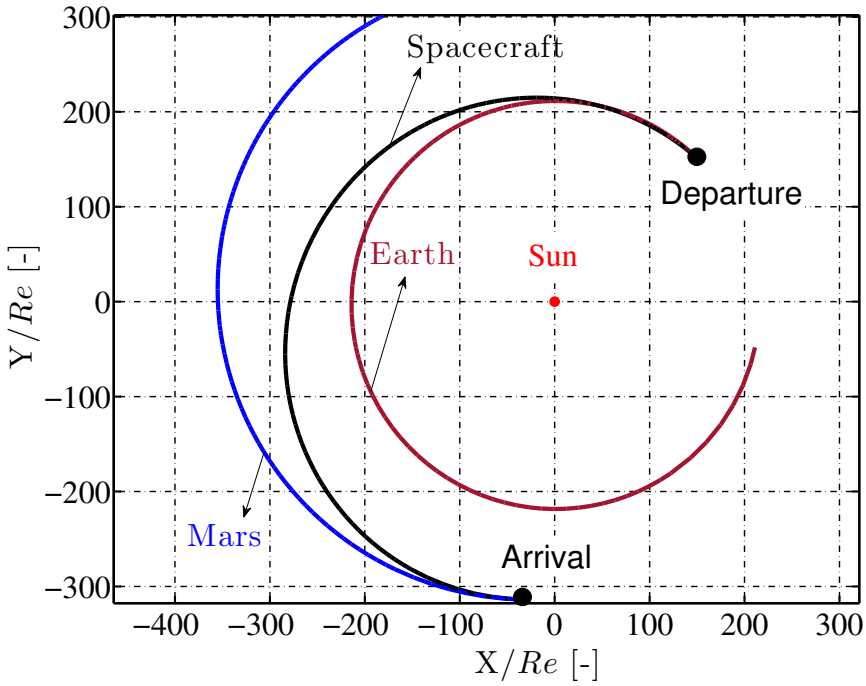

Figure 3.6: Lambert's problem. The departure planet is the Earth, and the arrival planet is Mars. The departure date is on 7 November 1996 TT and the arrival on 12 September 1997 TT.

One of the aim of designing such a trajectory is to confirm that the propagator is able to detect the condition: enter a sphere of influence. The case of a spacecraft traveling between the Earth and Mars in 309 days is chosen. The departure date is on 7 November 1996 TT and the arrival date on 12 September 1997 TT. In Figure 3.6, the spacecraft leaves the trajectory of the Earth (red) and intercepts the Mars's orbit (blue). The transfer orbit is an ellipse with the Sun at one of the foci. The x-axis and y-axis are expressed in dimensionless variables in the heliocentric inertial coordinate system. R_e is the photosphere radius of the Sun. IOP detects that the spacecraft crosses the sphere of influence of Mars. At this stage, the change of coordinate system between the heliocentric and Mars inertial coordinate system is performed. The norm of the initial position in the Mars inertial coordinate system is 5.56×10^5 km, which is 0.5 m within the sphere of influence at this specific date. The routine has been tested for any departure and arrival planets.

The properties of the sphere of influence have been discussed in this chapter. The sizes of the SOI are small at the scale of the solar system, but they are large view of the planets. It has been shown that an error linked to planetary ephemerides is added each time a change of coordinate system occurs. These errors can be significant. The following chapter introduces the different perturbations acting on the spacecraft. Up to now, only the motion due to the primary attractions of the central bodies has been considered.

Chapter 4

Perturbations

The objective of this chapter is to improve the fidelity of the propagation by taking into account the perturbations acting on the spacecraft. Perturbations induce deviations from the idealized two-body motion. Up to now, the motion of spacecraft is only due to the primary attraction of its associated central body. The primary attraction consists of the central body gravitational attraction modelled as a perfect sphere. The term perturbation comes from its small magnitude compared to the primary attraction[1]. However, as shown throughout the chapter, the perturbations impact the spacecraft trajectories significantly and should be taken into account to obtain realistic propagation.

The chapter is divided into four sections. The first section defines the general form of the perturbed equations of motion. The second and third sections discuss the perturbations acting on the spacecraft within and outside the spheres of influence. The chapter concludes with the possible solutions to improve the fidelity of the propagation.

4.1 Perturbed equations of motion: general form

The equations of the relative motion between the spacecraft and the central body are given by Vallado [24]

$$\ddot{\mathbf{r}} = -\frac{\mu}{r^3}\mathbf{r} + \mathbf{a}_{\text{perturbed}}, \tag{4.1}$$

where $\ddot{\mathbf{r}}$ stands for the acceleration vector, μ [km^3/s^2] stands for the gravitational parameter of the central body, $\mathbf{r}$ stands for the position vector and r stands for the norm of the position vector. The first term, $-\frac{\mu}{r^3}\mathbf{r}$, represents the primary attraction of the central body. The second term, $\mathbf{a}_{\text{perturbed}}$, represents perturbations.

All the equations of motion used in this chapter are written in dimensionless form. The characteristic time τ [s] and length λ [km] are introduced in that context. They are defined as

$$\tau = \sqrt{\frac{R_{\text{e}}^3}{\mu}}\ ;\ \lambda = R_{\text{e}}, \tag{4.2}$$

[1]The atmospheric drag constitutes an exception. This perturbation is able to deorbit a spacecraft at very low altitude ($\approx$ 100 km for the Earth). It is not considered in the thesis.

where R_e [km] stands for the equatorial radius of the central body. The equatorial radii and gravitational parameters are given in Appendix A.1. The values come from GMAT. The following dimensionless quantities are obtained

$$\tilde{\mathbf{r}} = [\tilde{x};\tilde{y};\tilde{z}]^T = \frac{\mathbf{r}}{\lambda} ; \tilde{t} = \frac{t}{\tau} ; \frac{d}{d\tilde{t}} = \tau\frac{d}{dt} ; \frac{d^2}{d\tilde{t}^2} = \tau^2\frac{d^2}{dt^2}, \tag{4.3}$$

where $\tilde{\mathbf{r}}$ stands for the dimensionless position vector and $\tilde{t}$ stands for the dimensionless time. The other quantities are the dimensionless derivatives.

An accurate orbit propagation requires the numerical integration of Equation 4.1. The equations are integrated in the inertial coordinate systems to avoid taking into account the additional contributions due to a rotating coordinate system. The user provides six keplerian elements $(a, e, i, \omega, \Omega, \phi)$ as initial conditions. The initial keplerian elements are first converted into initial Cartesian position and velocity vectors. Then, using the characteristic variables, the dimensionless initial conditions are obtained with

$$\tilde{\mathbf{r}}_0 = \mathbf{r}_0/\lambda \tag{4.4}$$
$$\tilde{\dot{\mathbf{r}}}_0 = \dot{\mathbf{r}}_0 \times \tau/\lambda. \tag{4.5}$$

4.2 Motion within the spheres of influence

The aim of this section is to build the models of the dimensionless J_2 perturbation $\mathbf{a}_{J2}$, dimensionless point mass gravity perturbations $\mathbf{a}_{\text{PMG}}$ and dimensionless solar radiation pressure perturbation $\mathbf{a}_{\text{SRP}}$ within the spheres of influence. The total perturbation $\mathbf{a}_{\text{perturbed}} = \mathbf{a}_{J2} + \mathbf{a}_{\text{PMG}} + \mathbf{a}_{\text{SRP}}$ within the SOI. The validation of these models is performed and the results are discussed.

4.2.1 J_2 perturbation

The planets are not perfect spheres as supposed in the two-body assumption. Several contributions must be added to the primary attraction of the central body to model the exact form of its gravitational field.

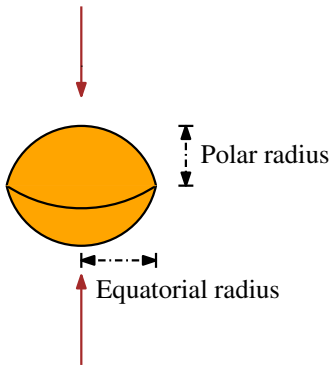

Figure 4.1: Shape of the planets taking into account the flattening of the poles.

Among these contributions, the J_2 perturbation is much higher than the other contributions. For example, it is respectively at least three and two orders of magnitude higher than the other

gravitational contributions in the case of the Earth and Mars (GMAT [18], Vallado [24]). In fact, IOP only includes the J_2 contribution in addition to the primary attraction of the planets to model their gravitational fields. The impact of this choice will be discussed in section 4.4. Indeed, this section is devoted to the perturbations that are not taken into account in IOP.

Planets	*Oblateness* (-)
Venus	0.000
Mercury	0.000
Earth	0.003353
Mars	0.00648
Neptune	0.01708
Uranus	0.02293
Jupiter	0.06487
Saturn	0.09796

Table 4.1: Planetary Oblatenesses in increasing order of magnitude. The values come from [6].

The J_2 contribution comes from the flattening of the poles. Instead of being spheres, the planets look like oblate spheroids. The resulting shape is shown in Figure 4.1. The oblateness is introduced to characterize the planetary flattening of the poles. This coefficient equals 0 for a perfect sphere. The oblatenesses of the different planets are provided in Table 4.1. It is defined by Curtis [6]

$$\text{Oblateness} = \frac{\text{Equatorial radius} - \text{Polar radius}}{\text{Equatorial radius}}. \tag{4.6}$$

For example, the Earth possesses an oblateness of 0.003353. The positive sign means that its equatorial radius is higher than its polar radius. The contribution of J_2 to the perturbed vector, $\mathbf{a}_{\text{perturbed}}$, is

$$\mathbf{a}_{J2} = \frac{3J_2}{2\tilde{r}^4}\left[\frac{\tilde{x}}{\tilde{r}}\left(5\frac{\tilde{z}^2}{\tilde{r}^2}-1\right)\mathbf{I} + \frac{\tilde{y}}{\tilde{r}}\left(5\frac{\tilde{z}^2}{\tilde{r}^2}-1\right)\mathbf{J} + \frac{\tilde{z}}{\tilde{r}}\left(5\frac{\tilde{z}^2}{\tilde{r}^2}-3\right)\mathbf{K}\right], \tag{4.7}$$

where **I**, **J** and **K** stand for the principal directions in the planetocentric inertial coordinate system defined in section 1.2, $\tilde{\mathbf{r}} = [\tilde{x};\tilde{y};\tilde{z}]^T$ stands for the dimensionless position vector of the spacecraft in this coordinate system and J_2 represents the dimensionless coefficient taking into account the effects of the flattening of the poles. This coefficient is deduced from observations of spacecraft motions in the planetary gravitational fields. The J_2 coefficients are summarized in Table 4.2. They are ordered in increasing J_2 coefficients. For a solid spheroid rotating about its axis of symmetry, the J_2 coefficient is computed by [19]

$$J_2 = \frac{2}{3}\text{Oblateness} - \frac{\omega_{\text{P}}^2 R_{\text{e}}^3}{\mu}, \tag{4.8}$$

where ω_{P} is the angular rotational velocity. Therefore, J_2 is directly linked to the oblateness as can be seen by comparing Table 4.1 and Table 4.2.

Planets	J_2 (-)
Venus	2.7×10^{-5}
Mercury	6.0×10^{-5}
Earth	1.1×10^{-3}
Mars	2.0×10^{-3}
Neptune	4.0×10^{-3}
Uranus	1.2×10^{-2}
Jupiter	1.5×10^{-2}
Saturn	1.6×10^{-2}

Table 4.2: Truncated planetary J_2 coefficients. The values come from Vallado [24].

Two cases are differentiated. If the initial semi-major axis a is positive and the initial eccentricity e smaller than 1, the resulting orbit consists of a nearly closed orbit around the considered planet. This type of orbit has been described in the case of the International Space Station ISS in a previous report[2]. The impact of the J_2 perturbation on all the orbital elements are discussed. A propagation lasting one day was considered. The J_2 perturbation has been validated with the S3L propagator developed by the University of Liège in this report. A distance of 1.07 m has been found between the final positions after one day of propagation.

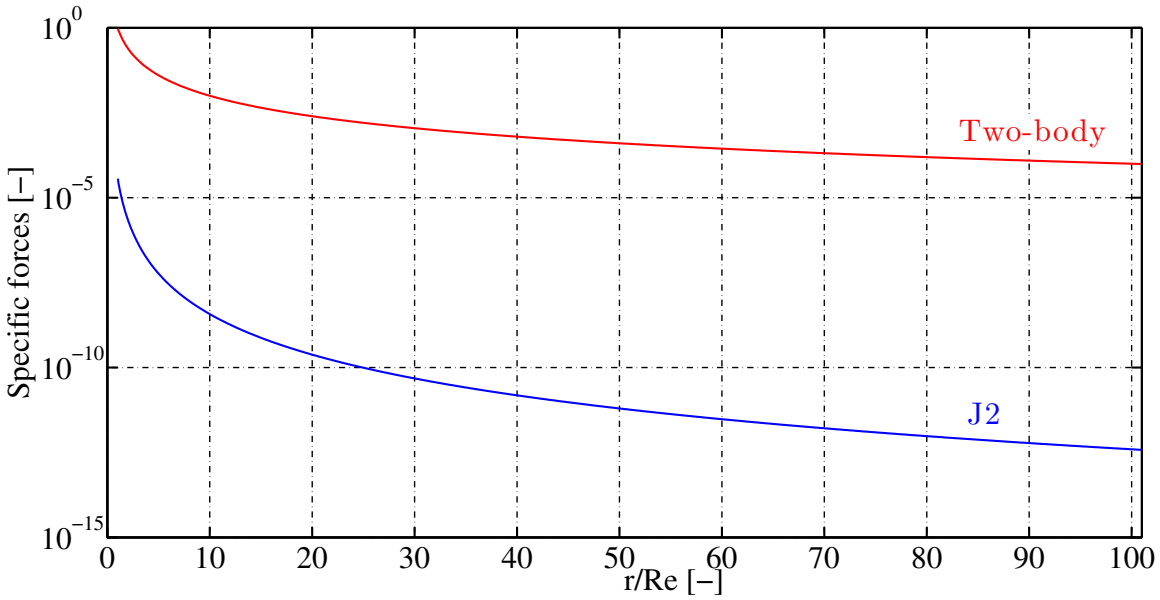

Figure 4.2: The figure represents the evolution of the dimensionless two-body and J_2 specific forces in the case of spacecraft trajectories escaping Venus. The evolution is valid for any orbits escaping Venus. The dimensionless position and specific forces are obtained with the Venus equatorial radius R_e and its gravitational parameter.

[2]CAMBERLIN Loïc, Pichâ Thibault, *Orbital propagator*, Astrodynamics course, November 2017.

The second case consists of a negative semi-major axis and an eccentricity higher than 1. It means that the spacecraft is located on an orbit escaping the considered planet. This type of orbit is needed to design interplanetary missions. The case of Venus is selected. The aims are to prove that the J_2 perturbation can be turned off outside the spheres of influence and to explain the point mass gravity assumption. The evolution of the dimensionless two-body and J_2 specific forces are represented in Figure 4.2. The y-axis is in logarithmic scale. Logarithmic scales are used for data that cover different orders of magnitude and to demonstrate some power-law scaling in the thesis. The x-axis represents the dimensionless distance measured from the centre of Venus. The curves stop when the spacecraft crosses the sphere of influence. It happens close to 101 Venus's radii which correspond to the mean radii of the SOI computed in the previous chapter. The magnitude of the flattening of the poles perturbation in Equation 4.7 is proportional to the J_2 coefficient. The dimensionless primary attraction, $-\frac{\tilde{\mathbf{r}}}{\tilde{r}^3}$, is proportional to 1. As a result, the starting value of the specific forces differ from about 5 orders of magnitude in Figure 4.2. Indeed, the Venus J_2 coefficient is 2.7×10^{-5}. The J_2 specific force decreases drastically when the spacecraft moves away from Venus. More specifically, it decreases as $1/r^4$. The J_2 specific force is only 0.15% with respect to its initial value at $5\times R_{\mathrm{e}}$ of Venus. The two-body attraction decreases more slowly with an inverse square law. The magnitude of the flattening of the poles perturbation at the end of the propagation in Figure 4.2 is very small compared to the two-body attraction. It is about 8 orders of magnitude smaller. A similar result is found for the seven remaining planets. Therefore, the J_2 perturbation is turned off outside the spheres of influence. Its contribution is not taken into account for the motion of spacecraft outside the SOI explained in the second section of this chapter.

The situation differs for the primary attractions. Their magnitudes still affect significantly the spacecraft trajectories outside the spheres of influence. As a result, the contributions of the planets and the Sun primary attractions are turned on everywhere in the solar system. The next perturbation within the spheres of influence comes from the gravitational attractions of the planets other than the central body, and the Sun. As explained above, the flattening of the poles perturbation, which constitutes the main departure from the primary gravitational attraction, can be neglected outside the spheres of influence. Therefore, the gravitational attractions of the other planets, and the Sun can be modelled as point mass gravity attractions without lost of accuracy. Indeed, according to the Newton's Shell Theorem [30], a spherically symmetric body affects external objects gravitationally as though all of its mass were concentrated at a point at its centre.

4.2.2 Point Mass Gravity perturbations

The perturbed motion of the spacecraft arising from the point mass gravity (PMG) perturbations of the Sun and the eight planets is studied. The contribution of point mass gravity perturbations to the perturbed vector, $\mathbf{a}_{\text{perturbed}}$, is

$$\mathbf{a}_{\text{PMG}} = \frac{1}{\mu}\sum_{k}\mu_{\text{k}}\times\left(\frac{\overbrace{\tilde{\mathbf{r}}_{\text{k}}-\tilde{\mathbf{r}}}^{Direct\ term}}{\|\tilde{\mathbf{r}}_{\text{k}}-\tilde{\mathbf{r}}\|^3}-\frac{\overbrace{\tilde{\mathbf{r}}_{\text{k}}}^{Indirect\ term}}{\|\tilde{\mathbf{r}}_{\text{k}}\|^3}\right), \tag{4.9}$$

where $\tilde{\mathbf{r}}$ and $\tilde{\mathbf{r}}_{\text{k}}$ stand respectively for the spacecraft and the k^{th} point mass dimensionless position vectors in the planetocentric inertial coordinate system associated to the central body. μ_k stands for the gravitational parameter of the k^{th} point mass. The subscript k denotes the seven planets

other than the central body and the Sun. Knowing planetary ephemerides and using the change of coordinate systems between heliocentric and planetocentric coordinate systems, the point mass gravity perturbations can be taken into account. The bracket in Equation 4.9 contains two terms. The first term is the direct term[3]. It takes into account the gravitational impact of the k^{th} celestial body on the spacecraft. The second term is the indirect term[4]. It takes into account the force of the k^{th} celestial body on the central body. This force changes the position of the central body which affects the specific force acting on the spacecraft.

The subsection is divided into two parts. The first part studies the contributions of the different PMG perturbations on orbits escaping the central body. The second part discusses the impact of the Sun point mass gravity perturbation on the orbital elements.

Escape orbits

Orbits escaping the planets are chosen to study the contributions of the different PMG perturbations on spacecraft trajectories. More specifically, the aim is to understand which celestial bodies contribute the most to the spacecraft trajectories in the different spheres of influence. The initial orbital elements of escape orbits have to be defined. All interplanetary trajectories start from a parking orbit. A departure hyperbola starting from a typical parking orbit of the Earth is defined. This test case is thereafter transposed to the other planets. The objective is to avoid multiplying the test cases. First, the eccentricity is higher than 1 to escape the planets. An eccentricity of 1.1 is arbitrarily selected. A parking orbit with an altitude of 166 km is chosen. This altitude was used for Apollo 16 and Apollo 17 lunar missions.

Planets	*Semi-major axis* (km)
Mercury	-26,057
Venus	-62,179
Earth	-65,441
Mars	-35,630
Jupiter	-716,580
Saturn	-604,340
Uranus	-257,250
Neptune	-254,350

Table 4.3: Initial semi-major axes.

The periapsis radius r_{p} of the departure hyperbola is equal to R_{e}+166 km. Indeed, the escape orbit starts at the periapsis of the hyperbola. It also means that the initial true anomaly is equal to 0. The periapsis radius varies from one planet to another in function of their equatorial radii. Knowing the periapis radius and the eccentricity, the semi-major axis can be extracted from

$$r_{\text{p}} = a(1 - e). \tag{4.10}$$

[3]The notation comes from GMAT [18].
[4]The notation comes from GMAT [18].

The initial semi-major axes are summarized in Table 4.3. Kennedy Space Centre is one of the typical launch sites on Earth. Its latitude is 28.5°. The inclination of the possible orbits admits as lower bound the latitude of the launch site. Therefore, the inclination of the orbit cannot be smaller than 28.5°. The classical range of inclination associated with Kennedy Space Centre is between 28.5° and 52.5° [29]. An inclination of 28.5° is chosen. The last two orbital elements consist of the argument of periapsis and the longitude of the ascending nodes. They are arbitrarily chosen to 5°.

The propagation lasts one day. The duration is not too long to prevent the spacecraft from crossing the spheres of influence. In this case, the change of coordinate system is performed and the error discussed in section 3.2 is added to the global error. The aim of this section is to study the point mass gravity perturbations. Therefore, only the errors linked to these gravitational perturbations are of interest. A statistical analysis is performed to obtain general results. The dates from 1 January 1900 12:00:00 TT to 1 January 2050 12:00:00 TT are swept out with a time step of five years. For each of these dates, a propagation of one day is performed and the contributions associated with each of the celestial bodies are computed. A statistical analysis is needed due to the fact that the contributions of the different celestial bodies depend on their time-varying positions in the solar system as can be seen in Equation 4.9.

The first test case is Mercury. The averages of the point mass gravity contributions are dominated by the Sun. Indeed, the Sun represents 99.99% of the total point mass gravity perturbations. How to explain this fact? The driven parameters of the point mass perturbations are the gravitational parameters μ_k, and the distances between the spacecraft and the celestial bodies. The higher the gravitational parameter is, the higher the point mass gravity perturbation is. The gravitational parameters are defined as the product of the universal gravitational constant and the masses. The universal gravitational constant being the same for all the celestial bodies, the key parameters are the masses. Table 4.4 provides in decreasing order of magnitude the gravitational parameters. These values are truncated values. As written in section 3.1, the mass of the Sun represents 99.8% of the total mass in the solar system. As a result, its gravitational parameter is much larger than the other gravitational parameters. This, coupled with the fact that Mercury is the closest planet to the Sun explains its major contribution. Indeed, the smaller the distance between the celestial body and the spacecraft is, the higher its contribution is.

Celestial bodies	μ (km^3/s^2)
Sun	1.3×10^{11}
Jupiter	1.3×10^{8}
Saturn	3.8×10^{7}
Neptune	6.8×10^{6}
Uranus	5.8×10^{6}
Earth	4.0×10^{5}
Venus	3.2×10^{5}
Mars	4.3×10^{4}
Mercury	2.2×10^{4}

Table 4.4: Truncated gravitational parameters of the eight planets and the Sun.

If the Sun is removed from the problem, the averages of the contributions of the planetary PMG perturbations are given in Figure 4.3. The first planetary contributor is Jupiter in Table 4.4. Its mass is one thousand times smaller than the Sun, but it is larger than the masses of the other planets. Figure 4.3 shows that, even if Jupiter is located far from Mercury, it constitutes the main contributor due to its large mass. The two other notable contributors are Venus and the Earth. These two planets do not possess the higher gravitational parameters. The reason comes from their close proximity to Mercury. The remaining planets contribute to a negligible extent. Indeed, Mars possesses one of the smallest gravitational parameters and the outer planets are located far to Mercury.

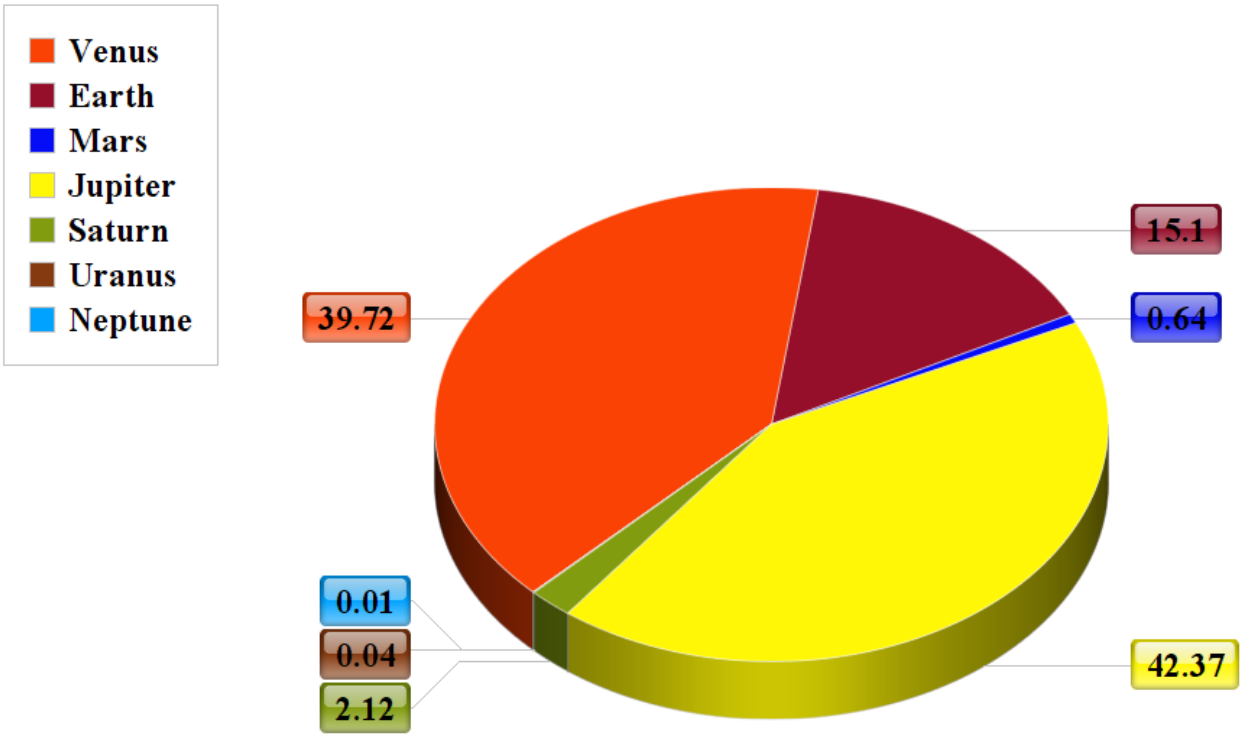

Figure 4.3: The central body is Mercury. Escape orbits are considered. The dates from 1 January 1900 12:00:00 TT to 1 January 2050 12:00:00 TT are swept out with a time step of five years. For each of these dates, a propagation of one day is performed. The figure provides the averages of the contributions of point mass gravity perturbations if the Sun is removed from the computations.

What is the contribution of the Sun if an orbit escaping the farthest planet from the Sun, Neptune, is chosen? Its contribution decreases to 99.85%, but it still dominates the other PMG perturbations. Figure 4.4 is obtained if the Sun is removed. Jupiter constitutes the main contributor as in the previous case. The difference with Mercury comes from the fact that the outer planets become the major planetary contributors whereas the effects of the inner planets become negligible.

In light of these results, one could wonder about the impact of the planetary point mass gravity perturbations on the spacecraft trajectories within the SOI. The ideal case is chosen to highlight the results. The central body is Mars, which is the planet located the closest to Jupiter. The two previous pie charts provide the average contributions of the different planets. In fact, the current percentages depend on the distances between the central body and the other bodies. If the departure

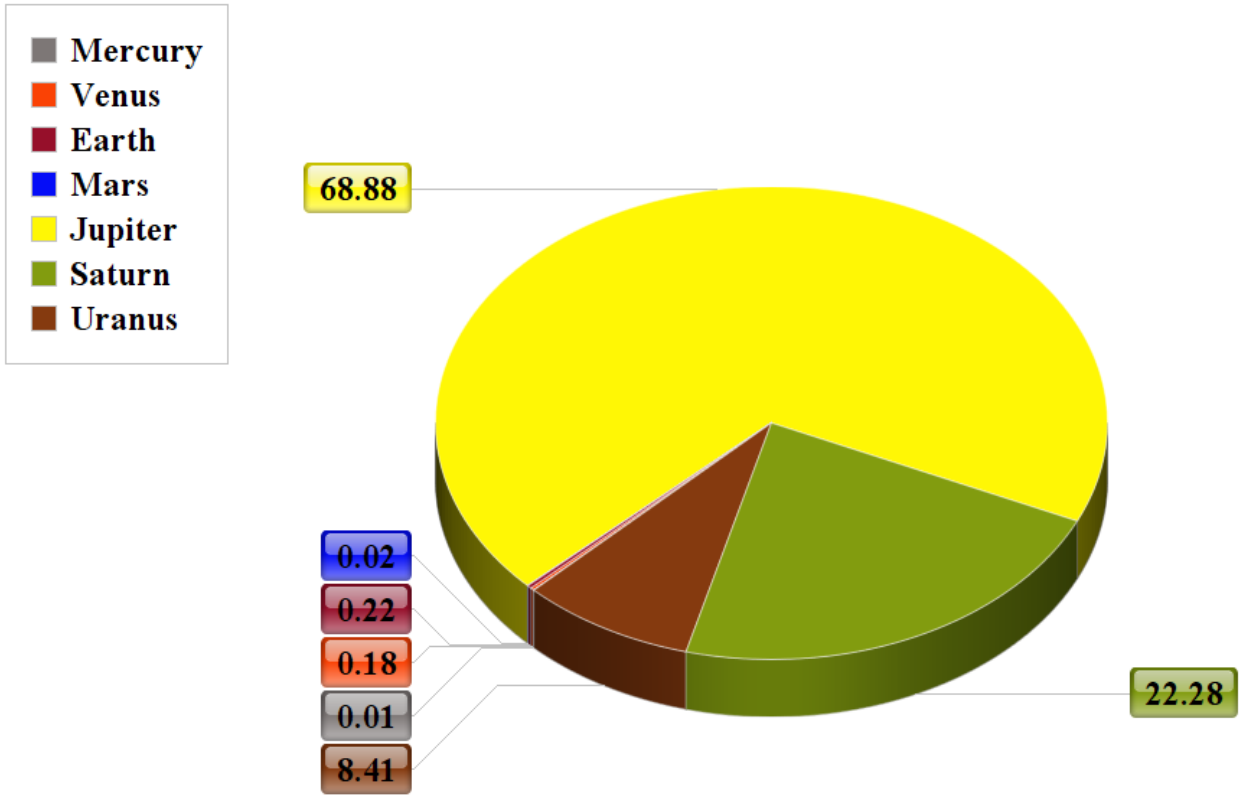

Figure 4.4: The central body is Neptune. Escape orbits are considered. The dates from 1 January 1900 12:00:00 TT to 1 January 2050 12:00:00 TT are swept out with a time step of five years. For each of these dates, a propagation of one day is performed. The figure provides the averages of the contributions of point mass gravity perturbations if the Sun is removed from the computations.

date is on 1 January 2045 12:00:00 TT, the distance between Jupiter and Mars is minimum and the PMG perturbation of Jupiter is therefore maximum. One focuses on the final position and velocity of the spacecraft after four days of propagation. This duration is close to the location where the spacecraft crosses Mars SOI. GMAT is used as reference. The primary attraction of Mars as well as the point mass gravity perturbations of the seven remaining planets are taken into account in GMAT. If only the primary attraction of Mars is included in IOP, the final positions and velocities computed with GMAT and IOP differ respectively of 8 m and 6 $\times 10^{-5}$ m/s. Even in a situation where the impacts of the PMG perturbations are maximized, the effects on the spacecraft trajectory within a sphere of influence are small. As a result, the planetary point mass perturbations should be taken into account only if a high-fidelity propagation is needed. Indeed, including these additional perturbations increase the computational time. A complete study of the computational time and other numerical parameters will be carried out in Chapter 5. This example is used to perform a first validation of the point mass gravitational models implemented in IOP. If the primary attraction and the planetary point mass perturbations are included in IOP, the final positions and velocities computed with GMAT and IOP differ only of 0.004 m and 3×10^{-8} m/s. In the case of the positions, it means that the PMG models included in IOP almost compensates the 8 m due to the point mass gravity perturbations. Other validations will be performed throughout this subsection. So the dominant perturbation comes from the Sun. This perturbation is also included in GMAT at this stage. IOP only

contains the primary attraction of Mars. In this case, the final positions computed with GMAT and IOP differ from 187 km! In contrast to the planetary perturbations, the Sun point mass perturbation must be taken into account to obtain realistic propagation. If the point mass model of the Sun is also included in IOP, the gap reduces to 23 m. The impact of the Sun is significant. This example is also used to compare the Sun PMG magnitude with the primary attraction magnitude to confirm that it remains a perturbation. In addition, this example is used to quantify the importance of the direct term with respect to the indirect term given in Equation 4.9. The last point to explore is the origin of the error of 23 m in the Sun point mass attraction model included in IOP.

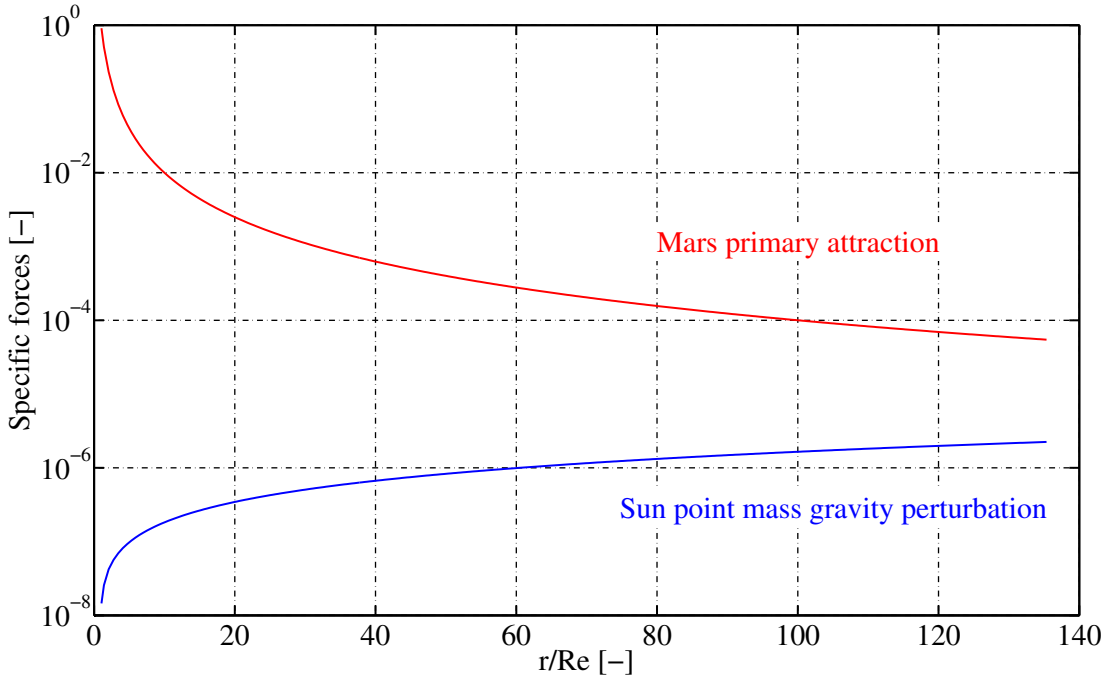

Figure 4.5: A trajectory escaping Mars is considered. The propagation lasts four days starting on 1 January 2045 12:00:00 TT. The dimensionless position and specific forces are obtained with the Mars equatorial radius R_e and its gravitational parameter. The figure compares the magnitude of the Mars primary attraction and the Sun point mass perturbation.

The point mass perturbation of the Sun is small compared to the primary attraction when the spacecraft is located close to Mars. During the propagation, the spacecraft gets closer to the Sun and goes away from Mars. As a result, the point mass gravity attraction of the Sun increases whereas the primary attraction of Mars decreases. The propagation stops at about 140 Mars equatorial radii. As shown in section 3.1, the mean radius of the Mars SOI is 170 Mars equatorial radii. One can imagine that at this distance the magnitude of the two specific forces will be close which is the meaning of the SOI.

The importance of the direct term compared to the indirect term depends only on the distance between the spacecraft, the central body and the Sun (Equation 4.9). The contributions of the direct and indirect terms are almost equal within the spheres of influence. The direct term represents 50.02% and the indirect term represents 49.98%.

As explained previously, the point mass gravity perturbations are computed knowing the locations of the planets and the Sun in the solar system. However, these positions are not known exactly. Indeed, the VSOP87 planetary theory introduces errors. The errors appearing in the point mass gravity models are directly linked to these errors. This can be illustrated taking two extreme cases. For the propagation starting on 1 January 2045 12:00:00 TT described above, the distance between the Sun and Mars has an error of 15,015 km compared to DE405. The error in the final position of the spacecraft is equal to 23 m in this case. If the departure date is on 1 January 1990 12:00:00 TT, the error on Mars's position is equal to 6,759 km and the error in the final position of the spacecraft reduces to 11 m. The following example will confirm this fact.

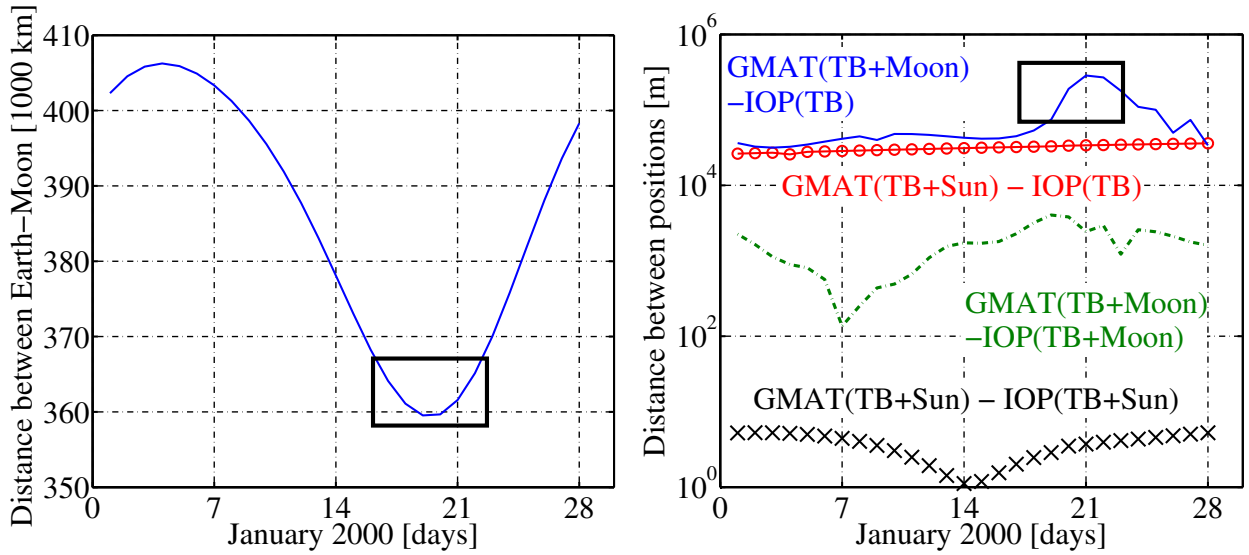

(a) Distance Earth-Moon

(b) Impacts of Moon and the Sun

Figure 4.6: The central body is the Earth. Escape trajectories are considered during the first 28 days of January 2000. The propagation lasts one day starting on [1,28] January 2000 12:00:00 TT. The left graph shows the distance between the Earth and Moon. The right graph contains four curves: the blue and red curves show respectively the impacts of Moon and the Sun on the final spacecraft positions. The green and dark curves show the errors between IOP and GMAT models. TB stands for two-body.

Our solar system is composed of other celestial bodies than the Sun and the planets. The moons are celestial bodies orbiting the planets. It means that that they are located within the planetary spheres of influence. The Earth has one moon, Mars has two moons and the giant planets (Jupiter to Neptune) have a series of moons. Some of them have a size comparable to that of Mercury. No moon orbits Mercury and Venus. The Moon orbiting the Earth is considered. Propagation lasting 1 day on the orbit escaping the Earth is considered for each day of January 2000. One month corresponds to the orbital period of the Moon around the Earth. The study focuses on the impact of the Moon on the final spacecraft positions. The right graph in Figure 4.6 shows that the Moon (blue curve) has a larger impact on the final spacecraft positions than the Sun (red curve). The Moon changes the final spacecraft position by 75 km on average, whereas the Sun changes it by 31 km on average. The gravitational parameter of the Moon is much smaller than the gravitational parameters of the planets and the Sun. However, the Moon is 389 times closer to the Earth than the Sun. NASA

provides a mean distance between the Earth and the Moon of 384,400 km which is close to the mean value on the left graph in Figure 4.6. The black rectangles in Figure 4.6 show that the impact of the Moon is maximum when the Moon is the closest to the Earth. The discussion above implies that high-fidelity propagation within the spheres of influence cannot be obtained if the Moon effects or more broadly the moons are not taken into account. Indeed, this is true in the SOI of the Earth. The Moon is negligible in the other spheres of influence due to its small gravitational parameter. Its perturbation is turned off outside the Earth's SOI. At this stage, the point mass gravity models are included in IOP. The averages of errors in final spacecraft positions for the Moon and Sun point mass gravity models are respectively of 1 km and 4 m. The approximate ephemerides of the Moon come from Astronomical Almanac which provides less accurate ephemerides than the VSOP87 planetary theory. As a result, the Moon point mass model gives rise to less accurate results. However, it reduces the error from 75 km to 1 km on average. In contrast, the Sun point mass gravity model reduces the error from 31 km to 4 m on average. The concept of a SOI cannot be applied to the moons. By definition, a moon is located within the sphere of its associated planet. If not, it would orbit the Sun like an asteroid. The contributions of the other moons are not taken into account in IOP.

The next part focuses on the impact of the point mass gravity perturbations on osculating orbital elements. The term osculating element has to be defined. If only the primary attraction of the central body is taken into account, a Keplerian orbit is obtained. The underlying orbital elements apart from the true anomaly are constant during all the propagation in this case. The perturbed orbit obtained by taking the point mass gravity perturbations into account differs from a simple Keplerian orbit. However, it is possible to define an osculating orbit in this case. An osculating orbit consists of an orbit that is tangent to the perturbed orbit at each time [24]. The osculating orbital elements vary in time due to the point mass gravity perturbations. It represents the most intuitive way to analyse the impact of a given perturbation. So Sun gives the dominant perturbation if the moons are not taken into account. Therefore, only the impact of the Sun on the osculating orbital elements is studied. The other planets have the same impact on the orbital elements, but it happens on a smaller scale. A nearly closed orbit around Mercury is chosen to highlight the effects. Indeed, Mercury is the closest planet to the Sun.

ISS Mercury

The aim is to define general cases as for the escape orbits. These orbits will also be used in the following perturbation. The case of the Earth International Space Station ISS is chosen. The initial conditions of the ISS on 13 October 2017 12:00:00 TT are written in Table 4.5.

Eccentricity e (-)	Semi-major axis a (km)	Inclination i (°)	RAAN Ω (°)	Argument of perigee ω (°)	True anomaly ϕ (°)
0.0012	6,779.77	51.71	167.35	44.16	74.45

Table 4.5: Orbital elements of the ISS on 13 October 2017 12:00:00 TT in the Earth inertial coordinate system [29].

Hypothetical cases are proposed. The ISS orbit is virtually transposed to the other planets. The date, spacecraft properties and initial orbital elements do not change apart from the semi-major axis.

Indeed, the ISS orbit on Earth at an altitude of about 400 km. The semi-major axis is given by $a = R_e + 400 = 6,779.77$ km where R_e stands for the equatorial radius. Replacing the equatorial radius of the Earth by the equatorial radii of the other planets gives the semi-major axis of the ISS on those planets. The semi-major axis of Mercury is 2,839 km using this procedure.

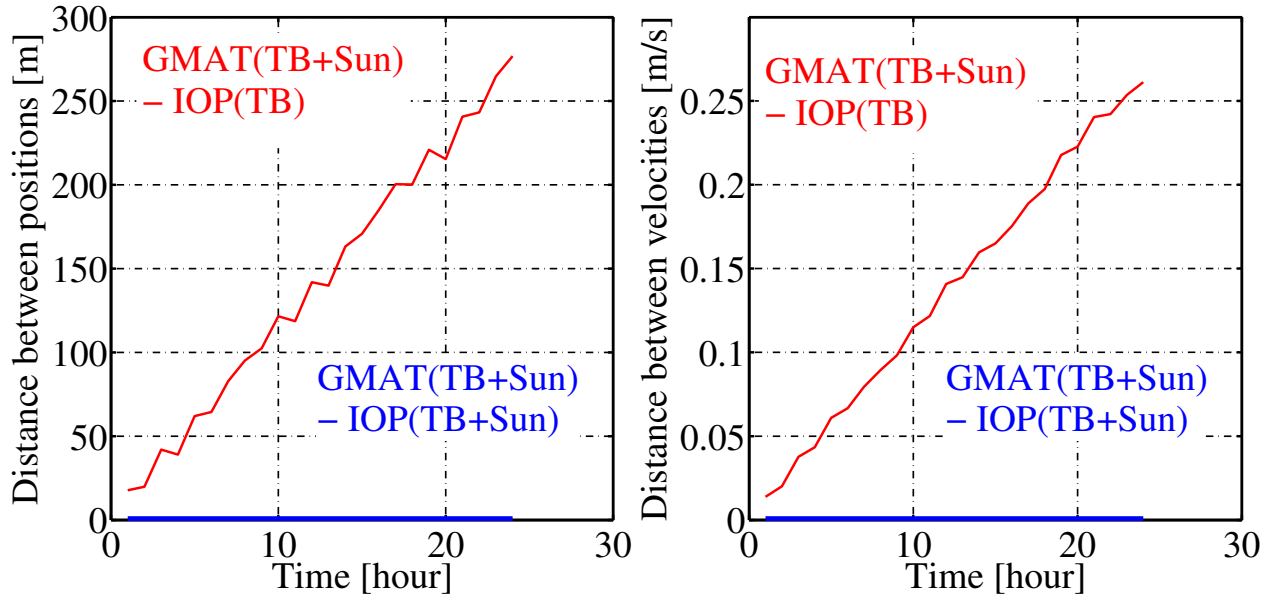

(a) Distance between positions

(b) Distance between velocities

Figure 4.7: The central body is Mercury. A nearly closed orbit is considered. The propagation lasts one day starting on 13 October 2017 12:00:00 TT. The figure gives the impact of the Sun point mass gravity perturbation on the positions and velocities (red curves) and validates the point mass gravity model included in IOP. The blue curves are close to 0.

Before analysing the results, the propagation is validated with GMAT. The Mercury's primary attraction and the point mass gravity perturbation of the Sun are included in GMAT. First, only the primary attraction of Mercury is included in IOP. The comparison with GMAT gives the impact of the Sun point mass gravity perturbation on the spacecraft positions and velocities. The propagation lasts one day. The distances between the positions and velocities are computed each hour and are represented in red in Figure 4.7. The averages of these distances for the positions and the velocities give respectively 120 m and 0.12 m/s. If the point mass gravity perturbation of the Sun is taken into account in IOP, it is expected that these values approach 0. The averaged values reduce to 0.003 m and 2×10^{-6} m/s in this case. The point mass gravity model included in IOP is therefore validated.

Let us focus on the impact of the Sun point mass gravity perturbation on the orbital elements. The six osculating orbital elements can be divided in two categories. The Sun affects the longitude of the ascending node and the argument of periapsis in a secular and in a periodic way [24]. The meaning of secular and periodic are the same as the ones discussed for planetary ephemerides. In contrast, the inclination, the eccentricity, the semi-major axis and the true anomaly are only affected in a periodic way [24]. Among the orbital elements, the argument of periapsis, longitude of the ascending node and the semi-major axis are analysed. The radial and tangential components of the point mass gravity specific force are not high enough to affect in secular way the eccentricity of

the orbit. The true anomaly exhibits 13 cycles from 0 to 360 °corresponding to the 13 orbits the spacecraft performed around Mercury in one day.

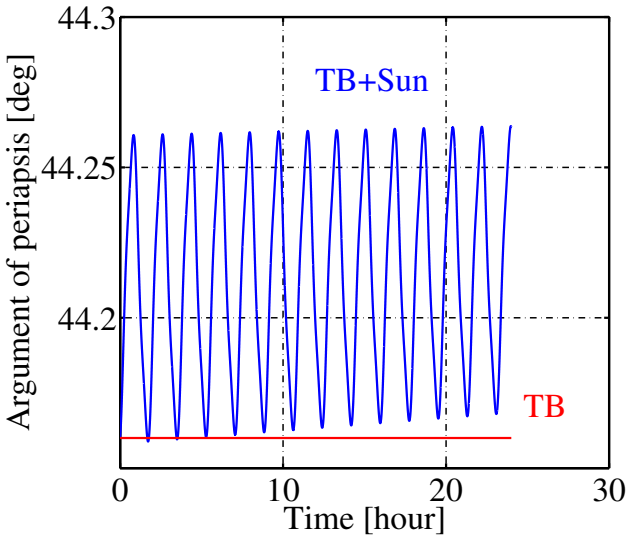

(a) Argument of periapsis.

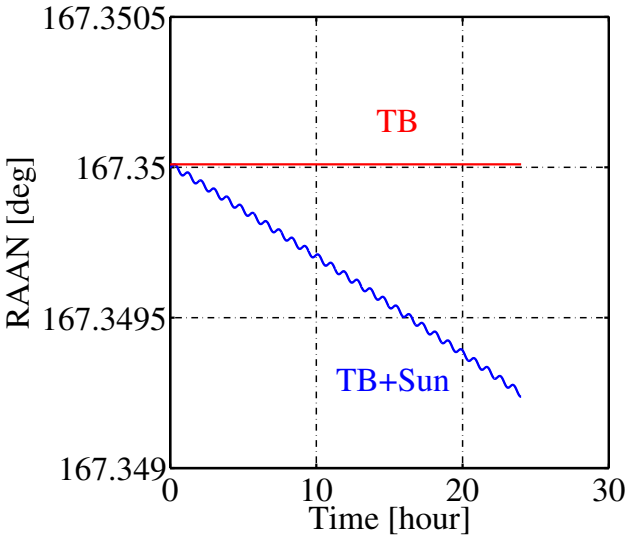

(b) Right ascension of the ascending node (RAAN).

Figure 4.8: The central body is Mercury. A nearly closed orbit is considered. The propagation lasts one day starting on 13 October 2017 12:00:00 TT. The figure compares the evolution of the RAAN and the argument of periapsis if the point mass gravity perturbation of the Sun is included (blue) or not (red).

The Sun does not lie in the spacecraft orbital plane. A force component is directed toward the Sun's orbital plane. The resulting torque tends to turn the orbital plane of the spacecraft toward the Sun's orbital plane. As a result, the spacecraft orbit precesses around the normal to the Sun's orbital plane [24]. The longitude of the ascending node and the argument of periapsis are affected in a secular and in a periodic way. The other orbital elements are only affected in a periodic way. The results are shown in Figure 4.8. The red curves represent the constant evolution of the orbital elements if only the primary attraction of Mercury is taken into account. The point mass gravity perturbation forces the orbit to deviate from the two-body elliptic orbit. The resulting curves are given in blue. The right ascension of the ascending node decreases with time. It means that the node line drifts Westward according to the convention defined in section 1.3. In contrast, the argument of periapsis increases with time meaning that the periapsis advances in the direction of the spacecraft's motion in the same convention. If the Sun and the planetary point mass perturbations are taken into account, the spacecraft orbital plane precesses simultaneously about the normals of the Sun's orbital plane and of each planetary equatorial planes. It gives rise to a complex precession. In fact, the planetary point mass gravity perturbations are small within the spheres of influence and the additional precessions are never observed.

The periodic variation of the semi-major axis over one orbit around Mercury is studied. This is represented in Figure 4.9. The initial inclination is modified so that the spacecraft and Sun orbital planes have the same inclination. The red line corresponds to the constant value of the semi-major axis if only the primary attraction of Mercury is included. During most of the propagation, the

osculating semi-major axis is higher than the two-body semi-major axis apart from the two portions where the blue curve is below the red one. These two portions are delimited with || on the centre graph in Figure 4.10. It consists of a top view of the orbital plane. The top and bottom graphs show that the osculating semi-major axis is smaller inside the orange region and higher outside the orange regions than the two-body semi-major axis. In addition, the centre graph show that the trajectory is close to a circle due to the small eccentricity of the ISS orbit.

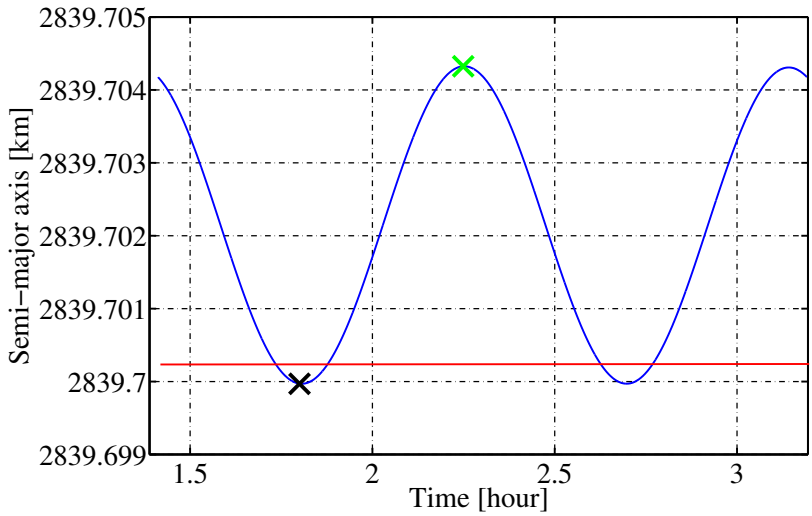

Figure 4.9: The central body is Mercury. A nearly closed orbit is considered. The propagation lasts one orbit around Mercury starting on 13 October 2017 12:00:00 TT. The figure compares the evolution of the semi-major axis if the point mass gravity perturbation is included (blue) or not (red).

The last part of this section explains why the minimum and maximum of the osculating semi-major axes occur at the green and black crosses. The black cross in Figure 4.9 represents the location where the unit position vector of the spacecraft $\mathbf{e}_S$ and the Sun $\mathbf{e}_\odot$ are perpendicular. It has to be stressed that during the considered orbit the position of the Sun is assumed to be fixed. In fact, the motion of the Sun is small in this short time interval. At this point, $\mathbf{e}_S \cdot \mathbf{e}_\odot$=0 and Equation 4.9 reduces to (Montenbruck [17])

$$\ddot{\mathbf{r}} \approx \frac{\mu_\odot r}{r_{P\odot}^3}(-\mathbf{e}_S), \tag{4.11}$$

assuming that the spacecraft is located much closer to Mercury than the Sun, which is the case for nearly circular orbits. $\mu_\odot$ stands for the gravitational parameter of the Sun, r and $r_{P\odot}$ stand respectively for the norm of the spacecraft position and the Sun position vectors in the planetocentric inertial coordinate system. The expression $-\mathbf{e}_S$ appearing in this equation means that the specific force of the Sun acting on the spacecraft is directed towards Mercury's center as shown on the centre graph in Figure 4.10. The osculating semi-major axis is therefore minimum. The black cross admits a symmetric point in the other orange region where the dot product is also equal to 0.

The green cross in Figure 4.9 represents the point where the dot product is equal to 1 which means that the spacecraft and the Sun are colinear ($\mathbf{e}_S$=$\mathbf{e}_\odot$) as represented on the graph at the centre in Figure 4.10. Equation 4.9 reduces to (Montenbruck [17])

$$\ddot{\mathbf{r}} \approx \frac{2\mu_\odot r}{r_{P\odot}^3}\mathbf{e}_S. \tag{4.12}$$

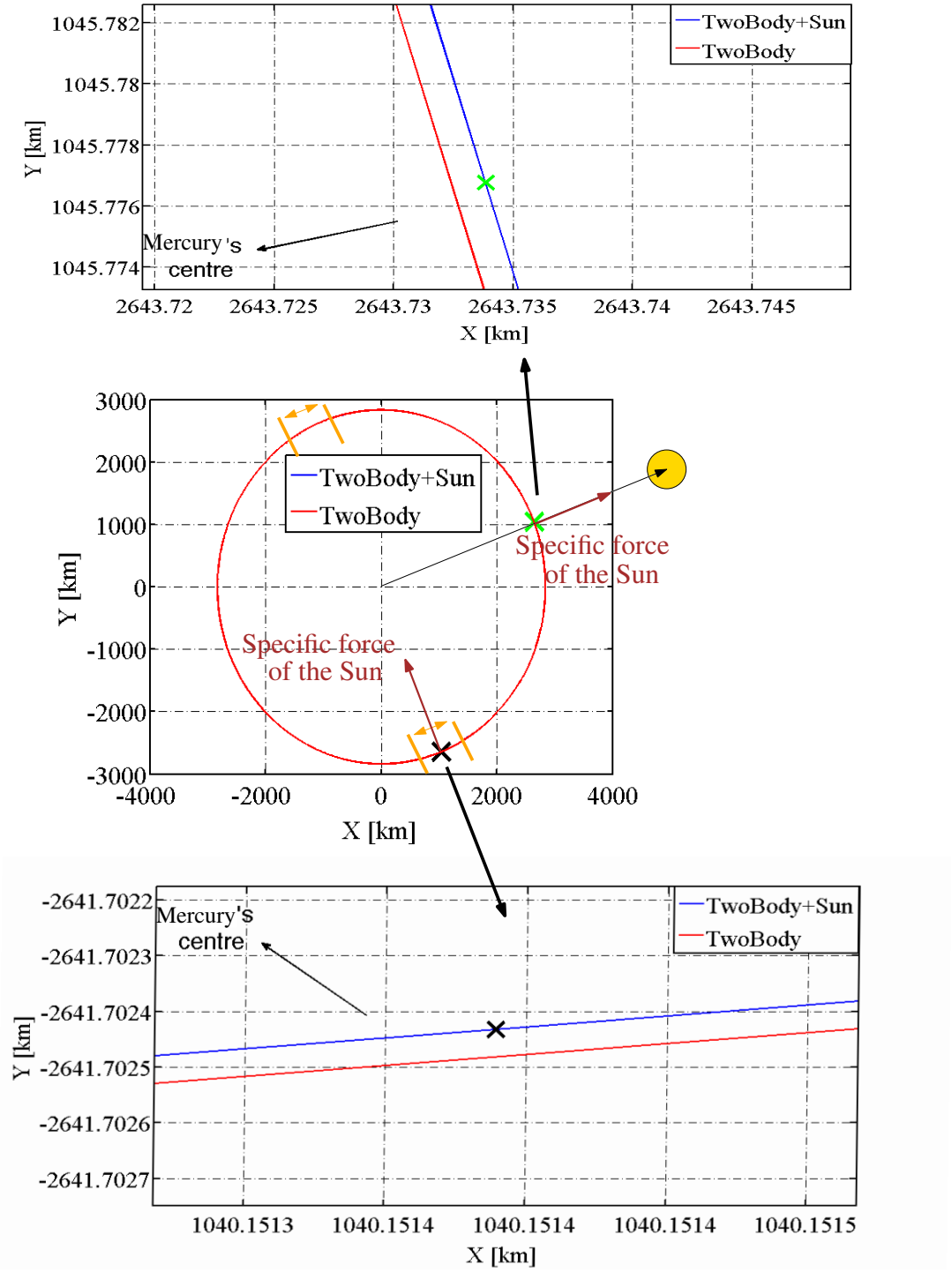

Figure 4.10: The graph at the centre shows the two-body ,and two-body plus point mass perturbation trajectories. The regions delimited by || are the locations where the osculating semi-major axis is smaller than the two-body semi-major axis. The black cross locates the point where the point mass specific force is directed away from Mercury. The graph at the bottom is a zoom on this region. The green cross is the location where the point mass specific force is directed toward Mercury. The graph at the top is a zoom on this region.

It means that the spacecraft experiences a specific force away from Mercury as represented on the graph at the centre in Figure 4.10. Therefore, the green cross corresponds to the point where the osculating semi-major axis is maximum in Figure 4.9. The point mass gravity attraction of the Sun has been discussed in this subsection. It is not the only perturbation coming from the Sun. The Sun emits photons in a continuous way. Photons are massless particles with a given energy and momentum. The photons exchange momentum with the spacecraft which disturbs its trajectory within the spheres of influence. The following subsection is devoted to this perturbation.

4.2.3 Solar radiation pressure perturbation

The problem of the solar radiation pressure (SRP) is addressed. Up to now, the perturbations do not take into account the ballistic properties of spacecraft. The gravitational attractions are independent of the mass, the material properties and surface area of spacecraft. These parameters become of primary importance in the case of the solar radiation pressure perturbation. Two situations are considered. In the first situation, the spacecraft is located in full illumination . It means that no osculating bodies eclipse the spacecraft. The second situation is opposed to the first one. The central body is located between the Sun and the spacecraft. The spacecraft is therefore in eclipse and the solar radiation pressure perturbation is equal to 0.

The subsection is divided into three parts. The first part explains the different choices made to build the solar radiation and eclipse models. The second part is devoted to the validation of the eclipse and solar radiation models. GMAT is used as reference. The third part concludes with the study of the solar radiation magnitudes in the different spheres of influence.

General Model

The contribution of the solar radiation pressure to the perturbed vector, $\mathbf{a}_{\text{perturbed}}$, is

$$\mathbf{a}_{\text{SRP}} = \nu \, \frac{R_{\text{e}}^2}{\mu} \, C_{\text{r}} \, P_{\text{SR}} \, \frac{A_{\text{Sun}}}{m} \, \frac{\mathbf{r}_{\odot S}}{r_{\odot S}}, \tag{4.13}$$

where ν [-] stands for the shadow coefficient, $C_{\text{r}} \in$ [1,2] [-] stands for the reflectivity coefficient, P_{SR} [kN/km^2] stands for the solar radiation pressure, A_{Sun} [km^2] stands for the spacecraft surface area facing the Sun, m [kg] stands for the mass of the spacecraft and $\frac{\mathbf{r}_{\odot S}}{r_{\odot S}}$ stands for the unit position vector of the spacecraft with respect to the Sun in the planetocentric inertial coordinate system. The gravitational parameter μ and the equatorial radius R_{e} are those of the planet at the centre of the sphere of influence. They are used to obtain dimensionless equations. Among these parameters, the user provides the reflectivity coefficient, the mass of the spacecraft and the spacecraft surface area. All these parameters are assumed constant over time. In real missions, the spacecraft changes attitude over time. As a result, the surface facing the Sun and the reflectivity coefficient also change over time, which modifies the amplitude of the solar radiation pressure perturbation. In addition, a constant mass implies that an unpowered flight is considered. The thrust coming from the spacecraft's engine is not taken into account in IOP. Models have to be built for the surface area facing the Sun, the solar radiation pressure and the shadow coefficient ν.

The spacecraft is modelled as a sphere of radius R_{S} (cannonball model). The surface area perpendicular to the Sun is constant and given by

$$A_{\text{Sun}} = \pi R_{\text{S}}^2. \tag{4.14}$$

The solar radiation pressure is the ratio between the radiation intensity S and the constant speed of the photons denoted c. The radiation intensity evolves with the inverse square of the distance R between the Sun's centre and the spacecraft. It can be expressed as [7]

$$S = S_{\odot} \left(\frac{R_{\odot}}{R} \right)^2, \tag{4.15}$$

in which $S_{\odot}$ stands for the constant radiated power intensity at the surface of the Sun (photosphere) and $R_{\odot}$ stands for the radius of the photosphere. $S_{\odot}$ is given by the Stefan-Boltzman law assuming that the photosphere is a black-body. The values are summarized in Table 4.6

Variables	Unit	Value
σ	W/m^{2}K^4	5.67×10^{-8}
$T_{\odot}$	K	5777
$R_{\odot}$	km	695990
$S_{\odot}$	W/m^2	$\sigma\, T_{\odot}^4$

Table 4.6: Constants used in the solar radiation pressure perturbation.

The selected model for the radiation intensity can be compared to key quantities known in the case where the central body is the Earth. At this stage, R is assumed to be the distance between the Sun and the Earth, instead of the distance between the Sun and the spacecraft. This assumption is often made for nearly closed orbits around the Earth. The solar radiation intensity is computed over 30 orbits of the Earth around the Sun starting on 13 October 2017 12:00:00 TT using the VSOP87 planetary theory.

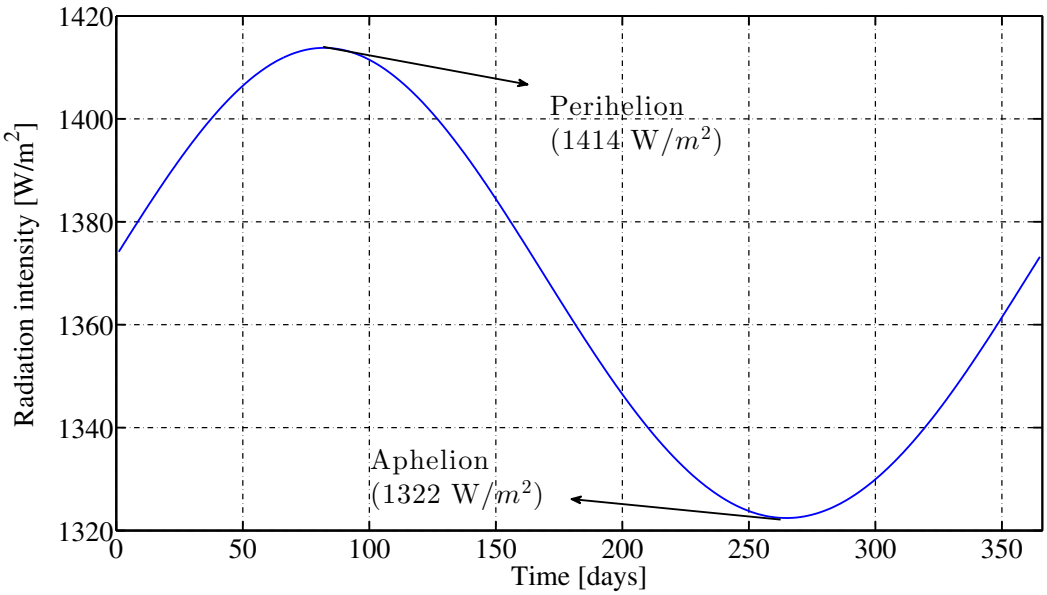

Figure 4.11: Evolution of the radiation intensity over one orbit of the Earth around the Sun.

The average is over 30 orbits in order to avoid exceeding the domain of validity of the ephemerides (1900-2050). It leads to a flux of 1367 W/m^2 which corresponds to the traditional solar constant proposed for orbits around the earth ([6] and [17]). The associated solar radiation pressure is 4.56×10^{-6} [N/m^2] which only represents 5×10^{-9} % of the mean sea-level atmospheric pressure (101325 Pa). This small digression gives a first preview of the fact that the solar radiation perturbations are small compared to the other perturbations in the vicinity of the planets. The radiation intensity over the first orbit is represented in Figure 4.11. The radiation intensity is maximum at perihelion (1414 W/m^2) and minimum at aphelion (1322 W/m^2) due to the inverse square law. Excape orbits are needed to travel between the different planets. Therefore, the distance R is the distance between the Sun and the spacecraft.

At this stage, models of the surface area and the solar radiation pressure are built. The last model is relative to the shadow coefficient ν. The eclipse model explained in Curtis [7] is chosen. A binary value is associated with the shadow coefficient ν. In full illumination, the shadow coefficient is equal to 1, whereas it is equal to 0 in shadow. A spacecraft in eclipse is represented on the right graph in Figure 4.12. The position of the spacecraft and the Sun are used to determine if the central body eclipses the spacecraft. θ represents the angle between these two position vectors. A and B represent the tangent to the planet passing through the Sun and spacecraft centres. These tangents define the angles $\theta_\odot$ and θ_S. The angles can be computed using the properties of right-angle triangles. The spacecraft is in shadow if

$$\theta_\odot + \theta_S < \theta \tag{4.16}$$

and the shadow coefficient is equal to 0 in this case. On the left graph in Figure 4.12, the limit case where the spacecraft enters in full illumination is shown. The angles are such that $\theta_\odot + \theta_S = \theta$.

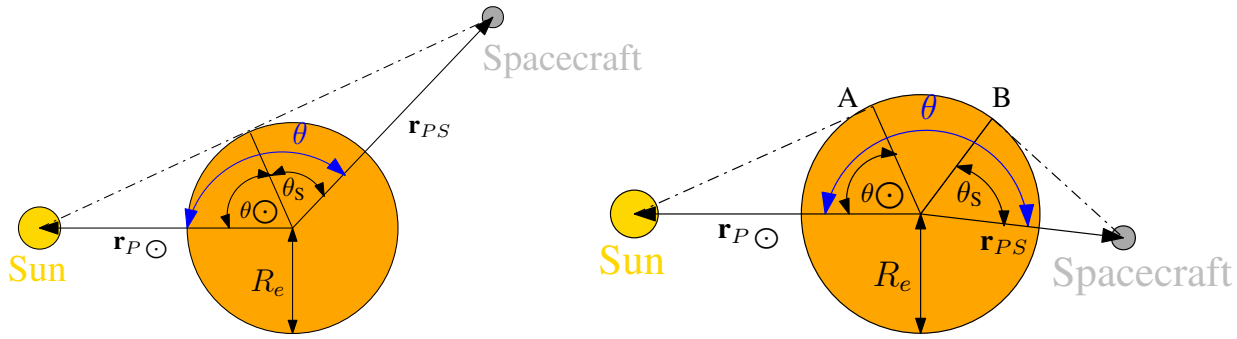

(a) Limit case: full illumination

(b) Shadow case

Figure 4.12: Eclipse model used in IOP. $\mathbf{r}_{PS}$ and $\mathbf{r}_{P\odot}$ denote respectively the position of the spacecraft and the Sun in the planetocentric coordinate system at a given time. R_e is the equatorial radius of the considered central body. The graphs are inspired by Curtis [7].

A efficient tracking of the Sun is needed to determine the shadow region. The VSOP87 planetary theory gives the position of the planets with respect to the Sun. By reversing these vectors and applying the change of coordinate systems, the position of the Sun with respect to the planet is known in the planetocentric coordinate system. In the case of the Earth, the tracking of the Sun can be compared with the classical method. The method is the one proposed by the Astronomical Almanac (National Almanac Office, 2013) explained in Curtis [6], Montenbruck [17] and Vallado [24]. According to Montenbruck, this method is accurate to about 0.1-1 %. The VSOP87 planetary leads to

an accuracy about $8 \times 10^{-4} - 0.02$ %. For example, the position of the Sun in the geocentric inertial coordinate system is computed on 2 April 1994 00:00:00 TT. The results are compared with the Development Ephemeris 405. The VSOP87 planetary theory leads to an error of 16,141 km whereas the method proposed by Astronomical Almanac leads to an error of 208,630 km.

The general model of the solar radiation pressure perturbation is defined. The next step is to validate the SRP model. The International Space Stations are chosen to validate the eclipse model. The ISS orbit the planets at an altitude of about 400 km. This altitude is suitable to test the eclipse condition. The results are compared with GMAT.

International Space Stations

The case of the Earth's International Space Station is first discussed. The ballistic properties of the ISS are a mass m =410,500 kg and an surface area facing the Sun A_{Sun} =1,641 m^2 [29]. The reflectivity coefficient is arbitrarily taken to 1.8.

The time spent in eclipse is computed for one orbit of the ISS around the Earth. The time needed to perform one orbit is the orbital period. Neglecting the impact of the solar radiation pressure perturbation, the orbital period is computed by

$$T = 2\pi\sqrt{\frac{a^3}{\mu}}, \tag{4.17}$$

where a [km] stands for the semi-major axis and μ [km^3/s^2] stands for the gravitational parameter. This relation is valid for an elliptic orbit which is the case of the ISS orbit (0<e<1). An orbital period of 1h30 is found. GMAT provides an eclipse time of 2072 s, which represents 37.1 % of the orbital period. Taking a time step of 1 s in IOP, the shadow coefficient can be computed each second of the propagation. Then, the shadow region is localized. It consists of the series of 0 comprised in the ν=1 coefficients. The difference between the time at the end and at the beginning of the eclipse is computed. An eclipse percentage slightly higher is found (37.29 %). At the end of the propagation, the distances between the positions and velocities of GMAT and IOP are 0.27 m and 3×10^{-4} m/s. Let us recall that the distances are computed with

$$d_{\text{Pos}} = \|\mathbf{r}_{\text{IOP}} - \mathbf{r}_{\text{GMAT}}\| \tag{4.18}$$

$$d_{\text{Vel}} = \|\dot{\mathbf{r}}_{\text{IOP}} - \dot{\mathbf{r}}_{\text{GMAT}}\|. \tag{4.19}$$

In Figure 4.13, the difference between the positions and velocities of IOP and GMAT are computed each hour during one day. The red curves correspond to the distances between IOP and GMAT if the solar radiation pressure perturbation is not included in IOP. Only the primary attraction of the Earth is included at this stage. Mean distances of 2.23 m and 2×10^{-3} m/s are found for the positions and the velocities. It means that the impact of the solar radiation pressure is small for the ISS[5]. The blue curves correspond to the distances between IOP and GMAT if the solar radiation pressure model is included in IOP. Mean distances reduce to 0.078 m and 9×10^{-5} m/s in this case.

[5]The solar radiation pressure is small in the vicinity of the planets compared to the other perturbations. In addition, the ballistic properties of the ISS are so that the impact of the solar radiation pressure is smaller. This will be shown in section 4.3.1 devoted to the study of solar radiation pressure parameters.

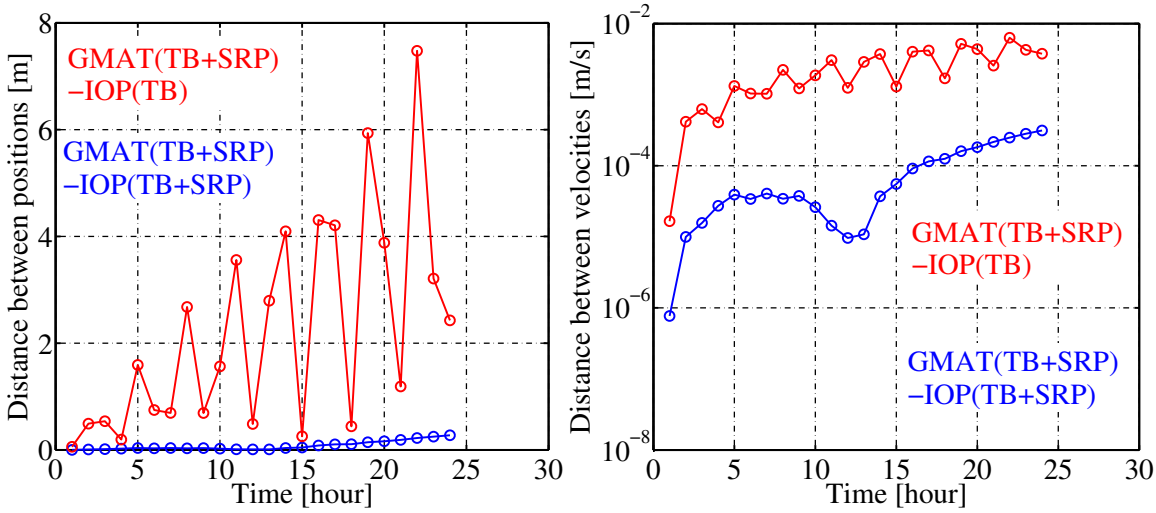

(a) Distance between positions

(b) Distance between velocities

Figure 4.13: The central body is the Earth. A nearly closed orbit is considered. The propagation lasts one day starting on 13 October 2017 12:00:00 TT. The figure gives the impact of the SRP on the positions and velocities (red curves) and validates the SRP model included in IOP. The blue curves are close to 0.

The procedure described above validates the eclipse model for the Earth. In fact, eclipses are possible with all the planets of the solar system. The same procedure is applied for the seven remaining planets considering the hypothetical ISS test cases described in the previous section. In Figure 4.13, it is shown that the distances between the positions and velocities at the end of the propagation can be used as indicators of the accuracy. They are therefore computed for the seven ISS after one day of propagation. The results are provided in Table 4.7. The maximum distances after one day are 59 cm and 5×10^{-4} m/s.

Planets	*Distance between Positions* (m)	*Distance between Velocities* (m/s)
Mercury	0.59	6×10^{-4}
Venus	0.14	1×10^{-4}
Mars	0.04	4×10^{-5}
Jupiter	0.06	2×10^{-5}
Saturn	0.06	2×10^{-5}
Uranus	0.01	3×10^{-6}
Neptune	0.01	6×10^{-6}

Table 4.7: The central body is the planet. Nearly closed orbits are considered. The propagation lasts one day starting on 13 October 2017 12:00:00 TT. The ballistic properties are: m = 410,500 kg, A_{Sun}=1,641 m^2, C_R=1.8. The table provides the differences in position and velocity between GMAT and IOP if the two-body attraction and the SRP perturbation are included in each propagator.

The differences between IOP and GMAT come mainly from two sources. The first source is the way ephemerides are computed. Indeed, the Sun is tracked in the sky during all the propagation and the solar radiation pressure acting on the spacecraft depends on the distance between the Sun and the spacecraft. Let us recall that ephemerides of GMAT come from numerical integration whereas IOP uses the VSOP87 planetary theory. The eclipse model constitutes the second source. GMAT uses one of the most accurate eclipse models which consists of the conical eclipse model. The conical model takes the size of the Sun into account and traces out the tangents to the planets starting from the extremities of the Sun. The region in black behind the planet in Figure 4.14 represents the umbra region (ν=0). The spacecraft does not receive direct light from the Sun in this region. The eclipse model used in IOP assimilates the Sun to a point. The tangents to the planet are traced out from this point at the centre of the Sun. The resulting umbra region is the blue region in addition to the black region in Figure 4.14. As a result, the eclipse model included in IOP overestimates the shadow region. In fact, GMAT replaces the blue region by a penumbra region where the shadow coefficient is between 0 and 1.

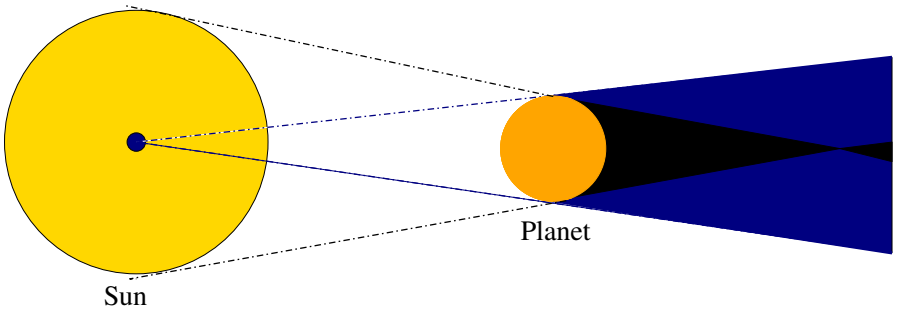

Figure 4.14: Representation of the difference between the umbra regions in IOP and GMAT.

Planets	R_e (km)	*Eclipse* GMAT (%)	*Eclipse* IOP (%)
Mercury	2,440	30.32	30.69
Mars	3,397	34.22	34.41
Venus	6,051	37.86	38.06
Neptune	25,269	40.73	44.36
Uranus	25,559	42.80	44.25
Saturn	60,268	40.28	46.34
Jupiter	71,492	39.92	45.99

Table 4.8: The central body is the planet. Nearly closed orbits are considered. The propagation lasts the time of one orbit around the planet starting on 13 October 2017 12:00:00 TT. The ballistic properties are: m = 410,500 kg, A_{Sun}=1,641 m^2, C_R=1.8. The table provides the difference in eclipse time between IOP and GMAT. The first column contains the equatorial radii in increasing order. The second and third columns compare the eclipse percentages in IOP and GMAT.

The sizes of the different shadow regions are exaggerated in Figure 4.14 and the difference between the predicted time spent in eclipse given in GMAT and IOP is not so large. The percentages

spent in eclipse over one orbit are given in Table 4.8. The difference between the two models increases with the equatorial radius. Indeed, the difference is larger for the outer planets than for the inner planets. The percentage of time the spacecraft spent in umbra is higher for IOP for the reason explained above. It has to be stressed that the percentage of one orbit spent in eclipse varies slightly in function of the position of the Sun with respect to the ISS orbits. The percentages provided in Table 4.8 are valid for the 13 October 2017 TT.

Is it the eclipse model included in IOP accurate enough? Are the larger errors for the outer planets detrimental? The difference between the positions and velocities after one day of propagation are computed if no eclipse model is included in IOP. In other words, the spacecraft is considered to be in full illumination during all its propagation. The results are given in Table 4.9. By comparing columns 1 and 2, and by comparing columns 3 and 4, the differences between IOP with and without eclipse models decrease when the distance between the Sun and the considered planet increases. Indeed, the solar radiation pressure decreases with the inverse square of this distance (Equation 4.15). Small differences are observed for the outer planets which are located far from the Sun. Therefore, the larger errors in terms of eclipse percentages for these planets impact weakly the spacecraft trajectories. For example, in the case of Neptune, IOP leads to the same results if the eclipse model is included or not. For Mercury, which is the planet located the closest to the Sun, the error on the position decreases from 11.23 m to 0.59 m by taking into account the eclipse model. To sum up, the eclipse model is sufficiently accurate and the implementation of a more advanced eclipse model is not mandatory.

Planets	*Distance between Positions (with)* (m)	*Distance between Positions (without)* (m)	*Distance between Velocities (with)* (m/s)	*Distance between Velocities (without)* (m/s)
Mercury	0.59	11.23	6×10^{-4}	1×10^{-2}
Venus	0.14	9.25	1×10^{-4}	7×10^{-3}
Mars	0.04	1.56	4×10^{-5}	1×10^{-3}
Jupiter	0.06	0.25	2×10^{-5}	2×10^{-4}
Saturn	0.06	0.07	2×10^{-5}	3×10^{-5}
Uranus	0.01	0.02	3×10^{-6}	1×10^{-5}
Neptune	0.01	0.01	6×10^{-6}	6×10^{-6}

Table 4.9: The central body is the considered planet. Nearly closed orbits are considered. The propagation lasts one day starting on 13 October 2017 12:00:00 TT. The ballistic properties are: m = 410,500 kg, A_{Sun}=1,641 m^2, C_R=1.8. The table provides the difference between the final positions and velocities computed with GMAT and IOP if the eclipse model is included or not in IOP.

The final remark comes from the fact the planets are considered to be spheres with radii equal to their equatorial radii in the eclipse models. In the section devoted to the J_2 perturbation, it has be shown that the planets exhibit a flattening at their poles. The flattening of the poles is small. It impacts significantly the spacecraft trajectories in terms of gravitational attraction, but its impact is negligible in the eclipse model. Therefore, the planets can be safely be modelled as spheres.

Escape orbits

The escape orbits described in section 4.2.2 are used. Two objectives are pursued. The first one is to study the magnitude of the solar radiation specific forces in the different spheres of influence. The second objective is to validate the propagator with a spacecraft possessing ballistic properties different from the ISS. Indeed, the ISS has a quite low area-to-mass ratio of 0.004 m^2/kg. The solar radiation pressure perturbation is proportional to this ratio (Equation 4.13). A spacecraft with a mass of 850 kg and a surface area of 50 m^2 is chosen. Nowadays, the spacecraft having the maximum area-to-mass ratio is the NASA's Echo 1 satellite. It possesses a surface area of 730 m^2 and a launch mass of 71 kg which gives an area-to-mass ratio of 10 m^2/kg. This satellite was used in the calculation of atmospheric density and solar radiation pressure in low Earth orbit.

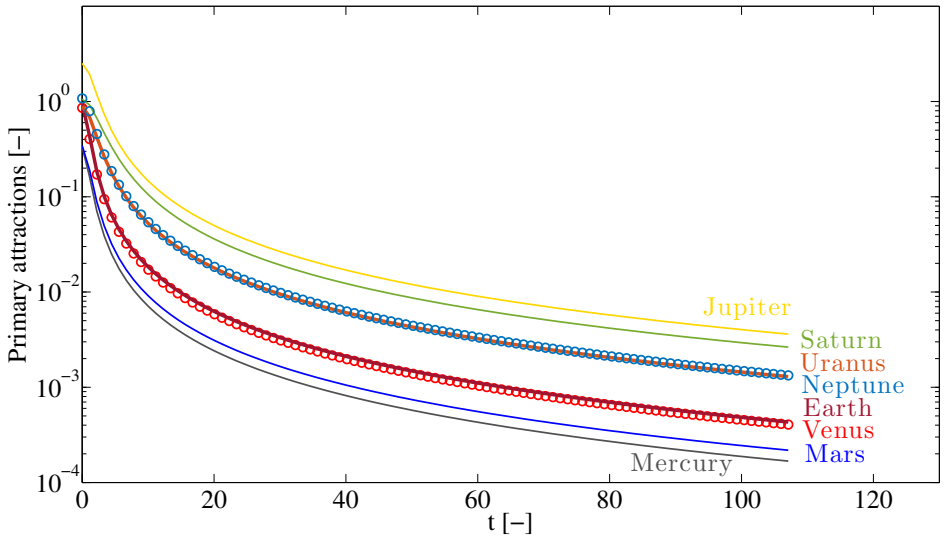

Figure 4.15: Evolution of the primary attractions on orbits escaping the planets.

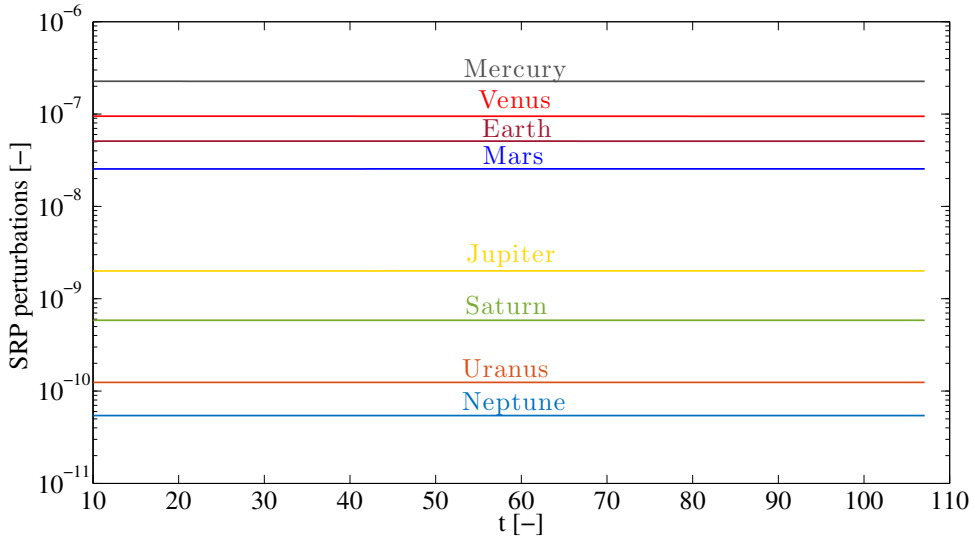

Figure 4.16: Evolution of the solar radiation specific forces on orbits escaping the planets.

Figure 4.15 and Figure 4.16 show the evolution of the primary attractions and solar radiation pressure perturbations for the escape trajectories of the eight planets. The characteristic variables used to obtain the dimensionless specific forces are the gravitational parameter and the equatorial radius of the Earth. Common characteristic variables are needed to compare the magnitudes of the different specific forces. The x-axes contain the dimensionless time. As explained in section 4.2.2, the planets with the higher mass exert the higher attractions on the spacecraft. Therefore, the primary attraction of Jupiter is the highest one. The primary attractions decrease when the spacecraft go away from the planets. Three elements distinguish the primary attractions and the solar radiation pressure perturbations. First, the magnitudes of the solar radiation pressure perturbations are very small compared to the primary attractions within the spheres of influence. Then, the solar radiation pressure perturbations are almost constant during the propagation. In the middle of nowhere, far from any planets, one can imagine that the solar radiation pressure perturbations become the dominant perturbation. The solar radiation pressure is therefore not turned off outside the spheres of influence. Eventually, the mass constitutes the main parameter for the primary attractions. For the solar radiation pressure, the distance between the Sun and the spacecraft matters. As a result, the solar radiation pressure is maximum for Mercury and is minimum for Neptune. This analysis consolidates the results in Table 4.9.

The last element to study is the impact of the solar radiation pressure on the spacecraft trajectories. The positions and velocities after one day of propagation are considered. First, the primary attraction and the SRP perturbation are included in GMAT. At this stage, only the primary attraction is included in IOP. The distances between the positions and velocities are computed. The results are given in the first and third columns in Table 4.10. The correlation between Figure 4.16 and these columns can be seen. For Mercury, the solar radiation pressure changes by 7,749 m and 0.2 m/s the final position and velocity of the spacecraft. In contrast, these changes are only of 2 m and 4×10^{-5} m/s for Neptune. The second step is to include the solar radiation pressure in IOP. The distances between positions and velocities must approach 0 if the solar radiation pressure model included in IOP is correct. For the eight planets, the maximum errors on the final positions and velocities are 52 cm and 1×10^{-5} m/s.

Planets	*TwoBody-GMAT Positions* (m)	*TwoBody+SRP-GMAT Positions* (m)	*TwoBody-GMAT Velocities* (m/s)	*TwoBody+SRP-GMAT Velocities* (m/s)
Mercury	7,749	0.52	2×10^{-1}	1×10^{-5}
Venus	3,846	0.28	9×10^{-2}	6×10^{-6}
Earth	1,807	0.17	4×10^{-2}	3×10^{-6}
Mars	989	0.04	2×10^{-2}	1×10^{-6}
Jupiter	67	0.04	2×10^{-3}	4×10^{-7}
Saturn	21	0.004	5×10^{-4}	1×10^{-7}
Uranus	4	0.004	1×10^{-4}	7×10^{-8}
Neptune	2	0.004	4×10^{-5}	9×10^{-8}

Table 4.10: The table gives the impact of the solar radiation pressure perturbation on the state of spacecraft and validates the solar radiation model included in IOP. Escape orbits are considered.

An spacecraft traveling from one planet to another spends most its time outside the spheres of

influence. Indeed, the spheres of influences are points at the scale of the solar system. The following section extents the results obtained within the SOI.

4.3 Motion outside the spheres of influence

The motion of the spacecraft outside the SOI is addressed. The flattening of the poles, solar radiation pressure and point mass gravity perturbations within the SOI have been studied in the previous section. The flattening of the poles and Moon point mass gravity perturbations are turned off outside the spheres of influence due to their small magnitudes. This section is therefore focused on the SRP and PMG perturbations outside the spheres of influence.

4.3.1 Solar radiation pressure perturbation

This subsection is devoted to the solar radiation pressure perturbation outside the spheres of influence. Eclipse and solar radiation pressure models have been validated in section 4.2.3. Propagation lasting one day have been considered. The magnitudes of the solar radiation pressure perturbations in the different SOI have also been discussed. The objectives of this subsection are the following ones. First, the modifications linked to the SRP model outside the spheres of influence are explained. Second, the impact of the parameters such as the reflectivity coefficient and the area-to-mass ratio on the spacecraft trajectories are studied. The third objective is to validate the SRP model with propagation longer than one day. Eventually, the effects of the solar radiation pressure on orbital elements is studied. The case study is the interplanetary trajectory between the Earth and Mars in 309 days defined in section 3.4.2.

Equation 4.13 is valid outside the spheres of influence. Two differences compared to the motion within the spheres of influence are distinguished. First, the spacecraft is always located in full illumination. No planets eclipse the spacecraft. As a result, the shadow coefficient ν equals 1 during all the propagation. The second difference comes from the fact that the motion is expressed in the heliocentric coordinate system. The Sun is located at the origin of the coordinate system, which simplifies the computations. Indeed, the position of the Sun does not need to be expressed in the planetocentric inertial coordinate systems and no change of coordinate systems is therefore required.

Solar radiation parameters

Area-to mass ratio and reflectivity coefficient parameters change the magnitude of the SRP perturbation acting on the spacecraft. The area-to-mass ratio is first considered. Three trajectories are represented on the right graph in Figure 4.17. The red curve represents the trajectory in the two-body approximation. It is used to understand the impact of the solar radiation pressure. The green curve represents a spacecraft with a low area-to-mass ratio called low spacecraft. It is the case of the ISS. The aim is to prove that the ballistic properties of the ISS are such that the solar radiation pressure affects its trajectory weakly as written in section 4.2.3. The black curve represents the trajectory of a spacecraft with a classical area-to-mass ratio of 0.0588 m^2/kg. The Sun is located at (0,0) and it is represented by a yellow circle on the right graph.

The positive sign in Equation 4.13 means that the solar radiation pressure is directed away from the Sun. It pushes the spacecraft away from it. The higher the area-to-mass ratio the higher the gap

with the two-body trajectory. The low spacecraft ratio spacecraft stays close to the two-body trajectory with its low area-to-mass ratio which confirms the discussions of the previous section. More specifically, the SRP modifies its trajectory on an average of 3,898 km during the first 300 days of propagation whereas it changes on a average of 57,368 km the classical spacecraft trajectory. It can be concluded that very large spacecraft with a very low mass are the most affected by the solar radiation pressure. The left graph recalls that the solar radiation pressure perturbation impacts moderately the spacecraft trajectories. The red and green curves are hidden behind the black one. Moreover, the three spacecraft reaches the SOI of Mars even if the trajectories are designed with Lambert's problem. Lambert's problem assumes two-body approximation. The right graph presented above represents a zoom on the black rectangle. Even if the solar radiation pressure perturbation impacts moderately the spacecraft trajectories, it is taken into account to obtain high-fidelity propagation.

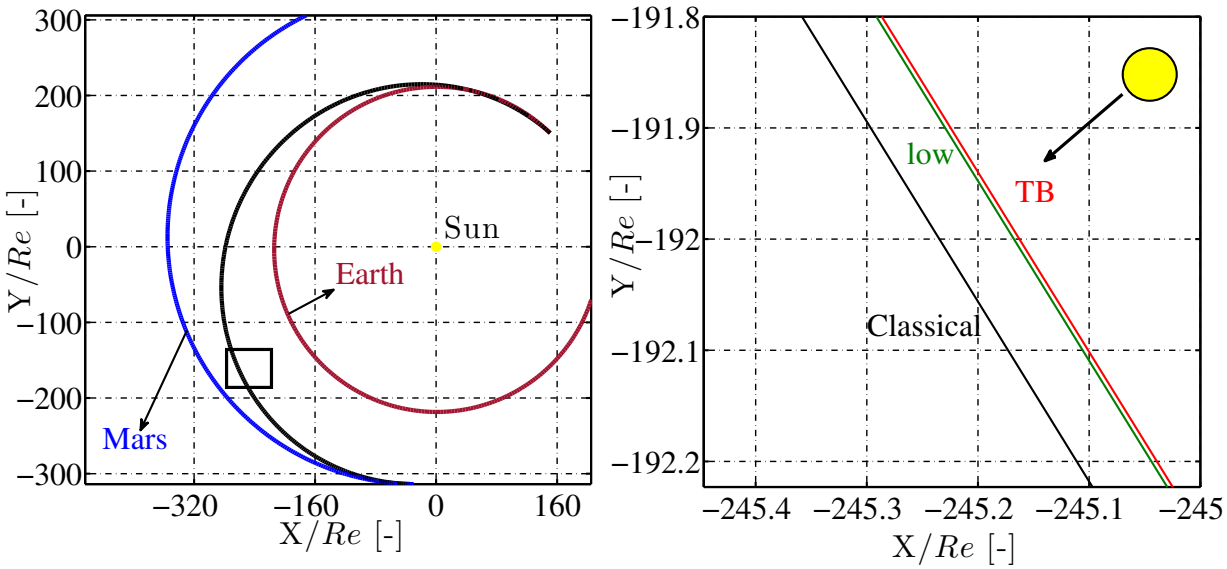

(a) Trajectories joining the Earth and Mars.

(b) Zoom on the right graph (black rectangle).

Figure 4.17: Trajectories joining the Earth and Mars. The figure shows the impact of the area-to-mass ratio parameter. TB stands for two-body approximation. The low spacecraft and the classical spacecraft have respectively an area-to-mass ratio of 0.004 m^2/kg and 0.0588 m^2/kg. R_e is the radius of the Sun photosphere. It is used to obtain dimensionless variables. The departure date is on 7 November 1996 TT. The arrival date is on 12 September 1997 TT.

The solar radiation pressure perturbation is also proportional to the reflectivity coefficient. This coefficient is between 1 and 2. The extreme values correspond respectively to a purely absorbing and reflecting surface. A purely reflecting surface means that the momentum transferred from photons is twice as large. These values represent ideal cases. Spacecraft surfaces have a reflectivity coefficient between 1 and 2 depending on the spacecraft material properties. For example, solar panels have a reflectivity coefficient equal to 1.21. The interpretation of its impact on the spacecraft trajectory is similar to the area-to-mass ratio parameter.

The SRP model with long propagation is studied. Only propagation lasting one day has been considered until now. The ballistic properties of the classical spacecraft, the primary attraction of

the Sun and the solar radiation pressure perturbation are included in GMAT. First, only the primary attraction is included in IOP. The distances between IOP and GMAT during the propagation are given in red in Figure 4.18. At the beginning of the propagation, the solar radiation pressure affects strongly the motion of the spacecraft and then its effects progressively decrease. It comes from the fact that the spacecraft goes from the Earth to Mars. The solar radiation pressure decreases as the square of the distance from the Sun. The distance is 154,644 km after 300 days of propagation. The second step consists of including the solar radiation pressure model in IOP. The distances between IOP and GMAT are represented in blue in this case. The blue curve represents the error linked to the solar radiation model included in IOP. The error follows the same evolution as the distance between the two-body attraction and GMAT. After 300 days of propagation, the distance is 11 km which represents an error of 0.007 %. The solar radiation pressure model is therefore correct.

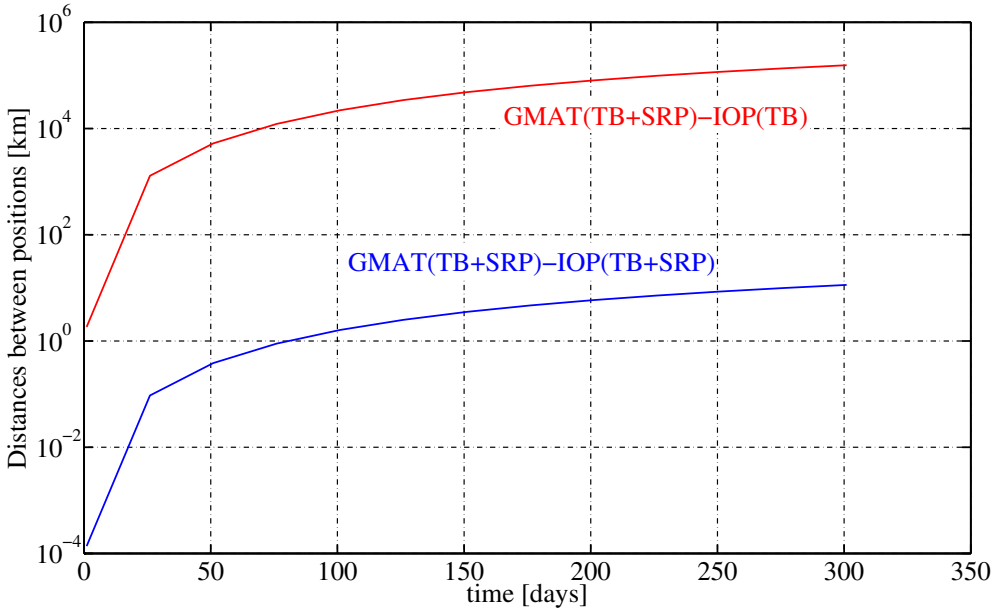

Figure 4.18: The central body is the Sun. The departure date is on 7 November 1996 TT. The departure and arrival planets are respectively the Earth and Mars. The figure shows the impact of the solar radiation pressure perturbation on the spacecraft trajectory (red). It also validates the SRP model included in IOP. The ballistic properties are: m = 850 kg, A_{Sun}=50 m^2, C_R=1.8.

The last part focuses on the orbital elements. The Variation-of-Parameters equations given in Vallado [24], Blitzer [3] show that the solar radiation pressure affects all the orbital elements in a periodic way and induce change in the periapsis height in the case of motion within SOI. Let us focus on the semi-major axis. The variation of the semi-major axis is given by Blitzer [3]

$$\Delta a = 2\frac{a^2}{\mu} F \Delta r_{\odot}, \tag{4.20}$$

where F stands for the solar radiation force and $\Delta r_{\odot}$ stands for the relative displacement of the spacecraft relative to the Sun. When the spacecraft goes from the Earth to Mars, the distance between the Sun and the spacecraft increases: $\Delta r_{\odot} > 0$. It implies that $\Delta a > 0$ according to Equation 4.20 and the semi-major axis increases as can be seen on the right graph in Figure 4.19. The first 300

days of propagation are considered. The correlation between the semi-major axis and the energy is given by Blitzer [3]

$$\Delta a = 2\frac{a^2}{\mu}\Delta\xi, \tag{4.21}$$

where ξ represents the energy. The energy increases when the semi-major axis increases. Physically, the dot product of the SRP force and the spacecraft's velocity vector is positive when it moves away from the Sun which increases its speed and its energy. One can imagine that if the spacecraft comes back to the Earth. The velocity vector is directed in an opposite direction of the solar radiation force. The dot product is negative leading to a deceleration (energy loss). The change in a is therefore zero over one orbit. The spacecraft is trapped by the Sun's gravitational attraction which means that its energy is always negative. A positive energy arises when the spacecraft escapes the solar system.

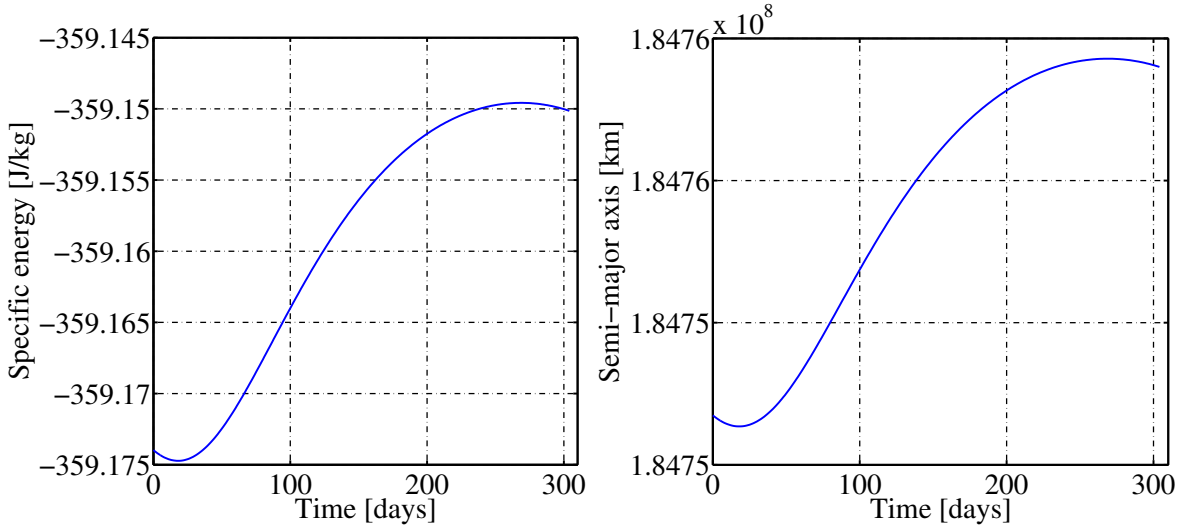

(a) Specific energy

(b) Semi-major axis

Figure 4.19: The central body is the Sun. The departure date is on 7 November 1996 TT. The departure and arrival planets are respectively the Earth and Mars. The ballistic properties are: m = 850 kg, A_{Sun}=50 m^2, C_R=1.8. The figure gives the evolution of the semi-major axis and energy during the first 300 days of propagation.

4.3.2 Point Mass Gravity perturbations

This subsection is devoted to the point mass gravity perturbations on interplanetary trajectories such as the Earth to Mars trajectory explained in the previous section. In section 4.2.2, the averages of the contributions of each point mass gravity perturbation have been quantified in the different SOI. In addition, the impact of the Sun PMG perturbation on the orbital elements has been studied. Section 4.2.2 has also highlighted the existence of new bodies affecting significantly the spacecraft trajectories within the spheres of influence: the moons.

The first objective of this section is to explain the differences between the motion within and outside SOI. The second one is to understand how each planet affects the spacecraft trajectory during interplanetary missions. More specifically, the evolution of each PMG perturbation is studied. The

motion outside SOI gives the spacecraft the opportunity to get closer to new types of bodies such as the asteroids and dwarf planets. Their impacts are not any more negligible as for motion within SOI. The dwarf planet Pluto is used as a test case to highlight the effects of the bodies other than the planets.

The general expression of the contribution coming from the point mass gravity perturbations remain unchanged

$$\mathbf{a}_{\text{PMG}} = \frac{1}{\mu}\sum_{k}\mu_{\text{k}} \times \left(\overbrace{\frac{\tilde{\mathbf{r}}_{\text{k}} - \tilde{\mathbf{r}}}{\|\tilde{\mathbf{r}}_{\text{k}} - \tilde{\mathbf{r}}\|^3}}^{Direct\ term} - \overbrace{\frac{\tilde{\mathbf{r}}_{\text{k}}}{\|\tilde{\mathbf{r}}_{\text{k}}\|^3}}^{Indirect\ term} \right). \tag{4.22}$$

The difference comes from the fact that all the positions are expressed in the heliocentric coordinate system which corresponds to the output system of the VSOP87 planetary ephemerides. No change of coordinate systems is required. In addition, the subscript k denotes the eight planets and the dwarf planet Pluto in this case.

The interplanetary trajectories designed with Lambert's problem cannot be used with the point mass gravity perturbation. Some modifications have to be introduced to study the impact of the PMG perturbations. For example, the Earth to Mars trajectory studied in the previous section assumes that the initial position of the spacecraft corresponds to the Earth itself. If the point mass gravity perturbations are introduced, the numerator and denominator of the Earth direct term in Equation 4.22 are close to 0. It prevents the convergence of the code. The solution is to introduce a small change in the initial true anomaly.

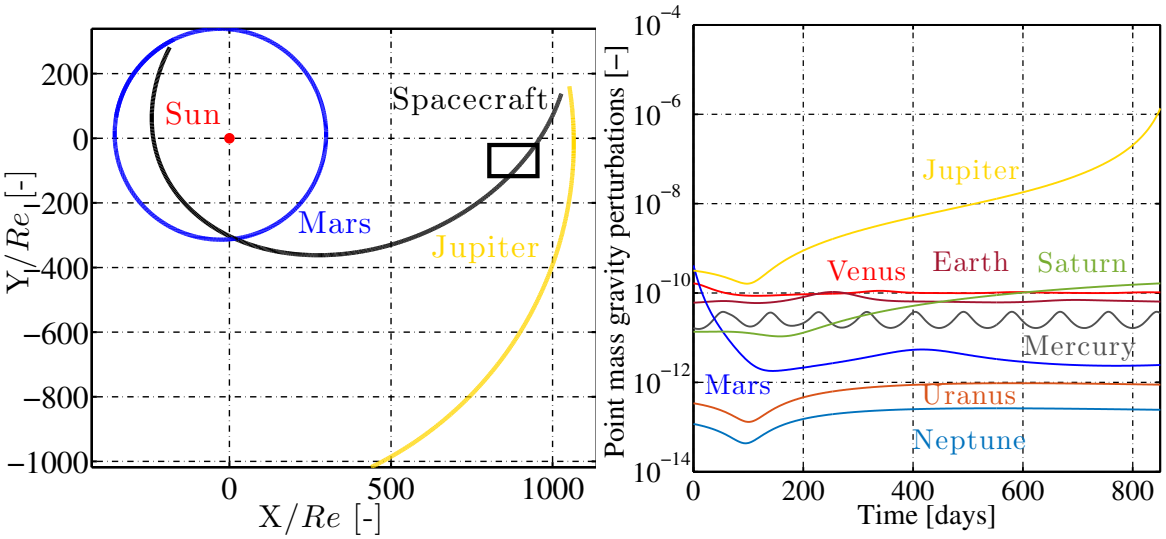

(a) Trajectories joining Mars and Jupiter.

(b) Evolution of the point mass gravity perturbations.

Figure 4.20: The central body is the Sun. The departure date is on 7 November 1996 TT. The departure and arrival planets are respectively Mars and Jupiter.

The following test case is proposed. An interplanetary trajectory between Mars and Jupiter lasting 802 days ($\approx$ 2 years) is chosen. It is shown on the left graph in Figure 4.20. The right graph

provides the evolution of the planetary PMG perturbations during the propagation. At the beginning, Mars has the dominant effect. Indeed, the spacecraft is within the Mars sphere of influence. Its contribution decreases drastically outside SOI due to its small gravitational parameter. Jupiter becomes the first contributor outside the spheres of influence. Its contribution increases during the propagation. The spacecraft gets closer to it. The right graph in Figure 4.20 also shows that the conclusions drawn in the case of motion within SOI remain valid. The Earth and Venus have significant contributions due to their close proximity to the spacecraft. The contributions of Uranus and Neptune affect the trajectory weakly due to their large distance with the spacecraft. Saturn has a high gravitational parameter and the spacecraft gets closer to it during the propagation. At the end, it becomes the second contributor.

There is a difference between the motion within and outside the spheres of influence. Even if the order is the same in terms of PMG contributors, the impact on the spacecraft trajectories is much larger in the case of motion outside SOI. The distance between the two-body trajectory and the trajectory taking into account the PMG perturbations is represented on the left graph in Figure 4.21. This distance is mainly due to Jupiter apart from the strong increase in the beginning due the combined effect of Jupiter and Mars. In section 4.2.2, it has been shown that the planetary PMG perturbations change only the final position by 8 m after 4 days of propagation compared to the two-body trajectory. A motion lasting four days inside the SOI of Mars was considered. The position changes by 828 km compared to the two-body trajectory between the days 300 and 304 in the Mars-Jupiter trajectory. The planetary point mass gravity perturbation must be included in the motion outside the spheres to obtain realistic propagation, whereas it is included to obtain high-fidelity propagation within the SOI.

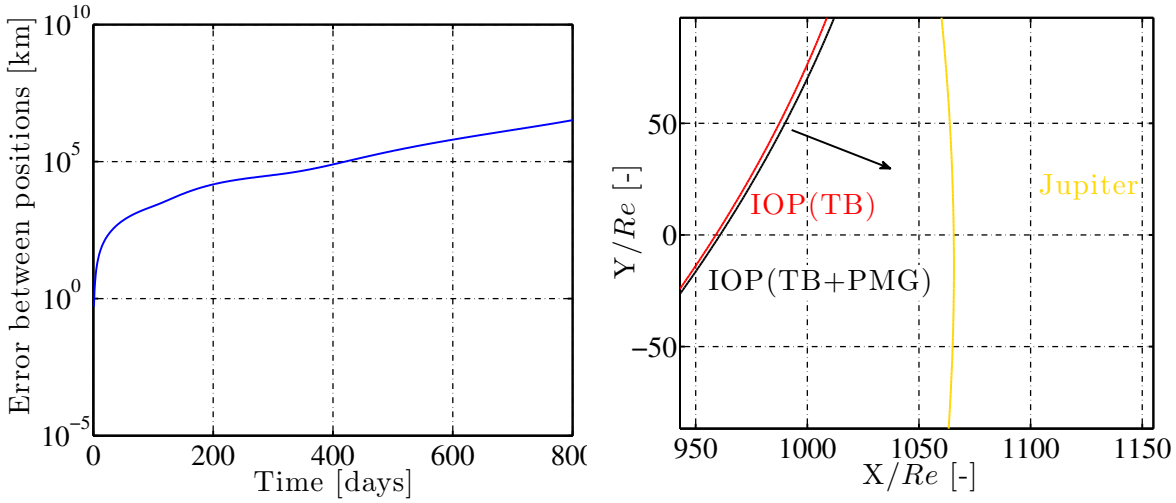

(a) Distance between positions.

(b) Zoom on the black rectangle.

Figure 4.21: The central body is the Sun. The departure date is on 7 November 1996 TT. The departure and arrival planets are respectively Mars and Jupiter. The left graph shows the distance between the two-body and two-body+PMG trajectories. The right graph shows the effects of the Jupiter point mass perturbation on the trajectory.

If a zoom is performed on the black rectangle in Figure 4.20, it is seen that Jupiter attracts the spacecraft close to it (right graph in Figure 4.21). In fact, each planet tries to attract the spacecraft

within its sphere of influence. The resulting motion depends on the strength of the attractions and the distance between the spacecraft and the planets.

The spacecraft can pass close to new kinds of celestial bodies during interplanetary missions. It includes asteroids and dwarf planets. Only the dwarf planets respond to the point mass gravity approximation. Indeed, the asteroids have complex shapes departing considerably from a sphere. New gravitational models have to be built for these celestial bodies. The focus is on the dwarf planet Pluto. For example, the mission New Horizons has visited Pluto. This celestial body is located farther than Neptune. A trajectory starting from Neptune and lasting 30 years is chosen. The spacecraft goes in the direction of Pluto during all the propagation. It is represented on the left graph in Figure 4.22. The red and blue curves on the right graph represent the distances with GMAT if the Pluto PMG is included or not in IOP. The point mass gravity perturbation of Pluto only disturbs the final spacecraft position by 80 km in 30 years. It comes from the fact that Pluto is a dwarf planet which means that its mass is small. As a result, its gravitational parameter is 22 times smaller than the gravitational parameter of Mercury. Mercury is the planet with the smallest gravitational parameter. If the spacecraft comes very close to Pluto, the impact on the spacecraft trajectory would be significant. An exact modelling of the interplanetary spacecraft trajectory implies to include the gravitational perturbations of each celestial body in our solar system. The two-body approximation is chosen to compute the Pluto ephemerides. The errors are represented in blue in Figure 4.22. The Pluto point mass gravity model only reduces to 69 km the error on the final spacecraft position. It provides an idea of the accuracy obtained if the two-body ephemerides were chosen instead of the VSOP87 planetary theory.

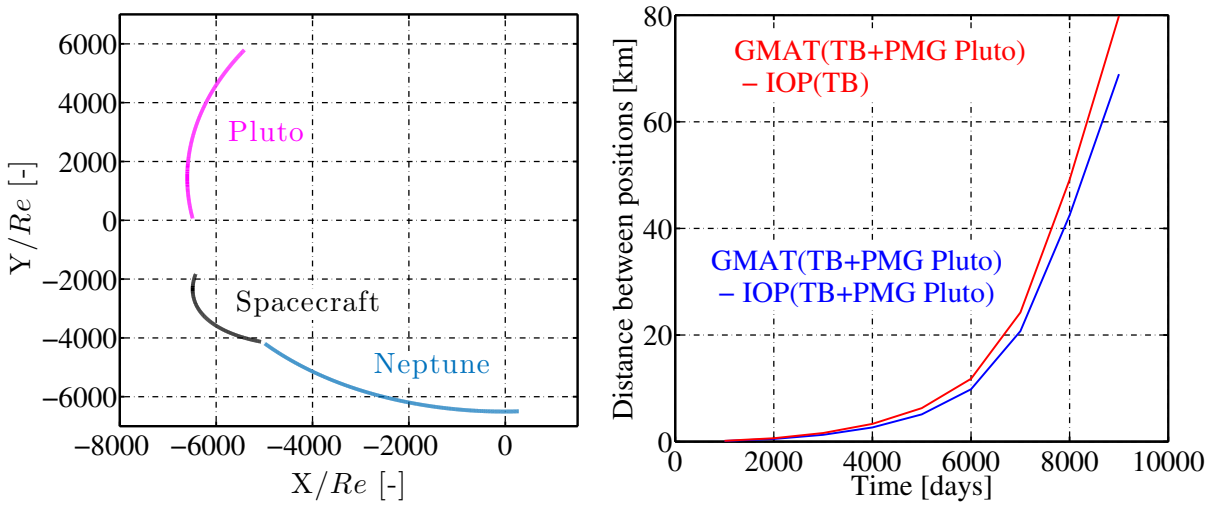

(a) Trajectory between Neptune and Pluto.

(b) Distance between positions.

Figure 4.22: The departure date is on 7 November 1960 TT. The departure planet is Neptune. The propagation lasts 30 years. The left graph shows the trajectory. The right graph shows the impact of the Pluto PMG on the spacecraft trajectory. The blue curve shows the accuracy obtained with two-body ephemerides.

4.4 Possible improvements

The case of an orbit escaping the Earth is chosen to illustrate the different improvements. The propagation lasts five days. The distances between the idealized two-body trajectory and the trajectory followed if each perturbation is turned on separately are computed. The results are given in Figure 4.23.

First, the improvements associated with the gravitational field of the central body are discussed. The flattening of the poles is the main departure from the spherical gravitational attraction. However, there exist many small other corrections to model perfectly the planetary gravitational fields. GMAT provides the corrections for the Earth, Mars and Venus. The gravitational field of the Earth is the most well-known. The corrections are given up to 360×360. The corrections are known respectively up to 80×80 and 75×75 for Mars and Venus in GMAT [18]. A routine can be implemented to read these coefficients in the files and to apply the corresponding corrections to the spacecraft. The form of the files are standardized. Therefore, a general routine can be written. Figure 4.23 shows that the gravitational field is the fourth contributor if the J2 contribution is retrieved. It represents 3.3% of the total perturbed trajectory for the Earth. After one day of propagation, it changes the final position by 47 km. This contribution increases for nearly closed orbits around the planets. The smaller the altitude is the higher its contribution is. The contributions of the complete gravitational field of planets are negligible for motions outside the spheres of influence.

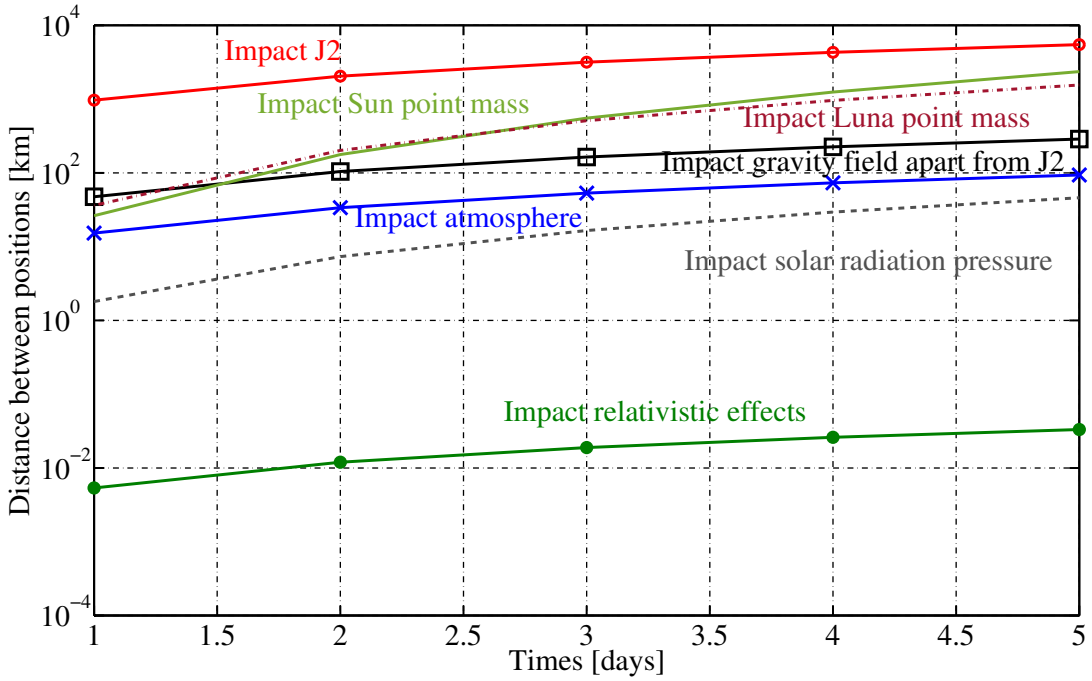

Figure 4.23: The distances between the idealized two-body trajectory and the trajectory followed if each perturbation is turned on separately are computed. The case of an orbit escaping the Earth is chosen to illustrate the different improvements. The propagation lasts five days. The results are computed with GMAT.

Another perturbation linked to the central body is the atmosphere. The impact of the atmosphere is significant at low altitude. For the Earth, the impact of the atmosphere is negligible above 1200 km [4]. The atmospheric density at each point around the considered planet must be known to model the impact of the atmosphere on the spacecraft. This represents a difficult topic. Each planet has an atmosphere. However, the impacts of the atmospheres of Mercury and Mars are negligible due to their small sizes [29]. Jacchia–Roberts atmospheric model is used for the test case. The escape orbit starts at an altitude of 166 km where the impact of the atmosphere is dominant. It represents the fifth contributor. It represents 1% of the total trajectory perturbation. The errors on the positions become significant for nearly closed orbits at small altitude around the different planets. After one day of propagation, it changes the final position by 15 km.

Some minor contributions can be included if a very high-fidelity propagation is required such that relativistic corrections, solid and ocean tides. For example, the relativistic corrections only disrupts of 5 m the spacecraft trajectory after one day of propagation. In addition, the fact that the J2000 frame is not perfectly inertial can be taken into account.

The perturbations taken into account in IOP are also represented in Figure 4.23. How can be improved the different models? What are their contributions on the spacecraft motion? The main contributor is the flattening of the poles perturbations. It represents 64% of the total perturbed trajectory. After one day of propagation, it changes the final position by 968 km. Its impact decreases when the spacecraft goes away from the planets. The point mass gravity models can be improved by taking into account the different moons and asteroids. The shape of the moons must be close to a sphere so that the point mass assumption is valid. The asteroids do not fulfill these requirements and another model should be used. For the Earth test case, the point mass perturbations of Moon and Sun are the second and third contributors. Moon is dominant in the first two days of propagation when the spacecraft is within the sphere of influence of the Earth. After that, the Sun becomes the dominant perturbation. The last perturbation taken into account in IOP is the solar radiation pressure. The shape of the spacecraft can be modelled with higher accuracy by modelling the spacecraft as box-wings constituted of six flat plates [17]. In addition, the planetary albedo can be taken into account. Planetary albedo is a measurement of the amount of light reflected from the surface of a planet. Venus has the highest albedo: 0.84, whereas the Earth has an albedo of 0.37. In general, the direct solar radiation pressure dominates the albedo. However, their contributions can be of comparable magnitude on some sun-synchronous orbits [10]. Eventually, the most advanced conical eclipse model can be implemented.

Chapter 5

Main algorithm and application

The previous chapters focused on the validation of the propagator and the physical interpretation of the results. The objective of this chapter is to study the algorithms behind IOP and to apply the propagator to Cassini-Huygens mission. The chapter begins with the presentation of the main algorithm. Then, the choices of the numerical integrators and parameters are discussed. The chapter concludes with the application of the propagator to the Cassini-Huygens mission.

5.1 Main algorithm

The general procedure followed by the propagator is shown in Figure 5.1. The codes are provided in Appendix C. The inputs required by the propagator and the outputs are first presented. The initial position and velocity vectors of the spacecraft are given by six orbital elements: $(a, e, i, \omega, \Omega, \phi)$. In addition, the input SOI_{flag} allows the user to indicate in which coordinate system the initial conditions are expressed. Table 5.1 provides the coordinate systems associated with the different values of the variable SOI_{flag}. SOI_{flag} is linked to the distance between Sun and the planets. For example, Venus is the second planet from the Sun. $SOI_{\text{flag}} = 2$ in this case. $SOI_{\text{flag}} = 10$ is arbitrarily associated with the Sun.

SOI_{flag}	*Inertial coordinate system*
1	Mercury
2	Venus
3	Earth
4	Mars
5	Jupiter
6	Saturn
7	Uranus
8	Neptune
10	Heliocentric

Table 5.1: This table provides the coordinate systems associated with the different values of the variable SOI_{flag}.

If a number between 1 and 8 is introduced for the input SOI_{flag}, the spacecraft starts in the sphere of influence of the associated planet. Otherwise, the spacecraft starts outside the SOI of the

eight planets. The following input consists of the departure date in terrestrial time ($Year$, $Month$, Day, $Hour$, $Minute$, $Second$). The choice of terrestrial time is driven by the ephemerides expressed in this time system. The departure date allows the propagator to locate the planets, the Moon, the Sun and the dwarf planet Pluto in the solar system during all the propagation. This information is needed to design interplanetary trajectories, to perform change of coordinate systems and to take into account the perturbations acting on the spacecraft. The ballistic properties ($m, A_{\text{sun}}, C_{\text{R}}$) are also needed to properly model the impact of the solar radiation pressure on the spacecraft. The user can decide which perturbations it wishes to take into account. The inputs ($onOffJ2, onOffSRP, onOFFPMG$) are equal to 1 if the flattening of the poles, solar radiation pressure and point mass gravity perturbations are respectively activated. Otherwise, they are put to 0. The general form of the equations of motion (Equation 4.1) allows the propagator to add each effect linearly. If more than one perturbation is activated, the effects can be combined by summing the different contributions. The last three inputs are directly related to the outputs. The first two ones are the duration of the propagation $duration$ and the time step dt at which the user wishes to know the position and the velocity vectors of the spacecraft. IOP always return the positions and the velocities of the spacecraft in the heliocentric inertial coordinate system at the desired time steps. The last input, SOI_{target}, indicates a planetocentric coordinate system in which the positions and velocities of the spacecraft wish to be known. The spacecraft trajectory can be visualized from any planets. SOI_{target} is between 1 and 8.

The output t_vector contains the times in terrestrial time at the desired time steps: t_vector = $[0\ dt\ 2dt\ \ldots\ duration]^T$. It consists of a n×1 vector. r_helio and $rdot\_helio$ are respectively the positions and velocities of the spacecraft in the heliocentric coordinate system at the times contained in t_vector. The positions are given in km and the velocities are given in km/s. Their sizes are 3×n. r_planet and $rdot\_planet$ are respectively the positions and velocities of the spacecraft in the planetocentric coordinate system specified by SOI_{target}. This is of particular interest when the spacecraft is located on nearly closed orbits around a given planet. The last two outputs are related to the detection of events. te_vector contains the times at which the spacecraft entered or left a sphere of influence. For example, this output gives the time needed to reach the sphere of influence of Jupiter for the interplanetary trajectory explained in section 4.3.2. If a longer propagation was considered, the second time in this vector would give the time the spacecraft spent in the sphere of influence of Jupiter. The last output, $location$, contains the regions in which the spacecraft has gone through. In the case of Mars-Jupiter trajectory, this output gives: $[10\ 5]^T$. The spacecraft starts in the heliocentric coordinate system. Then, it passes through the sphere of influence of Jupiter (SOI_{flag}= 5).

Figure 5.1 shows the procedure to convert the inputs into outputs. The propagator starts with the initialization of key variables. First of all, the initial orbital elements and the input SOI_{flag} are used to compute the initial position and velocity vectors. The departure date is used to determine the initial Julian date $jd_$init in terrestrial time. The Julian dates in days are needed to evaluate the positions and velocities of the Sun, the planets, the Moon and the dwarf planet Pluto during all the propagation. After a time t [s] of propagation, the current Julian date is given by

$$jd = jd\_\text{init} + \frac{t}{86400}, \tag{5.1}$$

where 86,400 corresponds to the number of seconds in one day. At this stage, the propagator enters in the loop while. The propagation stops when the current time $t\_current$ exceeds the duration of the propagation specified by the user. The following example is chosen to illustrate the procedure.

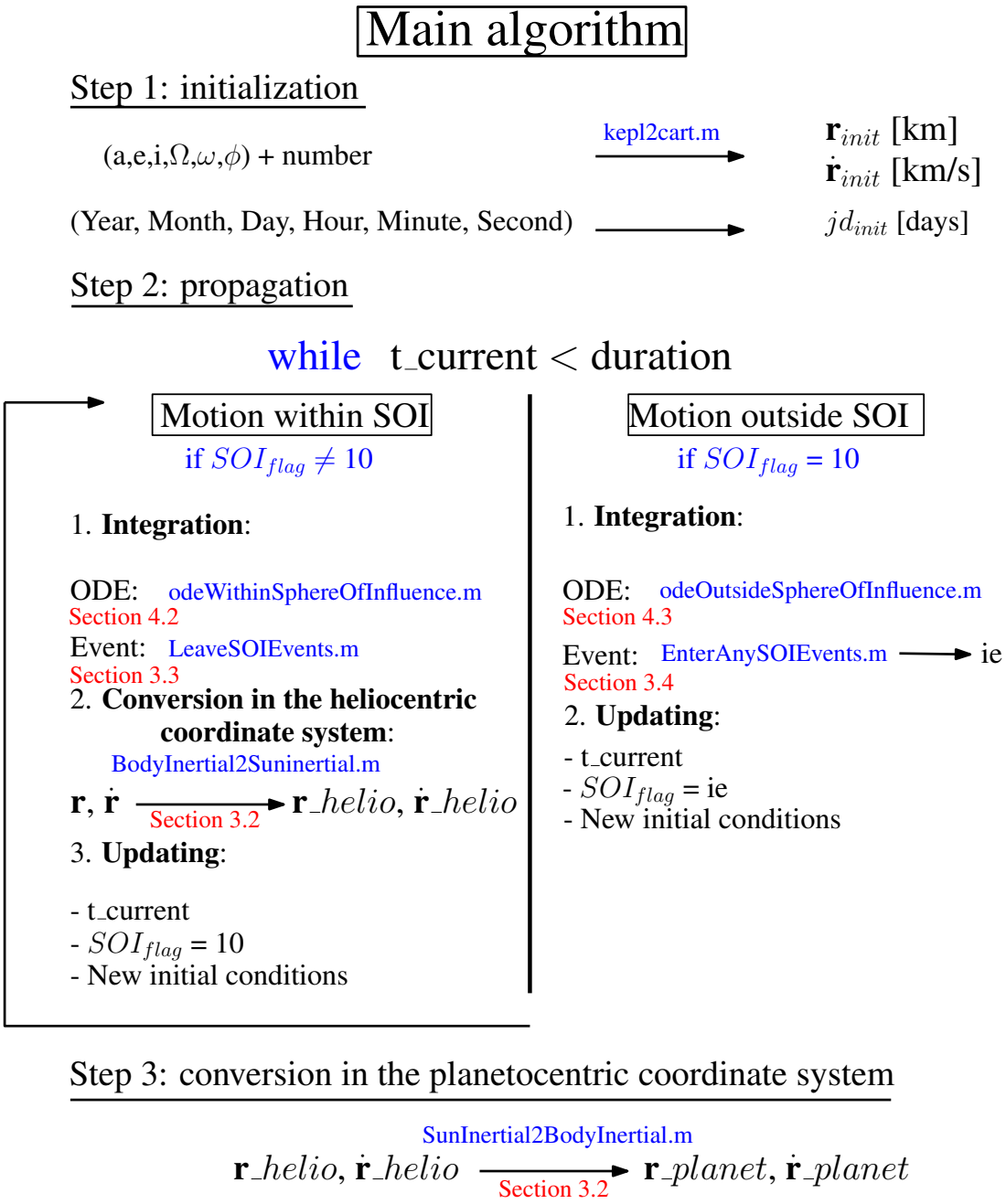

Figure 5.1: The figure describes the main algorithm behind IOP. The files .m written in blue correspond to the MATLAB functions used at the different steps. The sections in red indicate the sections of the thesis in which the different topics have been discussed.

Consider a spacecraft starting in the SOI of Venus. SOI_{flag} associated to the initial coordinate system is 2. 2 is different from 10. Therefore, the propagator enters in the left part of the loop in Figure 5.1. The dimensionless initial conditions are obtained with the characteristic variables associated to Venus. The numerical integration is performed. The current time $t\_current$ is equal to 0. Each integration is initially designed to go from 0 to $duration$-$t\_current$. Two causes can stop the integration. First, the spacecraft never leaves the sphere of influence of Venus. In this case, the motion of the spacecraft is within the SOI of Venus during all the propagation. It represents the case of nearly closed orbits around Venus or if the duration is not long enough to cross the SOI of Venus.

The second cause happens if the spacecraft crosses the Venus's SOI. This event occurs at t_e and stops the integration. The time at which the event occurs does not necessarily match with one of the times in t_vector specified by the user. The propagator retains the time at which the event occurs and uses the past time specified by the user the closest from the event time as the current time. The position and velocity vectors of the spacecraft at the event time are deleted. Before pursuing the integration, the positions and velocities until the current time are converted in the heliocentric coordinate system. At this stage, r_helio and $rdot\_helio$ are full until the current time. r_planet and $rdot\_planet$ are empty. Indeed, the user does not necessarily require the positions and velocities of the spacecraft in the Venus inertial coordinate system. te_vector contains the time at which the spacecraft has left the SOI of Venus and $location$ contains the numbers 2 and 10.

If the current time is shorter than the duration, the propagator moves into the right part of the loop in Figure 5.1. The final position and velocity of the previous integration converted in the heliocentric coordinate system are used as initial conditions. As previously, two cases are considered. First, the spacecraft can end its propagation in the heliocentric coordinate system. The integration lasts $duration\text{-}t\_current$ seconds. Otherwise, the integration stops due to the fact that the spacecraft enters the SOI of a planet. The steps used at the end of the first integration are repeated apart from the conversion in the heliocentric coordinate system. The event returns the SOI_{flag} of the sphere of influence the spacecraft is just crossing. A third integration is performed within the sphere of influence of this planet. The procedure described above is repeated until the current time exceeds the duration of the propagation. The final operation is to convert all the heliocentric positions and velocities in the planetocentric coordinate system specified by the user.

5.2 Tolerance and ordinary differential equation solvers

The motion of spacecraft is described by ordinary differential equations. The dimensionless time is the independent variable. Numerical integrators are needed to predict the positions and the velocities of the spacecraft. The second order ordinary differential equations can be recast as

$$\dot{\mathbf{U}} = f(\mathbf{U}, t), \tag{5.2}$$

where $\mathbf{U} = [\mathbf{r}\ \dot{\mathbf{r}}]^T$ defines the state of the spacecraft. Only the results of the numerical integration have been discussed until now. The numerical choices behind the results are still unknown. This section is devoted to this topic.

A first choice between constant time step and variable-time step solvers has to be performed. The ideal time step is linked to the variation of the solution. A small time step is needed when the solution varies rapidly to capture all the physics. In contrast, a higher time step can be chosen if the solution varies slowly. It allows the propagator to reduce the computational time. The variation of the solution depends on the shape of the orbits and their associated parameters. For example, the solution varies rapidly at the periapsis of a highly elliptic orbit and varies slowly at apoapsis. A rule of thumb said that automatic step size should be used for orbits with eccentricities greater than 0.1. IOP allows us to compute all types of orbits. A variable time step is the most suitable option in this case. The drawback of this choice appears in the case of circular orbits [24]. The velocity is almost constant during all the propagation. The variable time step solver spends its time to perform trial and error. At the end, it always comes back to the same size of time step. A constant time step reduces the computational time in this case.

The second choice is about absolute and relative tolerances. The tolerances are linked to the accuracy of the solution. The absolute tolerance avoids abnormally huge results as the one obtained by a division by zero for example [21]. The relative error allows the solver to choose the size of the adaptive time step [21]. In fact, the relative tolerance is the key driver of an accurate solution. The absolute tolerance is only useful in extreme cases and is arbitrarily taken equal to the relative tolerance. The smaller the relative tolerance is the higher the accuracy of the solution. The orbits escaping the planets are chosen to select the tolerances. The propagation lasts one day. The errors on the final spacecraft position are shown in function of the relative tolerances on the right graph in Figure 5.2. It is shown that the spacecraft propagation requires stringent error tolerances. The solutions start to converge at a tolerance of 10^{-10}. At 10^{-12}, the solutions reach a plateau. Indeed, the solutions for a tolerance of 10^{-14} are very close to those obtained with a tolerance of 10^{-12}. The absolute and relative tolerances of 10^{-12} are therefore chosen. It has to be stressed that the relative tolerance enables us to control the truncation errors. Truncation errors come from the inexact numerical solutions of the differential equations. However, the computers can carry only finite number of digits. This introduces round-off errors. These uncontrolled errors become significant for long propagation and fast-varying solutions. Indeed, fast-varying solutions decrease the time steps which increase the amount of round-off errors [17].

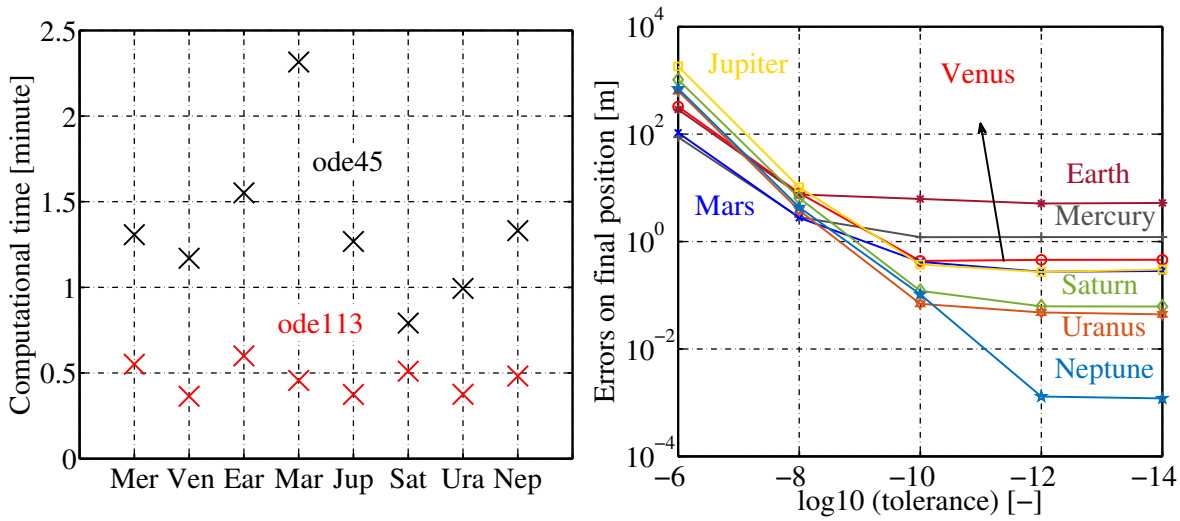

(a) Comparison of the computational time.

(b) Tolerances.

Figure 5.2: Numerical choices.

The third choice is the solver. MATLAB provides two variable-time step solvers: ode45 and ode113. The first one uses the Runge-Kutta methods. ode45 is based on the Runge-Kutta of order 4 and 5. The comparison between the two solutions allows the solver to determine if the time-step should be increased or decreased [24]. It is performed by comparing the local truncation error with the specified relative tolerance. The strength of the Runge-Kutta methods is to be single step methods. Only the previous state is used to compute the current state. The second solver, ode113, is based on the Adams-Bashforth Moulton method of orders 1 to 13. It consists of a multi-steps method. It means that the state of the spacecraft at time t_{n+1} is deduced from the state at previous times. It requires single step methods (Runge-Kutta methods) as starter because the back values are not yet available [24]. If the same absolute and relative tolerances are entered in the two solvers, the

accuracy of the solution is identical. Only the time needed to reach the solution differentiates the two solvers. The profiler of MATLAB is used to determine the time the algorithm spent in IOP. This tool is useful to compare different routines. However, the absolute time does not give the truth about the time needed to compute the propagation. The time taken by the profiler to perform its analysis is taken into account in the total time. The profiler is therefore used to obtain the general trends. The results are given on the left graph in Figure 5.2. All the perturbations are activated. The time spent in IOP is shown if ode113 or ode45 are respectively chosen as solvers. ode113 is more efficient than ode45 for the problems with stringent error tolerances considered. It is on average 53 seconds faster than ode45.

5.3 Cassini-Huygens mission

This section focuses on the study of the Cassini-Huygens mission. More specifically, the aims are to recreate the trajectory and the velocity of the Cassini-Huygens mission in the heliocentric coordinate system. This implies to discuss fly-by manoeuvres. The main objective of the Cassini-Huygens mission is to study the planet Saturn, its ring and its moons. It was launched on 15 October 1997 and spent 13 years orbiting Saturn. One of the challenges to perform such mission is to travel the 1,279,796,101 km separating the Earth and Saturn. There exist no launcher able to provide enough energy to Cassini-Huygens mass (5,720 kg) to reach Saturn directly. The flyby manoeuvre is introduced in that context. It uses the gravitational field of a planet to increase the spacecraft energy/velocity without propellant.

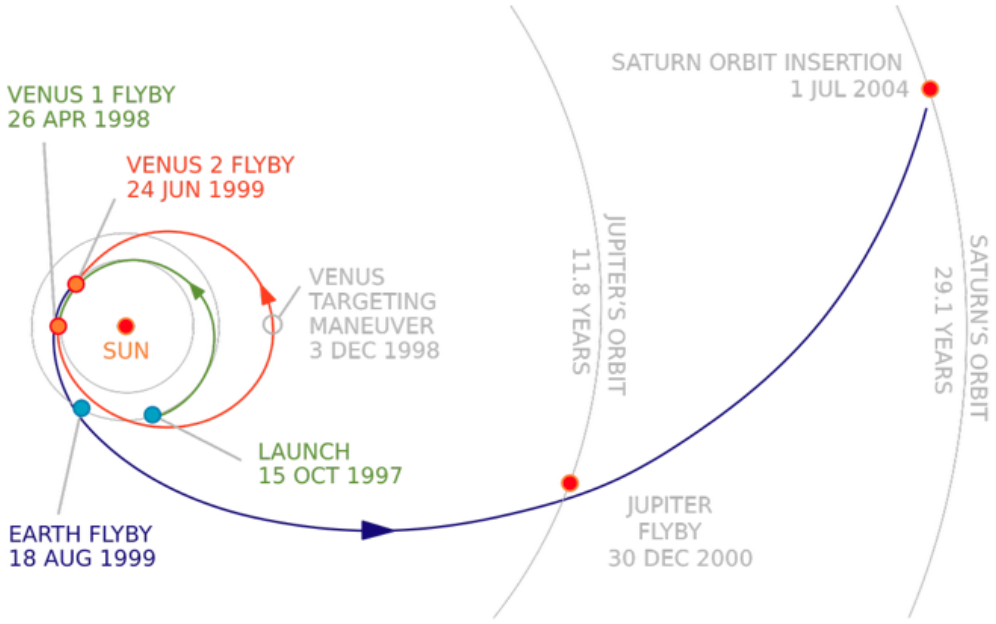

Figure 5.3: The figure represents the trajectory of the Cassini-Huygens mission and gives the departure and arrival dates as well as the departure and arrival planets of the Cassini-Huygens mission. The figure comes from [27].

Four flybys maneuvers have been performed during the mission. The dates and the flyby planets are given in Figure 5.3. It includes two flybys of Venus, one of the Earth and one of Jupiter. The

flybys of Venus and the Earth are used to obtain enough velocity. The one of Jupiter shortens the travel time by two years.

Flyby Planets	*Cassini* (km)	IOP (km)
Venus	284	3,000
Venus	603	609
Earth	1,166	1,166
Jupiter	9,720,000	9,721,907

Table 5.2: Closest approach between the spacecraft and the flyby planets. The first column is the values given by NASA. The second column contains the values obtained with IOP.

The departure and arrival dates as well as the departure and arrival planets given in Figure 5.3 are used to design the trajectories with Lambert's problem. The solar radiation pressure and point mass gravity perturbations are included in IOP. As explained in section 4.3.2, the code does not converge if the centre of the departure planet is used as initial position. A small change in initial true anomaly has to be introduced. How this degree of freedom can be used? It is used so that the closest approach of the flyby planets are as close as possible to the real values. The values provided by the NASA are given in the first column in Table 5.2. The second column provides the closest approach obtained with IOP. These values are obtained by trial and error.

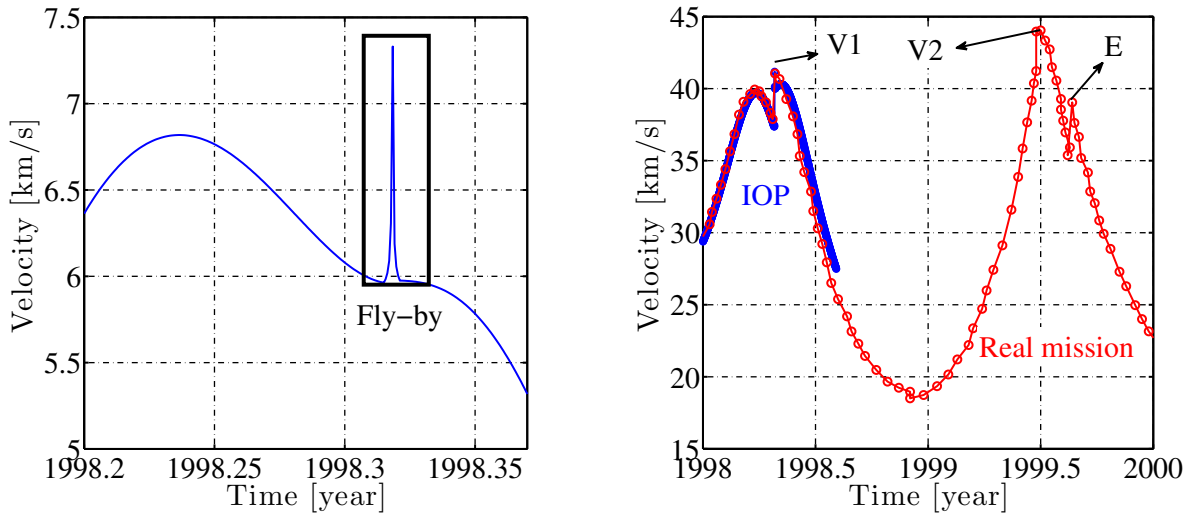

(a) View in the Venus coordinate system.

(b) View in the heliocentric coordinate system.

Figure 5.4: Velocities of Cassini-Huygens given in the Venus (left graph) and heliocentric (right graph) coordinate systems during the first flyby of Venus. V1 stands for the first flyby of Venus, V2 stands for the second flyby of Venus. E stands for the flyby of the Earth. The data of the red curve come from JPL Horizons Ephemeris System. The ballistic properties are: m=5,720 kg, A = 26.8 m^2.

The first fly-by of Venus is discussed. It is used to understand the physics behind the fly-by manoeuvre. The departure date is on 15 October 1997. The propagation stops 100 days after the

first flyby of Venus. The evolution of the Cassini-Huygens velocities in the Venus and heliocentric coordinate system are shown in Figure 5.4. The velocity in the Venus coordinate system is obtained by introducing $SOI_{\text{target}} = 2$ in IOP. The left graph shows the evolution of the velocity predicted by IOP during the fly-by in the Venus coordinate system.

The spacecraft arrives at Venus and performs a gravity-assist maneuver also called fly-by trajectory. The flyby trajectory is an osculating hyperbola view from Venus. The velocity is given by

$$v = \sqrt{\mu(\frac{2}{r} - \frac{1}{a})} \tag{5.3}$$

assuming that the impact of the point mass gravity attractions and solar radiation pressure are neglected during the fly-by. In the first part of the flyby, the spacecraft goes to the periapsis of the hyperbola, i.e, the closest point from Venus. The norm of the position in the Venus coordinate system decreases so that the spacecraft velocity increases in Equation 5.3. The spacecraft velocity decreases when the spacecraft goes away from the periapsis. At the end of the fly-by, the spacecraft has the same velocity as at the beginning. It is due to the fact that the specific forces applied to the spacecraft are conservative apart from the SRP which has a negligible impact during the flyby. The energy is conserved.

This explanation highlights the fact that the increase in velocity is only visible in the heliocentric coordinate system. The right graph in Figure 5.4 contains two curves. The red curve is the data provided by JPL Horizons Ephemeris System. The first three flybys are represented. The blue curve is the evolution of the velocity during the first flyby predicted by IOP. According to the Kepler's second law, 'a line segment joining a spacecraft and the Sun sweeps out equal areas during equal intervals of time'. Therefore, the spacecraft velocity increases when it goes closer to the Sun and decreases when it goes away from the Sun [14]. The distance between the spacecraft and the Sun decreases when the spacecraft goes from the Earth to Venus. As a result, its velocity increases when the spacecraft approaches Venus.

Then, the spacecraft performs the fly-by. The spacecraft velocity increases between the beginning and the end of the gravity assist manoeuvre. The duration of the flyby is small compared to the time the spacecraft spent on the interplanetary trajectory. The change of velocity can be assimilated to an impulse manoeuvre. It means that the change of velocity is immediate. The magnitude of the change of velocity depends on the gravitational parameter of the flyby planet and the proximity between the spacecraft and the flyby planet. The smaller the distance is the higher the change in velocity is. On the right graph in Figure 5.4, the change of velocity predicted by IOP is 2.94 km/s. The curve corresponding to the real velocity still increases when the velocity predicted by IOP starts to decrease. IOP underestimates the gain in velocity. It comes from the fact that the closest approach of the real mission is 284 km. The trajectory designed with IOP passes to at a higher altitude: 3,000 km. The real change of velocity is 3.7 km/s. The change in spacecraft energy with respect to the Sun is provided through an exchange of angular momentum of Venus, in orbit around the Sun, to the spacecraft. The mass of Venus is much larger than the spacecraft mass. Therefore, its change of velocity is negligible [11]. The relative error is used to assess the accuracy of the results. It is defined as

$$\epsilon_{\text{rel}} = \frac{v_{\text{IOP}} - v_{\text{real}}}{v_{\text{real}}} \tag{5.4}$$

A mean relative error of 0.84% is found between the beginning of the mission and 100 days after the fly-by of Venus.

The second flyby planet is also Venus. A special event happens during this second manoeuvre. Figure 5.3 indicates that a Venus targeting manoeuvre is performed on 3 December 1998. In fact, the launch and manoeuvre errors as well as the small perturbations acting on the spacecraft can prevent the arrival to Venus. Trajectory Correction Manoeuvre (TCM) is therefore applied to the spacecraft. 22 TCM's have been used in total during the Cassini-Huygens mission. These manoeuvres used thrusters which are not modelled in IOP. Only ballistic flights are considered. Therefore, the zoom present on the right graph in Figure 5.5 shows that the red curve changes abruptly whereas the blue curve follows its smooth change of velocity. This event creates a gap between the change of velocity of the real mission and the one predicted by IOP after the TCM. As a result, the mean relative error increases to 2.24% for the part of the mission simulated in Figure 5.5. The left graph represents the impact of a flyby on the spacecraft trajectory. At the end of the propagation, the spacecraft is on an orbit with a higher osculating semi-major axis which means an orbit with higher energy than the orbit at the beginning of the propagation. This gain is due to the fly-by. It is 3,1 km/s. The spacecraft trajectory predicted by IOP (left graph in Figure 5.5) is close to the one given in Figure 5.3.

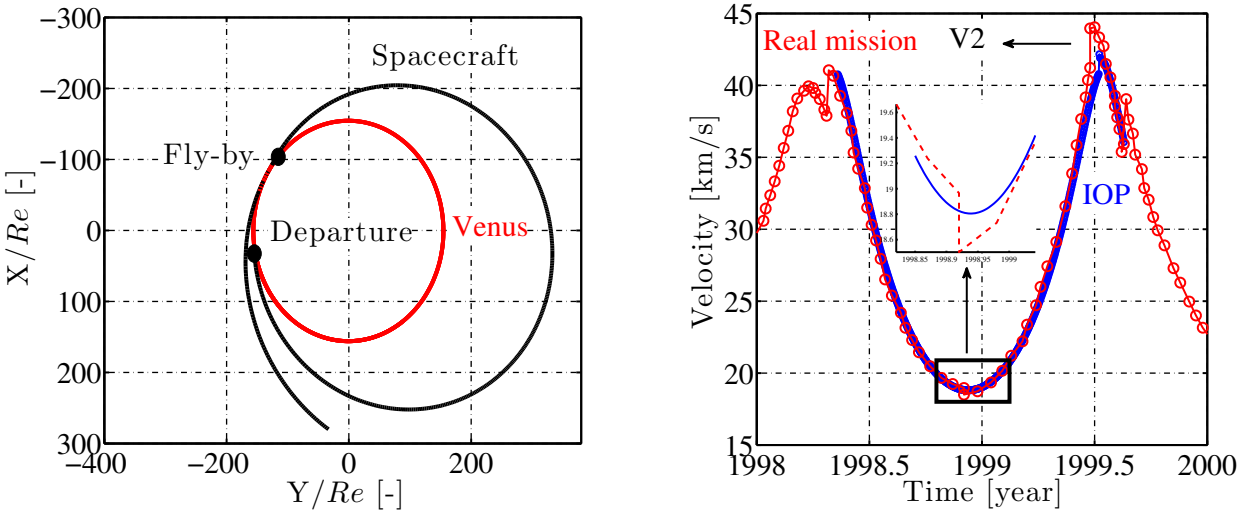

(a) Trajectory predicted by IOP.

(b) View in the heliocentric coordinate system.

Figure 5.5: Second flyby. The data of the red curve come from JPL Horizons Ephemeris System. The ballistic properties are: m=5,720 kg, A = 26.8 m^2.

The last two flybys are about the Earth and Jupiter. As written in Table 5.2, the closest distance between the Earth and the spacecraft are the same for IOP and the real mission. However, choosing this constraint helps to reduce the gap between IOP and the real mission. It does not ensure that they follow the same osculating flyby hyperbola. As a result, the change in velocity predicted by IOP, 4.4 km/s ,is realistic, but it is not the exact value: 4.1 km/s. Comparing Figure 5.3 and Figure 5.6 highlights the similarities between the real trajectory and the one designed by IOP. The mean relative error is 0.97% for the third simulation.

The magnitude of the change of velocity depends on the gravitational parameter of the flyby planet and the proximity of the periapis of the flyby hyperbola. In the case of Jupiter, the gravitational parameter is the highest. However, the change of velocity is moderate due to the fact that the flyby is performed far from Jupiter at the scale of Jupiter. Jupiter possesses an important radiation belt.

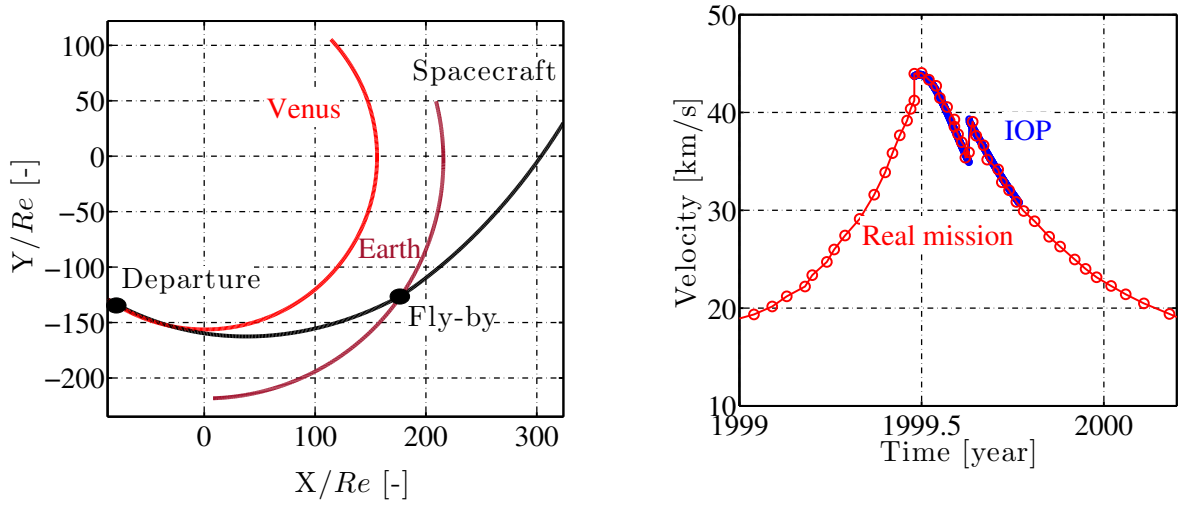

(a) Trajectory predicted by IOP.

(b) View in the heliocentric coordinate system.

Figure 5.6: Third flyby. The data of the red curve come from JPL Horizons Ephemeris System. The ballistic properties are: m=5,720 kg, A = 26.8 m^2.

It is detrimental for the spacecraft to get close to it. For example, the radiation could destroy the on-board electronics. The remarks done for the Earth are still valid. The IOP trajectory is close to the real one as can be seen in Figure 5.7. IOP gives ΔV=1.28 km/s and the real change of velocity ΔV=2.1 km/s. The change of velocity is underestimated as for the first flyby of Venus. The closest approach is significantly higher in the case of IOP. As a result, the mean relative error is 2.83%. The last part of the trajectory between Jupiter and Saturn is not represented. The spacecraft goes away from the Sun and its velocity decreases.

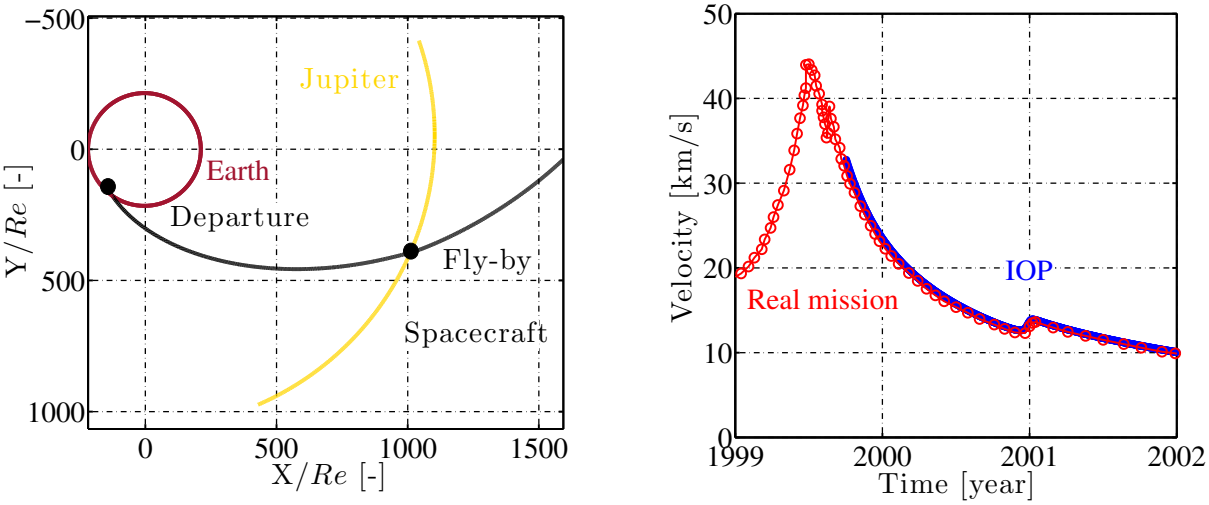

(a) Trajectory predicted by IOP.

(b) View in the heliocentric coordinate system.

Figure 5.7: Fourth flyby. The data of the red curve come from JPL Horizons Ephemeris System. The ballistic properties are: m=5,720 kg, A = 26.8 m^2.

IOP allows to recreate the mission with a high degree of confidence during the first four years. The average of the relative errors is $1.95\ \%$. However, the 61 moons orbiting Saturn are not included in IOP. It prevents the simulation of the end of cassini-Huygens mission. In addition, orbital manoeuvres, which consist of one of the orbital propagator pillar, should be included in IOP to recreate the manoeuvres around Saturn and its moons. For example, the manoeuvres are needed to correct launch errors, to insert spacecraft within nearly closed orbits, to change the inclination and the semi-major axis of an orbit. The additional perturbation linked to the manoeuvres is the thrust coming from the vehicle's engines. It implies also that the mass is not constant any more.

Conclusion

The objective was to develop a high-fidelity orbital propagator for interplanetary space missions. The propagator should include accurate ephemerides of our solar system and high-fidelity dynamical models. More specifically, perturbations due to the non-sphericity of the attractors, the solar radiation pressure, eclipse models and point mass gravity attractions should be taken into account. Lambert's problem should also be included in the propagator.

The most basic method to compute planetary ephemerides is the two-body approximation. It describes the motion of a planet considering that the Sun and the selected planet as the only celestial bodies in the solar system. The semi-analytic method VSOP87 based on integrated ephemeris DE200 is implemented in IOP. Data provided by the authors of VSOP87 planetary theory are used to validate the results. The positions of the planets in the heliocentric coordinate system for 77 dates have been provided. The mean error between IOP and these data only represents $2\times10^{-6}\%$ of the planetary semi-major axes. The Development Ephemeris DE405 is one of the most used and accurate integrated Development Ephemerides. DE405 is used to assess the accuracy of the results. The semi-analytic method VSOP87 takes into account the secular and periodic perturbations between the considered planet and the other celestial bodies (planets and asteroids).

Planets	*Error between positions TwoBody-DE405* (km)	*Error between positions VSOP87-DE405* (km)
Mercury	9,974	281
Venus	7,261	903
Earth	19,434	13,196
Mars	74,682	4,782
Jupiter	1,240,540	63,502
Saturn	6,722,816	189,192
Uranus	38,842,630	567,825
Neptune	42,992,237	153,717

Table 5.3: Comparison between the two-body method and VSOP87 planetary theories. The values are averaged of the errors with DE405 computed on the 5th, 10th, 15th, 20th, 25th of each month for the years 1960-1970-1980-1990-2000-2010.

Table 5.3 contains the average of the errors computed on the 5th, 10th, 15th, 20th, 25th of each month for the years 1960-1970-1980-1990-2000-2010. For each of these dates, the errors between the positions computed with the two-body/VSOP87 and DE405 are computed. It means that each of

the values in Table 5.3 is the average of 360 errors. The table shows the improvements linked to the VSOP87 planetary theory. The errors represent respectively 0.003% and 0.01% of the semi-major axes of the inner planets (Mercury, Venus, Earth, Mars) and of the outer planets (Jupiter,Saturn, Uranus, Neptune).

The planetary formulation VSOP87 comes from the Development Ephemeris DE200. The accuracy of VSOP87 results directly from the observational data integrated in DE200. DE200 shows significant positional errors during the present epoch for all the four outermost planets (Jupiter to Neptune) [22]. Indeed, ephemerides of outer planets mainly rely on optical observations whereas inner planets are observed with satellite ranging. A semi-analytic method based on the most advanced Development Ephemeris DE405 could be implemented to improve the results. The best solution to compute planetary ephemerides is to couple the propagator with tabulated data computed by numerical integration. The propagator interpolates the data to obtain ephemerides at the desired dates. The accuracy of the point mass gravity and solar radiation pressure models is directly linked to the accuracy of planetary ephemerides. The J_2 perturbation is independent of the ephemerides. It has been validated with the S3L propagator developed by the University of Liège. A distance of 1.07 m has been found between the final positions after one day of propagation.

The dominant point mass gravity perturbations within the spheres of influence come from the moons. The close proximity between the moons and the spacecraft is the key parameter explaining this fact. Only Earth's moon called Moon is modelled in IOP. The Sun is the second contributor due its large gravitational parameter. Propagation lasting one day have been performed each day on January 2000 on an orbit escaping the Earth. The Moon changes the final spacecraft position by 75 km on average compared to the two-body trajectory, whereas the Sun changes it by 31 km on average compared to the two-body trajectory. These distances represent the errors with respect to GMAT the point mass gravity models included in IOP should compensate. It is expected that these values approach 0. The averages of errors in final spacecraft positions for the Moon and Sun point mass gravity models reduce respectively to 1 km and 4 m. The approximate ephemerides of the Moon come from Astronomical Almanac which provides less accurate ephemerides than the VSOP87 planetary theory. As a result, the Moon point mass model gives rise to less accurate results. However, it reduces the error from 75 km to 1 km on average. In contrast, the Sun point mass gravity model reduces the error from 31 km to 4 m on average.

The planetary point mass gravity perturbations are included to obtain high-fidelity propagation within the SOI. In the case of a spacecraft escaping Mars during four days, the planetary point mass gravity perturbations only change the final position by 8 m after 4 days of propagation compared to the two-body trajectory. The planetary point mass gravity models included in IOP reduce this distance to 0.004 m. In contrast, the planetary point mass perturbations change significantly the spacecraft trajectories outside the spheres of influence. The position changes by 828 km compared to the two-body trajectory between the days 300 and 304 in a Mars-Jupiter trajectory. The moons have negligible impact outside the spheres of influence due to their small gravitational parameters.

A cannonball model and the eclipse model proposed in Curtis [6] are chosen to model the solar radiation pressure perturbation. The case of the Earth's International Space Station is considered. The difference between the positions and velocities of IOP and GMAT are computed each hour during one day. The Earth's primary attraction and solar radiation pressure are included in GMAT. If only the primary attraction of the Earth is included in IOP, mean distances of 2.23 m and 2×10^{-3} m/s

are found with GMAT. If the solar radiation pressure model is included in IOP, mean distances reduce to 0.078 m and 9×10^{-5} m/s in this case. The eclipse model included in IOP overestimates the shadow region compared to the conical eclipse model included in GMAT. However, for Mercury, which is the planet located the closest to the Sun, the error on the final position decreases from 11.23 m to 0.59 m by taking into the eclipse model. The distance, 11.23 m, is found considering that the spacecraft is in full illumination during the one day of propagation around Mercury. Eventually, the solar radiation pressure model is validated with long propagation. The case study is an interplanetary trajectory between the Earth and Mars in 309 days. After 300 days of propagation, the error compared to GMAT is 11 km which represents an error of 0.007 $\%$.

Some perturbations should be added to obtain a high-fidelity orbital propagator until the limit defined by the Neptune's orbit. For nearly closed orbits at low altitude around the planets, the perturbations coming from the atmospheres should be added. For example, the impact of the atmosphere is negligible above 1200 km for the Earth [4]. In addition, the gravitational corrections other than the J_2 should be added for nearly closed orbits around the planets. The smaller the altitude is the higher its impact is. At high altitude and for orbits escaping the planets within the spheres of influence, the point mass gravity perturbations of the moons are the dominant perturbations. The 178 moons other than Earth's moon should be added in the propagator [28]. The impacts of the first three contributions are negligible outside the spheres of influence. The asteroids and the dwarf planets should be added to the propagator to model with a high degree of confidence the motion of spacecraft outside the spheres of influence. The point mass gravity assumption is not valid any more in the case of asteroids. New gravitational models have to be built.

Lambert's problem is used to design interplanetary trajectories in the thesis. Given two position vectors $\mathbf{r}_1$ and $\mathbf{r}_2$, and the transfer time between these two positions t_T, Lambert's problem allows the propagator to compute the orbit connecting the two positions vectors as well as the initial and final velocity vectors. The algorithm has been validated with numerical examples given in Curtis [6] for both types of orbit (ellipse, hyperbola). In addition, the example given in Vallado [24] is considered. The reference solutions and the ones predict by IOP are given in Table 5.4. A slight difference (blue) appears between the reference solutions and IOP.

	Velocities	$\mathbf{E}_1$-component (km/s)	$\mathbf{E}_2$-component (km/s)	$\mathbf{E}_3$-component (km/s)
Reference	V_{init}	2.058913	2.915965	0
IOP	V_{init}	2.058913	2.915964	0
Reference	V_{final}	-3.451565	0.910315	0
IOP	V_{final}	-3.451565	0.910314	0

Table 5.4: Comparison between IOP and reference solutions

Lambert's problem coupled with the perturbation models is used to recreate the Cassini-Huygens mission. The aims are to recreate the trajectory and the velocity of the Cassini-Huygens mission in the heliocentric coordinate system. More specifically, the four first years of the mission are simulated. The assemble of the velocities linked to the four trajectories studied in Chapter 5 is given in Figure 5.8. The data of the reference curve (red curve) come from JPL Horizons Ephemeris System.

The mean relative error between the two curves is 1.95%. IOP allows us to recreate the velocities of the Cassini-Huygens mission in the heliocentric coordinate system with a high degree of confidence.

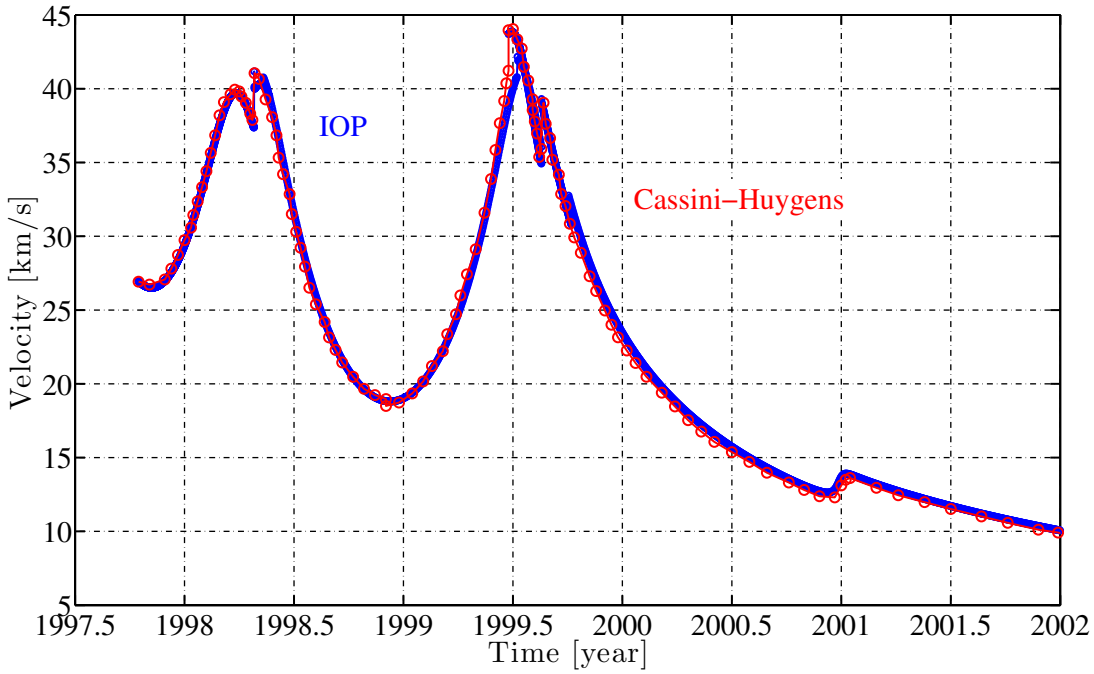

Figure 5.8: Cassini-Huygens mission: velocities in the heliocentric coordinate system.

Nowadays, only five spacecraft are located beyond Pluto's orbit : Pioneer 10, Pioneer 11, Voyager 1, Voyager 3 and New Horizons. There are about tens of billions of solar systems in the Milky Way galaxy. Many challenges are to come!

Appendix A

Constants

A.1 Planets, Sun, Pluto, Moon constants.

The constants linked to each celestial body are given in Table A.1. The gravitational parameters are used for the primary attractions and the point mass gravity perturbations. They are also used to obtain dimensionless equations. The masses are used to compute the radii of the spheres of influence. The J_2 coefficients are used in the flattening of the poles perturbations. The equatorial radii are used to obtain dimensionless equations.

	Gravitational parameter (km^3/s^2)	*Mass* (kg)	J_2 (-)	*Equatorial radius* (km)
Mercury	22032.080486418	3.3022×10^{23}	0.00006	2439.7
Venus	324858.59882646	4.869×10^{24}	0.000027	6051.9
Earth	398600.4415	5.9742×10^{24}	0.0010826269	6378.1363
Mars	42828.314258067	6.4191×10^{23}	0.001964	3397
Jupiter	126712767.8578	1.8988×10^{27}	0.01475	71492
Saturn	37940626.061137	5.685×10^{26}	0.01645	60268
Uranus	5794549.0070719	8.6625×10^{25}	0.012	25559
Neptune	6836534.0638793	1.0278×10^{26}	0.004	25269
Pluto	981.600887707	-	-	-
Sun	132712440017.99	1.9891×10^{30}	-	695990
Moon	4902.8005821478	-	-	-

Table A.1: Constants linked to each celestial body. The values are not truncated. The masses and J_2 coefficients come from Vallado, the equatorial radii and the gravitational parameters come from GMAT. The symbol - means that the values are not used.

Appendix B

Ephemerides

B.1 VSOP87 planetary theory: statistical analysis on planetary velocities

The conclusions drawn for the extreme values and the standard deviation of the positions are also valid for the velocities as can be seen in Table B.1.

Planets	*Error between velocities VSOP87-DE405* (m/s)	*Standard deviation* (m/s)	*Minimum* (m/s)	*Maximum* (m/s)
Mercury	0.3	0.2	0.03	0.9
Venus	0.8	0.3	0.04	1.6
Earth	13	1	9	15
Mars	2	0.7	0.3	3.5
Jupiter	11	0.4	8	17
Saturn	16	0.9	2	26
Uranus	15	0.6	3	26
Neptune	13	0.6	9	21

Table B.1: Statistical analysis on planetary velocities.

Appendix C

Codes

The chapter contains all the codes used in IOP. The codes are ordered in the same order presented in the thesis: constants, ephemerides, change of coordinate systems, Lambert's problem and the main algorithm.

C.1 Constants used in IOP

The file *Constants.m* is called by the different functions included in IOP. All the constants used in IOP are contained in this file.

```
%_____________________________________________________________________________
% Author: PICHA Thibault
%
%
% Academic year: 2017-2018
%
% DESCRIPTION : this file contains the constants relative to the 8 planets
% + pluto.
% Reference plane: ecliptic plane at J2000 Epoch. A structure is assigned
% at each planet. The different fields of the structures are:
%
% a             : semi-major axis                   [km]
% e             : eccentricity                      [-]
% i             : inclination                       [deg]
% J2            : flattening of the pole coefficient[-]
% L0            : mean longitude                    [deg]
% m             : mass                              [kg]
% n             : angular velocity                  [deg/day]
% Omega         : longitude of the ascending node   [deg]
% omegaBar      : longitude of the perihelion       [deg]
% Re            : equatorial radius                 [km]
% mu            : gravitational parameter           [km^3/s^2]
%
% INPUTS : /
% OUTPUTS: /
%
% Reference: Vallado appendix D apart from angular velocity.
% n come from:  Rauw Gregor, celestial mechanics and space trajectories.
```

```
% Gravitational parameters and equatorial radii come from GMAT.
%
% Function called : /
%_____________________________________________________________________________


% Conversion astronomical units to kilometres.
AU                      = 149597870;  % [km]

% Conversion arcsecond to degree.
arcsecond2degree        = 1/3600;

% Mercury
Mercury.a               = 0.387098310 * AU;
Mercury.e               = 0.205631752;
Mercury.i               = 7.00498625;
Mercury.J2              = 0.00006;
Mercury.L0              = 252.25090551;
Mercury.m               = 3.3022*10^23;
Mercury.n               = 14732.42 * arcsecond2degree;
Mercury.Omega           = 48.33089304;
Mercury.omegaBar        = 77.45611904;
Mercury.Re              = 2439.7;
Mercury.mu              = 22032.080486418;

% Venus
Venus.a                 = 0.72332982*AU;
Venus.e                 = 0.006771882;
Venus.i                 = 3.39446619;
Venus.J2                = 0.000027;
Venus.L0                = 181.97980084;
Venus.m                 = 4.869*10^24;
Venus.n                 = 5767.67 * arcsecond2degree;
Venus.Omega             = 76.67992019;
Venus.omegaBar          = 131.56370724;
Venus.Re                = 6051.9;
Venus.mu                = 324858.59882646;

% Earth
Earth.a                 = 1.0000010178*AU;
Earth.e                 = 0.016708617;
Earth.i                 = 0;
Earth.J2                = 0.0010826269;
Earth.m                 = 5.9742*10^24;
Earth.n                 = 3548.19 * arcsecond2degree;
Earth.L0                = 100.46644851;
Earth.Omega             = 0;
Earth.omegaBar          = 102.93734808;
Earth.Re                = 6378.1363;
Earth.mu                = 398600.4415;

% Mars
Mars.a                  = 1.52367934*AU;
Mars.e                  = 0.093400620;
Mars.i                  = 1.84972648;
Mars.J2                 = 0.001964;
```

```
Mars.m                  = 6.4191*10^23;
Mars.n                  = 1886.52 * arcsecond2degree;
Mars.L0                 = 355.43327463;
Mars.Omega              = 49.55809321;
Mars.omegaBar           = 336.06023398;
Mars.Re                 = 3397;
Mars.mu                 = 42828.314258067;

% Jupiter
Jupiter.a               = 5.202603191*AU;
Jupiter.e               = 0.048494851;
Jupiter.i               = 1.30326966;
Jupiter.J2              = 0.01475;
Jupiter.L0              = 34.35148392;
Jupiter.m               = 1.8988*10^27;
Jupiter.n               = 299.128 * arcsecond2degree;
Jupiter.Omega           = 100.46444064;
Jupiter.omegaBar        = 14.33130924;
Jupiter.Re              = 71492;
Jupiter.mu              = 126712767.8578;

% Saturn
Saturn.a                = 9.554909595*AU;
Saturn.e                = 0.055508622;
Saturn.i                = 2.48887810;
Saturn.J2               = 0.01645;
Saturn.L0               = 50.07747138;
Saturn.m                = 5.685*10^26;
Saturn.n                = 120.455 * arcsecond2degree;
Saturn.Omega            = 113.6655237;
Saturn.omegaBar         = 93.05678728;
Saturn.Re               = 60268;
Saturn.mu               = 37940626.061137;

% Uranus
Uranus.a                = 19.218446061*AU;
Uranus.e                = 0.046295898;
Uranus.i                = 0.77319617;
Uranus.J2               = 0.012;
Uranus.L0               = 314.05500511;
Uranus.m                = 8.6625*10^25;
Uranus.n                = 42.231 * arcsecond2degree;
Uranus.Omega            = 74.00594723;
Uranus.omegaBar         = 173.00515922;
Uranus.Re               = 25559;
Uranus.mu               = 5794549.0070719;

% Neptune
Neptune.a               = 30.11038687*AU;
Neptune.e               = 0.008988095;
Neptune.i               = 1.76995221;
Neptune.J2              = 0.004;
Neptune.L0              = 304.34866548;
Neptune.m               = 1.0278*10^26;
Neptune.n               = 21.534 * arcsecond2degree;
Neptune.Omega           = 131.78405702;
```

```
Neptune.omegaBar          = 48.1236905;
Neptune.Re                = 25269;
Neptune.mu                = 6836534.0638793;

% Pluto
Pluto.a                   = 39.544674*AU;
Pluto.e                   = 0.249050;
Pluto.i                   = 17.14216667;
Pluto.J2                  = 0;
Pluto.L0                  = 238.74394444;
Pluto.m                   = 1.5*10^22;
Pluto.n                   = 14.3 * arcsecond2degree;
Pluto.Omega               = 110.29713889;
Pluto.omegaBar            = 224.13486111;
Pluto.Re                  = 1151;
Pluto.mu                  = 981.600887707;

% Sun
Sun.m                     = 1.9891*10^30;
Sun.mu                    = 132712440017.99;
Sun.Re                    = 695990;

%---------------------------------Vectors-----------------------------------

% First element       : Mercury
% Second element      : Venus
% Third element       : Earth
% Fourth element      : Mars
% Fifth element       : Jupiter
% Sixth element       : Saturne
% Seventh element     : Uranus
% Eighth element      : Neptune
% Ninth element       : Pluto
% Tenth element       : Sun

% Semi-major axes vector [km]
a_bodies    = [Mercury.a; Venus.a; Earth.a ; Mars.a; Jupiter.a; Saturn.a; ...
               Uranus.a; Neptune.a; Pluto.a; 0];

% J2 vector [-]
J2_bodies   = [Mercury.J2; Venus.J2; Earth.J2; Mars.J2; Jupiter.J2; ...
               Saturn.J2; Uranus.J2; Neptune.J2; Pluto.J2; 0];

% Masses vector [kg]
m_bodies    = [Mercury.m; Venus.m; Earth.m; Mars.m; Jupiter.m; Saturn.m; ...
               Uranus.m; Neptune.m; Pluto.m; Sun.m];

% Equatorial radii vector [km]
Re_bodies   = [Mercury.Re; Venus.Re; Earth.Re; Mars.Re; Jupiter.Re; ...
               Saturn.Re; Uranus.Re; Neptune.Re; Pluto.Re; Sun.Re];

% Gravitational parameters vector [km^3/s^2]
mu_bodies   = [Mercury.mu; Venus.mu; Earth.mu; Mars.mu; Jupiter.mu; ...
               Saturn.mu; Uranus.mu; Neptune.mu; Pluto.mu; Sun.mu];
```

C.2 Ephemerides

The section is divided into two parts. The first part introduces the codes behind the planetary and Pluto ephemerides. The second part introduces Moon ephemerides.

C.2.1 Planets and dwarf planet Pluto

```
%_____________________________________________________________________________
% Author: PICHA Thibault
%
% Academic year: 2017-2018
%
% DESCRIPTION : this function computes the planetary positions and velocities
% (+ Pluto)in the heliocentric inertial coordinate system depending on the
% given Julian date (jd) in terrestrial time and the considered
% celestial body (number).
%
% INPUTS :
%
% - number                  [1,9] is the index of the celestial elements
%                           Size: 1x1 [-]
%
%                           => 1 : Mercury
%                           => 2 : Venus
%                           => 3 : Earth
%                           => 4 : Mars
%                           => 5 : Jupiter
%                           => 6 : Saturn
%                           => 7 : Uranus
%                           => 8 : Neptune
%                           => 9 : Pluto
%
%  - jd                     Current Julian date expressed in terrestrial
%                           time.
%                           Size: 1x1 [days]
%
%
% OUTPUTS:
%
%
%
% -  PositionPlanets        Position vector of the considered planet in the
%                           heliocentric inertial coordinate system.
%                           Size : 3x1 [km]
%
%
% -  VelocityPlanets        Velocity vector of the considered planet in the
%                           heliocentric inertial coordinate system.
%                           Size : 3x1 [km/s]
%
%
% -  Reference :            VSOP87.pdf
%                           Vallado p283-284-285 (procedure)
```

```
%
% -  Functions called :     CorrectionVSOP87.m
%                           Kepl2cart_planet.m
%_____________________________________________________________________________

function [PositionPlanets,VelocityPlanets] = ephemerideVSOP87(jd,number)


%------------- Step 1: correction of the orbital elements-----------------
%                       refercence : VSOP87.pdf
[a,e,incl,omegaBar,L,Omega]  = CorrectionVSOP87(jd,number);


%----------------Step2: resolution of Kepler's equation--------------------
% Argument of perihelion [deg].
omega                        = omegaBar - Omega; % [deg]

% Mean anomaly.
M                            = L - omegaBar;     % [deg]
M_rad                        = M * pi / 180;     % [rad]

% Newton-Raphson algorithm to solve Kepler's equation
% Initial guess proposed by Battin: (equation 5.4) p194.
E_nPlus1                     = M_rad + (e * sin(M_rad) ) / ...
                               (1 - sin(M_rad + e) + sin(M_rad));
E_n                          = E_nPlus1+10;


while abs(E_nPlus1-E_n)>10^-8
    E_n                      = E_nPlus1;
    E_nPlus1                 = E_n + (M_rad - E_n + e * sin(E_n))/ ...
                               (1 - e * cos(E_n));
end

 E                           = E_nPlus1 * 180 / pi;


%----------------Step3: conversion in cartesian elements------------------

% Conversion in AU and AU/day.
[PositionPlanets, VelocityPlanets] = Kepl2cart_planet(a , e, incl, Omega, ...
                                     omega, E);

% Conversion in km and km/s.
AU                           = 149597870; % [km]
PositionPlanets              = PositionPlanets * AU; % [km]
VelocityPlanets              = VelocityPlanets * 58.1324409 * 29.7846916749;
                               % [km/s]

end
```

Corrections of the orbital elements

```
%_____________________________________________________________________________
% Author: PICHA Thibault
%
%
% Academic year: 2017-2018
%
% DESCRIPTION : this function corrects the orbital elements using the VSOP87
% planetary theory depending on the given Julian date (jd) in terrestrial
% time and the considered celestial body (number).
%
% INPUTS :
%
% - number                  [1,9] is the index of the celestial elements.
%                           Size: 1x1 [-]
%
%                           => 1 : Mercury
%                           => 2 : Venus
%                           => 3 : Earth
%                           => 4 : Mars
%                           => 5 : Jupiter
%                           => 6 : Saturn
%                           => 7 : Uranus
%                           => 8 : Neptune
%                           => 9 : Pluto
%
%  - jd                     Current julian date expressed in terrestrial
%                           time.
%                           [days]
%
%
% OUTPUTS: corrected orbital elements
%
% - a                       Semi-major axis.
%                           [AU]
%
% - L                       Mean longitude.
%                           [deg]
%
% - e                       Eccentricity.
%                           [-]
%
% - omegaBar                Longitude of the perihelion.
%                           [deg]
%
% - Incl                    Inclination.
%                           [deg]
%
% - Omega                   Right ascension of the ascending node.
%                           [deg]
%
% REFERENCE :               VSOP87.pdf
%_____________________________________________________________________________
```

```
function [a,e,incl,omegaBar,L,Omega] = CorrectionVSOP87(jd,number)


% Thousands Julian years elapsed from J2000 in terrestrial time.
T_TT                            =  (jd - 2451545) / 365250;


% Conversions used throughout the file.
arcsec2degreeTimesT_TT          =  1/3600*T_TT;
T_TTTimes035                    =  0.35953620*T_TT;


%---------------------------------------Mercury-----------------------------
if number == 1

%% Secular corrections

% Semi-major axis [AU]
a         = 0.3870983098;

% Eccentricity [-]
e         = 0.2056317526 + 0.0002040653*T_TT;

% Inclination [deg]
incl      = 7.00498625 - 214.25629*arcsec2degreeTimesT_TT;

% Longitude of the ascending node [deg]
Omega     = 48.33089304 - 4515.21727*arcsec2degreeTimesT_TT;

% Longitude of the perihelion [deg]
omegaBar = 77.45611904 + 5719.1159*arcsec2degreeTimesT_TT;

% Mean longitude [deg]
L         = 252.25090552 + 5381016286.88982*arcsec2degreeTimesT_TT;

%% Periodic corrections

pimu = [69613;75645;88306;59899;15746;71087;142173;3086;0;0]* T_TTTimes035;
       %[rad]
Ca    = [4;-13;11;-9;-9;-3;-1;4;0;0]*10^-7; %[AU]
Sa    = [-29;-1;9;6;-6;5;4;0;0;0]*10^-7; %[AU]
qimu = [3086;15746;69613;59899;75645;88306;12661;2658;0;0] * T_TTTimes035;
       %[rad]
Cl    = [21;-95;-157;41;-5;42;23;30;0;0]*10^-7; %[rad]
Sl    = [-342;136;-23;62;66;-52;-33;17;0;0]*10^-7; %[rad]

%---------------------------------Venus-------------------------------------

elseif number == 2

%% Secular corrections

% Semi-major axis [AU]
a             = 0.723329820;
```

```
% Eccentricity [-]
e            = 0.0067719164 - 0.0004776521*T_TT;

% Inclination [deg]
incl         = 3.39466189 -30.84437*arcsec2degreeTimesT_TT;

% Longitude of the ascending node [deg]
Omega        = 76.67992019 - 10008.48154*arcsec2degreeTimesT_TT;

% Longitude of the perihelion [deg]
omegaBar     = 131.563703 + 175.4864*arcsec2degreeTimesT_TT;

% Mean longitude [deg]
L            = 181.97980085 + 2106641364.33548*arcsec2degreeTimesT_TT;

%% Periodic corrections

pimu = [21863;32794;26934;10931;26250;43725;53867;28939;0;0] ...
       *T_TTTimes035; %[rad]
Ca   = [-156;59;-42;6;19;-20;-10;-12;0;0]*10^-7; %[AU]
Sa   = [-48;-125;-26;-37;18;-13;-20;-2;0;0]*10^-7; %[AU]
qimu = [21863;32794;10931;73;4387;26934;1473;2157;0;0]*T_TTTimes035; %[rad]
Cl   = [-160;-313;-235;60;-74;-76;-27;34;0;0]*10^-7; %[rad]
Sl   = [524;-149;-35;117;151;122;-71;-62;0;0]*10^-7; %[rad]

%---------------------------------Earth-------------------------------------

elseif number == 3

T_TT=T_TT*10;
%% Secular change

% Semi-major axis [AU]
a            = 1.000001018;

% Eccentricity [-]
e            = 0.01670862 - 0.000042037 * T_TT - 0.0000001236 * T_TT^2 ...
               + 0.00000000004 * T_TT^3;


% Inclination [deg]
incl         = 0 + 0.0130546 * T_TT - 0.00000931 * T_TT^2 - 0.000000034 ...
               * T_TT^3;


% Longitude of the ascending node [deg]
Omega        = 0;


% Longitude of the perihelion [deg]
omegaBar     = 102.937348 + 0.3225557 * T_TT + 0.00015026 * T_TT^2 + ...
               0.000000478 * T_TT^3;


% Mean longitude [deg]
L            = 100.466449 + 35999.3728519 * T_TT - 0.00000568 * T_TT^2;
```

```
%% Periodic change

 pimu = [0;0;0;0;0;0;0;0;0;0]*T_TTTimes035; %[rad]
 Ca   = [0;0;0;0;0;0;0;0;0;0]*10^-7; %[AU]
 Sa   = [0;0;0;0;0;0;0;0;0;0]*10^-7; %[AU]
 qimu = [0;0;0;0;0;0;0;0;0;0]*T_TTTimes035; %[rad]
 Cl   = [0;0;0;0;0;0;0;0;0;0]*10^-7; %[rad]
 Sl   = [0;0;0;0;0;0;0;0;0;0]*10^-7; %[rad]

%--------------------------------Mars-----------------------------------

elseif number == 4

%% Secular corrections

% Semi-major axis [AU]
a            = 1.5236793419 + 3*10^-10*T_TT;

% Eccentricity [-]
e            = 0.0934006477+0.0009048438*T_TT;

% Inclination [deg]
incl         = 1.84972648-293.31722*arcsec2degreeTimesT_TT;

% Longitude of the ascending node [deg]
Omega        = 49.55809321-10620.90088*arcsec2degreeTimesT_TT;

% Longitude of the perihelion [deg]
omegaBar     = 336.06023395+15980.45908*arcsec2degreeTimesT_TT;

% Mean longitude [deg]
L            = 355.43299958+ 689050774.93988*arcsec2degreeTimesT_TT;

%% Periodic corrections

 pimu = [6345;7818;15636;7077;8184;14163;1107;4872;0;0]*T_TTTimes035;
        %[rad]
 Ca   = [124;621;-145;208;54;-57;30;15;0;0]*10^-7; %[AU]
 Sa   = [-621;532;-694;-20;192;-94;71;-73;0;0]*10^-7; %[AU]
 qimu = [10;6345;7818;1107;15636;7077;8184;532;10]*T_TTTimes035; %[rad]
 Cl   = [2268;-979;802;602;-668;-33;345;201;-55;0]*10^-7; %[rad]
 Sl   = [854;-205;-936;-240;140;-341;-97;-232;536;0]*10^-7; %[rad]


%-------------------------------------Jupiter-----------------------------

elseif number == 5

%% Secular corrections

% Semi-major axis [AU]
a            = 5.2026032092 + 19132*10^-10*T_TT;

% Eccentricity [-]
```

```
e            = 0.0484979255 + 0.0016322542*T_TT;


% Inclination [deg]
incl         = 1.30326698-71.55890*arcsec2degreeTimesT_TT;


% Longitude of the ascending node [deg]
Omega        =  100.46440702 + 6362.03561*arcsec2degreeTimesT_TT;


% Longitude of the perihelion [deg]
omegaBar     = 14.33120687+7758.75163*arcsec2degreeTimesT_TT;


% Mean longitude [deg]
L            = 34.35151874+ 109256603.77991*arcsec2degreeTimesT_TT;


%% Periodic corrections

 pimu = [1760; 1454;1167;880;287;2640;19;2047;1454;0]*T_TTTimes035; %[rad]
 Ca   = [-23437;-2634;6601;6259;-1507;-1821;2620;-2115;-1489;0] ...
        *10^-7; %[AU]
 Sa   = [-14614; -19828;-5869;1881;-4372;-2255;782;930;913;0] ...
        *10^-7; %[AU]
 qimu = [19; 1760; 1454; 287; 1167; 880; 574; 2640;19;1454] ...
        *T_TTTimes035; %[rad]
 Cl   = [7610;-4997;-7689; -5841; -2617; 1115; -748; -607;6074;354]* ...
        10^-7; %[rad]
 Sl   = [-56980;8016;1012; 1448;-3024;-3710; 318;503;3767;577]*10^-7;%[rad]



%--------------------------------------Saturn-----------------------------

elseif number == 6

%% Secular corrections

% Semi-major axis [AU]
a            = 9.5549091915 - 0.0000213896*T_TT;

% Eccentricity [-]
e            = 0.0555481426-0.0034664062*T_TT;


% Inclination [deg]
incl         = 2.48887878+91.85195*arcsec2degreeTimesT_TT;


% Longitude of the ascending node [deg]
Omega        = 113.66550252-9240.19942*arcsec2degreeTimesT_TT;


% Longitude of the perihelion [deg]
```

```
omegaBar     = 93.05723748+20395.49439*arcsec2degreeTimesT_TT;


% Mean longitude [deg]
L            = 50.0774443 + 43996098.55732*arcsec2degreeTimesT_TT;


%% Periodic corrections

 pimu = [574;0;880;287;19;1760;1167;306;574;0]*T_TTTimes035; %[rad]
 Ca   = [62911;-119919;79336;17814;-24241;12068;8306;-4893;8902;0] ...
        *10^-7; %[AU]
 Sa   = [139737;0;24667;51123;-5102;7429;-4095;-1976;-9566;0]*10^-7; %[AU]
 qimu = [19;574 ;287;306;1760;12;31;38 ;19;574]*T_TTTimes035; %[rad]
 Cl   = [-18549;30125;20012;-730;824;23;1289;-352;-14767;-2062] ...
        *10^-7; %[rad]
 Sl   = [138606;-13478;-4964;1441;-1319;-1482;427;1236;-9167;-1918] ...
        *10^-7; %[rad]

%--------------------------------------Uranus-----------------------------

elseif number == 7

%% Secular corrections

% Semi-major axis [AU]
a            = 19.2184460618-3716*10^-10*T_TT;


% Eccentricity [-]
e            = 0.0463812221-0.0002729293*T_TT;


% Inclination [deg]
incl         = 0.77319689-60.72723*arcsec2degreeTimesT_TT;


% Longitude of the ascending node [deg]
 Omega        = 74.00595701+2669.15033*arcsec2degreeTimesT_TT;


% Longitude of the perihelion [deg]
omegaBar     = 173.00529106+3215.56238*arcsec2degreeTimesT_TT;


% Mean longitude [deg]
L            = 314.05500511 + 15424811.93933*arcsec2degreeTimesT_TT;


%% Periodic corrections

 pimu = [204;0;177;1265;4;385;200;208;204;0]*T_TTTimes035; %[rad]
 Ca   = [389061;-262125;-44088;8387;-22976;-2093;-615;-9720;6633;0]* ...
        10^-7; %[AU]
 Sa   = [-138081;0;37205;-49039;-41901;-33872;-27037;-12474;18797;0] ...
        *10^-7; %[AU]
```

```
 qimu = [4;204;177;8;31;200;1265;102;4;204]*T_TTTimes035; %[rad]
 Cl   = [-135245;-14594;4197;-4030;-5630;-2898;2540;-306;2939;1986] ...
        *10^-7; %[rad]
 Sl   = [71234;-41116;5334;-4935;-1848;66;434;-1748;3780;-701]*10^-7;%[rad]

 %--------------------------------------Neptune---------------------------

elseif number == 8

% Secular corrections

% Semi-major axis [AU]
a =30.1103868694 - 16635*10^-10*T_TT;


% Eccentricity [-]
e = 0.0094557470 + 0.0000603263*T_TT;


% Inclination [deg]
incl = 1.76995259 + 8.12333*arcsec2degreeTimesT_TT;


% Longitude of the ascending node [deg]
Omega = 131.78405702 - 221.94322*arcsec2degreeTimesT_TT;


% Longitude of the perihelion [deg]
omegaBar = 48.12027554 + 1050.71912*arcsec2degreeTimesT_TT;


% Mean longitude [deg]
L =304.34866548 + 7865503.20744*arcsec2degreeTimesT_TT;


%% Periodic corrections

 pimu = [0;102;106;4;98;1367;487;204;0;0]*T_TTTimes035; %[rad]
 Ca   = [-412235;-157046;-31430;37817;-9740;-13;-7449;9644;0;0] ...
        *10^-7; %[AU]
 Sa   = [0;28492;133236;69654;52322;-49577;-26430;-3593;0;0]*10^-7; %[AU]
 qimu = [4;102;106;8;98;1367;487;204;4;102]*T_TTTimes035; %[rad]
 Cl   = [89948;2103;8963;2695;3682;1648;866;-154;-1963;-283]*10^-7; %[rad]
 Sl   = [-47645;11647;2166;3194;679;0;-244;-419;-2531;48]*10^-7; %[rad]

%--------------------------------------Pluto-----------------------------

elseif number == 9

% Semi-major axis [AU]
a         = 39.53758;

% Eccentricity [-]
e         = 0.250877;

% Inclination [deg]
```

```
incl      = 17.13233;

% Longitude of the ascending node [deg]
Omega     = 110.4065;

% Longitude of the perihelion [deg]
omegaBar  = 224.6148;

% Mean longitude [deg]
n_pluto   = 14.3/3600;
L         = 218.88735+n_pluto*(jd-2451545);

%% Periodic : /

pimu      = [0;0;0;0;0;0;0;0;0;0]*0.035953620*T_TT; %[rad]
Ca        = [0;0;0;0;0;0;0;0;0;0]*10^-7; %[AU]
Sa        = [0;0;0;0;0;0;0;0;0;0]*10^-7; %[AU]
qimu      = [0;0;0;0;0;0;0;0;0;0]*0.035953620*T_TT; %[rad]
Cl        = [0;0;0;0;0;0;0;0;0;0]*10^-7; %[rad]
Sl        = [0;0;0;0;0;0;0;0;0;0]*10^-7; %[rad]

end
%-----------------------------Periodic corrections-----------------------

correction_a      = sum(Ca(1:8,1).*cos(pimu(1:8,1))+Sa(1:8,1).* ...
                    sin(pimu(1:8,1)));
correction_lambda = sum(Cl(1:8,1).*cos(qimu(1:8,1))+Sl(1:8,1).* ...
                    sin(qimu(1:8,1)));
a                 = a +correction_a;
L                 = L + correction_lambda*180/pi;

end
```

Conversion Keplerian elements to planetary Cartesian position and velocity vectors

```
%_____________________________________________________________________________
% Author: PICHA Thibault
%
%
% Academic year: 2017-2018
%
% Description : this function converts Keplerian elements to
% Cartesian elements.
%
% INPUTS : Keplerian elements
% OUTPUTS: Position and velocity vectors in the heliocentric
% coordinate system.
%
%
% r             3x1 [AU]     Position vector
% rdot          3x1 [AU/day] Velocity vector
%
% 1 AU=149597870 km (p905 Vallado)
```

```
% 1 AU/TU=29.784 691 674 9 km/s (p905 Vallado) (s referred as solar s)
%_____________________________________________________________________________



function [r, rdot] = Kepl2cart_planet(a, e, incl, Omega, omega, E)

% Gravitational parameter of the sun.
mu                  = 1; % [AU^3/TU^2]

% Transformation matrix R (p 125 Vallado).
cOmega              = cosd(Omega);
sOmega              = sind(Omega);
comega              = cosd(omega);
somega              = sind(omega);
cInc                = cosd(incl);
sInc                = sind(incl);
CE                  = cosd(E);
SE                  = sind(E);

R11                 =   cOmega * comega - sOmega * somega * cInc;
R12                 = - cOmega * somega - sOmega * comega * cInc;
R13                 =   sOmega * sInc;
R21                 =   sOmega * comega + cOmega * somega * cInc;
R22                 = - sOmega * somega + cOmega * comega * cInc;
R23                 = - cOmega * sInc;
R31                 =   somega * sInc;
R32                 =   comega * sInc;
R33                 =   cInc;
R                   =   [R11, R12, R13; R21, R22, R23; R31, R32, R33];

% Position vector (p 125 Vallado).

% NB: expression expressed in terms of the
% eccentric anamoly E and not in terms of the true anomaly as proposed to
% use directly the results of Kepler's equation.

x_p_init(:,1)       = a * [CE - e; SE * sqrt(1 - e^2 ) ; 0 ];
r                   = R * x_p_init;

% Velocity vector (p 125 Vallado).
xdot_p_init(:,1)    = sqrt(mu / a)/( 1 - e * CE) * [ - SE ; CE * sqrt(1 ...
                       - e^2) ; 0];

rdot                = R * xdot_p_init / 58.1324409;

% 58.1324409 to go from AU/TU to AU/day p284 vallado.

end
```

C.2.2 Moon

```
%_____________________________________________________________________________
% Author: PICHA Thibault
%
% Academic year: 2017-2018
%
% DESCRIPTION : this function computes Moon ephemerides.
%
% INPUTS :
%
%  - jd                     Current Julian date expressed in terrestrial
%                           time.
%                           Size: 1x1 [days]
%
%
% OUTPUTS:
%
%
%
% -  r_m                    Position vector of the Moon in the geocentric
%                           inertial coordinate system.
%                           Size : 3x1 [km]
%
%
%
% - Reference :             Montenbruck
%
% - Function called : /
%
%_____________________________________________________________________________

function [r_m] = EphemerideMoon(jd)

% Number of Julian centuries since J2000.
T0                    = (jd - 2451545) / 36525;

% The mean longitude Lo of the Moon, the Moon's mean anomaly 1,
% the Sun's mean anomaly 1prime, the mean angular distance of the Moon from
% the ascending node F, and the difference D between the mean longitudes
% of the Sun and the Moon.
L0                    = 218.31617 + 481267.88088*T0 - 1.3972*T0; % [deg]
l                     = 134.96292 + 477198.86753*T0; % [deg]
lprime                = 357.52543 + 35999.04944*T0;  % [deg]
F                     = 93.27283 + 483202.01873*T0;  % [deg]
D                     = 297.85027 + 445267.11135*T0; % [deg]

% Conversion arcsecond to degree.
arcsecond2degree      = 1/3600; % [deg/arcsecond]

% Moon's longitude with respect to the equinox and ecliptic of the year
% 2000.
lambda_M  = L0 + 22640*arcsecond2degree*sind(l) + 769 * ...
            arcsecond2degree*sind(2*l) - 4586 *arcsecond2degree ...
```

```
            * sin(l-2*D) + 2370 *arcsecond2degree*sind(2*D) ...
            - 668 *arcsecond2degree * sind(lprime) - 412 * ...
            arcsecond2degree * sind(2*F) - 212 * arcsecond2degree * ...
            sind(2*l - 2 * D) - 206 * arcsecond2degree * ...
            sind(l+lprime-2*D) + 192 * arcsecond2degree * sind(l+2*D) ...
            - 165 * arcsecond2degree * sind(lprime - 2*D) + 148 * ...
            arcsecond2degree * sind(l-lprime) - 125 * arcsecond2degree ...
            * sind(D) - 110 * arcsecond2degree * sind(l+lprime) - 55 ...
            * arcsecond2degree * sind(2*F -2*D); % [deg]

lambda_M  = mod(lambda_M,360);  % [deg]

%  lunar latitude.
beta_M    = 18520 * arcsecond2degree * sind(F+lambda_M - L0 + 412 ...
            * arcsecond2degree *sind(2*F)+ 541 * arcsecond2degree * ...
            sind(lprime)) - 526 * arcsecond2degree * sind(F - 2*D) + 44 ...
            * arcsecond2degree * sind(l+F - 2*D) - 31 * arcsecond2degree...
            * sind(-l+F-2*D) - 25 * arcsecond2degree * sind(-2*l+F) ...
            - 23 * arcsecond2degree * sind(lprime + F - 2*D) + 21 * ...
            arcsecond2degree * sind(-l+F) + 11 * arcsecond2degree ...
            * sind(-lprime + F -2*D);
beta_M    = mod(beta_M,360);

% Moon's distance from the center of the Earth.
norm_r_M  = 385000 - 20905 * cosd(l) - 3699 * cosd(2*D-l) - 2956 * ...
            cosd(2*D) -570*cosd(2*l) + 246 * cosd(2*l - 2*D) ...
            - 205 * cosd(lprime - 2*D) -171 * cosd(l+2*D) ...
            - 152*cosd(l+lprime-2*D); % [km]

epsilon_J2000     = -23.439291111;  % [deg]
cos_epsilon       = cosd(epsilon_J2000);
sin_epsilon       = sind(epsilon_J2000);

% The ecliptic and equatorial coordinates differs from a rotation about the
% Vernal equinox of amplitude epsilon_J2000.
rot1              = [ 1               0                  0           ;...
                      0             cos_epsilon       sin_epsilon     ;...
                      0             -sin_epsilon       cos_epsilon    ];

r_m               = rot1 * [norm_r_M*cosd(lambda_M)*cosd(beta_M); ...
                    norm_r_M*sind(lambda_M)*cosd(beta_M); norm_r_M* ...
                    sind(beta_M)];

end
```

C.3 Change of coordinate system

C.3.1 Heliocentric and Earth inertial coordinate systems

```
%_____________________________________________________________________
% Author: PICHA Thibault

% Academic year: 2017-2018

% DESCRIPTION : this function rotates the position and velocity vectors
% between the axes of the heliocentric inertial coordinate system and the
% axes of the Earth inertial coordinate system at the J2000 epoch. It is
% used in the general change of coordinate system between heliocentric and
% planetocentric coordinate systems.
%
% INPUTS :
%
%
% - r_init               Position vector in heliocentric axes or Earth
%                        axes depending on the variable in2out (see below).
%                        Size: 3 x 1 [km]
%
% - rdot_init            Velocity vector in heliocentric axes or Earth
%                        axes depending on the variable in2out (see below).
%                        depending on the variable in2out (see below).
%                        Size: 3 x 1 [km/s]
%
%
% - in2out               = 1 if we go from mean equator to mean ecliptic.
%
%
%                        = -1  if we go from mean ecliptic to mean equator.
%
% OUTPUTS:
%
% - r_final              Position vector in heliocentric axes or Earth
%                        axes depending on the variable in2out (see below).
%                        Size: 3 x 1 [km]

% - rdot_final           Velocity vector in heliocentric axes or Earth
%                        axes depending on the variable in2out (see below).
%                        depending on the variable in2out (see below).
%                        Size: 3 x 1 [km/s]
%
%
%
% Reference:             GMTA 2017a
%
% FUNCTION CALLED : \
%_____________________________________________________________________

%% Validation 1 : HeliosphericCoordinateSystem.pdf p20. NB the velocity is
%% taken equal to the position (arbitrarily because if the position is
%% correct the velocity too).
```

```
% Mean ecliptic J2000:

%  r_init    = [-5.7840451;-3.0076174;3.3908496];
%  rdot_init = [-5.7840451;-3.0076174;3.3908496];
%  in2out    = -1;

% Mean equator J2000:

%  r_init    = [-5.7840451;-4.108237524144306;1.914682187679091];
%  rdot_init = [-5.7840451;-4.108237524144306;1.914682187679091];
%  in2out    = 1;
%_____________________________________________________________________________

function [r_final,rdot_final] = MJ2000Ec2MJ2000Eq(r_init,rdot_init,in2out)

% Obliquity of the ecliptic at epoch J2000 with respect to the mean equator
% at epoch J2000.
epsilon_J2000     = 23.439291111; % [deg]

cos_epsilon       = cosd(in2out*epsilon_J2000);
sin_epsilon       = sind(in2out*epsilon_J2000);

% The ecliptic and equatorial coordinates differ from a rotation about the
% Vernal equinox of amplitude epsilon_J2000.
rot1              = [ 1               0                 0           ;...
                      0             cos_epsilon       sin_epsilon    ;...
                      0             -sin_epsilon       cos_epsilon   ];

r_final           = rot1 * r_init;
rdot_final        = rot1 * rdot_init;
end
```

C.3.2 Heliocentric to planetocentric coordinate system

```
%_____________________________________________________________________________
% Author: PICHA Thibault
%
% Academic year: 2017-2018
%
% DESCRIPTION : when a spacecraft enters a sphere of influence, the change
% of coordinate system between the heliocentric inertial and planetocentric
% inertial coordinate systems is performed thanks to this function.
%
%
% INPUTS :
%
% - number                [1,8] is the index of the celestial elements
%                         It refers to the final inertial coordinate
%                         system we want to go.
%                         Size: 1x1 [-]
%
%                           => 1 : Mercury
```

```
%                             => 2 : Venus
%                             => 3 : Earth
%                             => 4 : Mars
%                             => 5 : Jupiter
%                             => 6 : Saturn
%                             => 7 : Uranus
%                             => 8 : Neptune
%
%
%
% - r_InertialSun           Position vector in the heliocentric inertial
%                           coordinate system.
%                           Size: 3 x 1  [km]
%
% - rdot_InertialSun        Velocity vector in the heliocentric inertial
%                           coordinate system.
%                           Size: 3 x 1  [km/s]
%
% OUTPUTS:
%
%
%  - r_InertialBody         Position vector in the body inertial coordinate
%                           system
%                           Size: 3 x 1  [km]
%
%
%  - rdot_InertialBody      Velocity vector in the body inertial coordinate
%                           system.
%                           Size: 3 x 1  [km/s]
%
%
%  Reference:               GMAT R2017a
%
% FUNCTIONS CALLED :        MJ2000Ec2MJ2000Eq.m
%                           ephemerideVSOP87.m
%                           MJ2000Eq2InertialBody.m
%_____________________________________________________________________________

function [r_InertialBody,rdot_InertialBody] = SunInertial2BodyInertial( ...
                              r_InertialSun,rdot_InertialSun,jd_SOI,number)

% The first step is to rotate the position and velocity vector in the axes
% of the Earth's inertial at the J2000 epoch.
[r_InertialSun_MJ2000Eq,rdot_InertialSun_MJ2000Eq] = ...
                      MJ2000Ec2MJ2000Eq(r_InertialSun,rdot_InertialSun,-1);

% The second step is to translate the origin of the Sun inertial coordinate
% system to the origin of the planetocentric inertial coordinate system.
% Before to do that, we need to express the vector from Sun to planet in
% the EarthJ2000. At this stage, it is in the ecliptic plane of reference. A
% rotation about the Vernal equinox has to be done.
[PositionPlanets,VelocityPlanets] = ephemerideVSOP87(jd_SOI,number);

% Planetary position and velocity vectors in the EarthJ2000 coordinate.
[r_Sun_planet_MJ2000eq,rdot_Sun_planet_MJ2000eq] = MJ2000Ec2MJ2000Eq( ...
                                       PositionPlanets,VelocityPlanets,-1);
```

```
% Translation
r_InertialBody_MJ2000eq    = r_InertialSun_MJ2000Eq - r_Sun_planet_MJ2000eq;
rdot_InertialBody_MJ2000eq = rdot_InertialSun_MJ2000Eq - ...
                             rdot_Sun_planet_MJ2000eq;


% The final transformation is the reverse transformation of the first one.
[r_InertialBody,rdot_InertialBody] = MJ2000Eq2InertialBody(number, ...
                        r_InertialBody_MJ2000eq,rdot_InertialBody_MJ2000eq);


end
```

Function called

```
%_____________________________________________________________________________
% Author: PICHA Thibault
%
% Academic year: 2017-2018
%
% DESCRIPTION : this function rotates the position and velocity vectors
% between an inertial coordinate system where the axes are those of the Earth
% inertial coordinate system to an inertial coordinate system where the
% axes are those of the planetocentric inertial coordinate system. The origin
%  of the coordinate system is the one of the target planet.
%
%
% INPUTS :
%
% - number                [1,8] is the index of the celestial elements
%
%                           => 1 : Mercury
%                           => 2 : Venus
%                           => 3 : Earth
%                           => 4 : Mars
%                           => 5 : Jupiter
%                           => 6 : Saturn
%                           => 7 : Uranus
%                           => 8 : Neptune
%
%
%
%
%  - r_MJ2000Eq            Position vector in the coordinate system where
%                          the axes are those of the Earth inertial
%                          coordinatesystem and the origin is the target
%                          planet.
%                          Size: 3x1 [km]
%
%
%
%  - rdot_MJ2000Eq         Velocity vector in the coordinate system where
```

```
%                           the axes are those of the Earth inertial
%                           coordinate system and the origin is the target
%                           planet.
%                           Size: 3x1 [km/s]
%
%
%
%
% OUTPUTS:
%
%
% - r_InertialBody          Position vector in the planetocentric inertial
%                           coordinate system
%                           Size: 3 x 1 [km]
%
%
% - rdot_InertialBody       Velocity vector in the planetocentric inertial
%                           coordinate system.
%                           Size: 3 x 1 [km/s]
%
%
%  Reference:               GMAT R2017
%
% FUNCTION CALLED : \
%_____________________________________________________________________________

function [r_InertialBody,rdot_InertialBody] = MJ2000Eq2InertialBody( ...
                                          number,r_MJ2000Eq,rdot_MJ2000Eq)

% Right ascension and declination of the Spin axis of the celestial body
% with respect to EarthMJ2000 (GMTA p41). [Degree]
alpha0           = [281.01; 272.76; -90; 317.68143; 268.05; 40.589; ...
                    257.311; 299.36+0.7*sind(357.85); 313.02];
delta0           = [61.45; 67.16; 90; 52.8865; 64.49; 83.537; -15.175; ...
                    43.46-0.51*cosd(357.85); 9.09];

% First rotation about the Z-axis.
sin_alpha0       =     sind(alpha0(number) + 90);
cos_salpha0      =     cosd(alpha0(number) + 90);

rot3_alpha0      =  [ cos_salpha0         sin_alpha0          0    ;...
                     -sin_alpha0         cos_salpha0         0    ;...
                         0                   0               1    ];

% Second rotation about the X-axis.
sin_delta0       =      sind(90 - delta0(number));
cos_delta0       =      cosd(90 - delta0(number));

rot1_delta0      =  [1                0                   0  ;...
                     0          cos_delta0       sin_delta0 ;...
                     0         -sin_delta0       cos_delta0 ];


% Position and velocity vectors in the planetocentric inertial system.
r_InertialBody    = rot1_delta0 * rot3_alpha0 * r_MJ2000Eq;
rdot_InertialBody = rot1_delta0 * rot3_alpha0 * rdot_MJ2000Eq;
```

```
end
```

C.3.3 Planetocentric to heliocentric coordinate system

```
%_____________________________________________________________________
% Author: PICHA Thibault
%
% Academic year: 2017-2018
%
% DESCRIPTION : when a spacecraft leaves a sphere of influence, the change
% of coordinate system between the planetocentric and heliocentric inertial
% coordinate systems is performed thanks to this function. It is also used
% to perform any change between planetocentric and heliocentric
% coordinate systems.
%
% INPUTS :
%
% - number                  [1,8] is the index of the celestial body the
%                           spacecraft is leaving.
%                           [-]
%
%
%                            => 1 : Mercury
%                            => 2 : Venus
%                            => 3 : Earth
%                            => 4 : Mars
%                            => 5 : Jupiter
%                            => 6 : Saturn
%                            => 7 : Uranus
%                            => 8 : Neptune
%
%
%
%  - r_InertialBody         Position vector in the planetocentric inertial
%                           coordinate system.
%                           Size: 3x1 [km].
%
%
%
%  - rdot_InertialBody      Velocity vector in the planetocentric inertial
%                           coordinate system.
%                           Size: 3x1 [km/s].
%
% - jd                      Julian date at which we perform the
%                           transformation in terrestrial time
%
%
%
% OUTPUTS:
%
%
% - r_InertialSun           Position vector in the heliocentric inertial
```

```
%                           coordinate system.
%                           Size: 3 x 1 [km].
%
% - rdot_InertialSun        Velocity vector in the heliocentric inertial
%                           coordinate system.
%                           Size: 3 x 1  [km/s].
%
%
% Reference:                GMTA R2017a
%
% FUNCTIONS CALLED :        InertialBody2MJ2000Eq.m
%                           ephemerideVSOP87.m
%                           MJ2000Ec2MJ2000Eq.m
% ______________________________________________________________________

function [r_InertialSun,rdot_InertialSun] = BodyInertial2Suninertial( ...
                           r_InertialBody,rdot_InertialBody,jd_SOI,number)


% The first step is to rotate the position and velocity vectors in the Earth's
% inertial axes at the J2000 epoch.
[r_InertialBody_MJ2000,rdot_InertialBody_MJ2000] = InertialBody2MJ2000Eq(...
                                  number,r_InertialBody,rdot_InertialBody);

% The second step is to translate the origin of the planetocentric
% coordinate system to the origin of the heliocentric inertial
% coordinate system. Before to do that, we need to express the vector
% from Sun to planet in the Earth's inertial coordinate system.
% At this stage, it is in the heliocentric inertial coordinate system.
% A rotation about the Vernal equinox has to be done.
[PositionPlanets,VelocityPlanets] = ephemerideVSOP87(jd_SOI,number);

% Planet position and velocity vectors in the EarthJ2000 coordinate system.
[r_Sun_planet_MJ2000,rdot_Sun_planet_MJ2000] = MJ2000Ec2MJ2000Eq(...
                                       PositionPlanets,VelocityPlanets,-1);

% Translation
r_InertialSun_MJ2000Eq      =  r_InertialBody_MJ2000 + r_Sun_planet_MJ2000;
rdot_InertialSun_MJ2000Eq   =  rdot_InertialBody_MJ2000 + ...
                               rdot_Sun_planet_MJ2000;

% The final step rotates the axes of the Earth inertial coordinate
% system on the axes of the Sun inertial coordinate system.
[r_InertialSun,rdot_InertialSun] = MJ2000Ec2MJ2000Eq(r_InertialSun_MJ2000Eq,...
                                                rdot_InertialSun_MJ2000Eq,1);
end
```

Function called

```
%_______________________________________________________________________
% Author: PICHA Thibault
%
% Academic year: 2017-2018
```

```
% DESCRIPTION : this function rotates the position and velocity vectors
% between an inertial coordinate system where the axes are those of the
% planetocentric inertial coordinate system to an inertial coordinate system
%  where the axes are those of the Earth inertial coordinate system. The
% coordinate system is the one of the considered planet. It is used during
% origin of the  a change of coordinate system between a planetocentric and
% a heliocentric inertial coordinate system.
%
%
% INPUTS :
%
% - number                [1,8] is the index of the departure celestial
%                         element
%
%                           => 1 : Mercury
%                           => 2 : Venus
%                           => 3 : Earth
%                           => 4 : Mars
%                           => 5 : Jupiter
%                           => 6 : Saturn
%                           => 7 : Uranus
%                           => 8 : Neptune
%
%
%
% - r_InertialBody         Position vector in the planetocentric inertial
%                          coordinate system.
%                          Size: 3 x 1 [km].
%
% - rdot_InertialBody      Velocity vector in the planetocentroc inertial
%                          coordinate  system.
%                          Size: 3 x 1 [km/s].
%
% OUTPUTS:
%
%
%  - r_MJ2000Eq           Position vector in the coordinate system where
%                         the axes are those of the Earth inertial coordinate
%                         system and the origin is the one of the departure
%                         planet.
%                         Size: 3x1  [km].
%
%
%  - rdot_MJ2000Eq        Velocity vector in the coordinate system where
%                         the axes are those of the Earth inertial coordinate
%                         system and the origin is the one of the departure
%                         planet.
%                         Size: 3x1 [km/s].
%
%
%  Reference:             GMTA R2017a
%
% FUNCTION CALLED : \
%_____________________________________________________________________________
```

```
function [r_MJ2000Eq,rdot_MJ2000Eq] = InertialBody2MJ2000Eq(number,...
                                        r_InertialBody,rdot_InertialBody)

% Right ascension and declination of the Spin axis of the celestial body
% with respect to the axes of the Earth inertial coordinate system.
% [Degree]
alpha0          = [281.01; 272.76; -90; 317.68143; 268.05; 40.589; 257.311;...
                   299.36+0.7*sind(357.85); 313.02];
delta0          = [61.45; 67.16; 90; 52.8865; 64.49; 83.537; -15.175; ...
                   43.46-0.51*cosd(357.85); 9.09];

% First rotation about the X-axis. The rotation matrix is the Euler
% matrix. The minus sign means that it is a clockwise rotation.
sin_delta0      =  sind(-(90 - delta0(number)));
cos_delta0      =  cosd(-(90 - delta0(number)));

rot1_delta0     =  [1               0                  0  ;...
                    0          cos_delta0       sin_delta0 ;...
                    0         -sin_delta0       cos_delta0 ];

% Second rotation about the Z-axis:
sin_alpha0      =   sind(-(alpha0(number) + 90));
cos_salpha0     =   cosd(-(alpha0(number) + 90));

rot3_alpha0     =   [ cos_salpha0         sin_alpha0          0    ;...
                      -sin_alpha0         cos_salpha0         0    ;...
                          0                    0              1    ];

% Transformation: position and velocity vectors  in the axes of the Earth
% inertial coordinate system.
r_MJ2000Eq      =  rot3_alpha0 * rot1_delta0 *  r_InertialBody;
rdot_MJ2000Eq   =  rot3_alpha0 * rot1_delta0 *  rdot_InertialBody;

end
```

C.4 Lambert's problem

```
%_____________________________________________________________________________
% Author: PICHA Thibault
%
% Academic year: 2017-2018
%
% DESCRIPTION : this function implements Lambert's problem. Given the
% initial, final vector position and the time of flight between these two
% position vectors, the function computes the Keplerian elements of the
% corresponding orbit and also the velocities at departure v_init and at
% arrival V_final.
%
% INPUTS :
%
% - r_init          Initial position of the spacecraft.
%                   Size: 3x1 [km]
%
% - r_final         Final position of the spacecraft.
%                   Size: 3x1 [km]
%
% - time_Flight     Transfert time between the initial and the final
%                   position.
%                   Size: 1x1 [s]
%
% - mu              Gravitational parameter of the main attractor
%                   Size: 1x1 [km^3/s^2]
%
% - type            = 1 if prograde trajectories (0<i<90), =0 if retrograde
%                   trajectory (90<i<180) (often take prograde)
%                   Size: 1x1 [-]
%
% OUTPUTS:
%
% - (a, e, incl,     Keplerian elements of the orbit
%   Omega, omega,    describing the trajectory joining
%   phi)             the two position vectors.
%
% -  v_init          Departure velocity.
%                    Size: 3 x1 [km/s].
%
% - v_final          Arrival velocity.
%                    Size: 3 x1 [km/s]
%
%  REFERENCE :       p263-270 Curtis
%
% FUNCTION CALLED :  cart2kepl.m
%
%
%
%_____________________________________________________________________________

%%  Validation 1: Example 5.2 Curtis p 270 (ellipse case)
```

```
% r_init      = [5000;10000;2100];
% r_final     = [-14600;2500;7000];
% time_Flight = 3600;
% mu          = 398600;
% type        = 1;

%% Validation 2: Example 5.3 Curtis p274 (hyperbolic case)

% r_init      = [273378;0;0];
% r_final     = [1.458209875172735e+05;1.275768331191671e+04;0];
% time_Flight = 13.5*60*60;
% mu          = 398600;
% type        = 1; => compare with v_1, e, h

%% Validation 3 : Vallado p467

% r_init      = [15945.34;0;0];
% r_final     = [12214.83899;10249.46731;0];
% time_Flight = 76*60;
% mu          = 398600.44418;
% type        = 1

%% Validation 4: p477 Curtis

% r_init        = [1.05*10^8;1.0466*10^8;988.33];
% r_final       = [-2.0833*10^7;-2.184*10^8;-4.0629*10^6];
% time_Flight   = 309*86400;
% mu            = 132.71*10^9;
% type          = 1;

%% Reverse process test

% r_init        = [1.514453905048841e+08;3.537732760553140e+07;
%                   8.721319269168037e+05];
% r_final       = [-4.804176489776150e+07;1.398470642756414e+08;
%                   -2.486049327415967e+05];
% time_Flight   = 309*86400;
% mu            = 1.32712428*10^11;
% type          = 1;
%_____________________________________________________________________________

function [a, e, incl, Omega, omega, phi,v_init,v_final] = LambertProblem( ...
                                        r_init,r_final,time_Flight,mu,type)

% Norm of the initial and final position vectors.
r_init_norm      = norm(r_init);
r_final_norm     = norm(r_final);

% DeltaPhi is the change in true anomaly. Its value depends on the Z-components
% of the cross product between r_init and r_final (Eq-5.26 Curtis)
% The condition "if" differentiates the prograde and retrograde trajectories.
% [deg].
DeltaPhi         =  acosd(r_init'*r_final / (r_init_norm *r_final_norm));

if cross(r_init,r_final)'*[0;0;1] <0 && type == 1 ||  cross(r_init,r_final)'*...
                                                    [0;0;1] >=0 && type == 0
```

```
    DeltaPhi     = 360 - DeltaPhi;
end


% Temporary variable temp [km] (Eq-5.35 Curtis).
temp             = sind(DeltaPhi) * sqrt(r_init_norm * r_final_norm/(1 - ...
                   cosd(DeltaPhi)));

% Newton-raphson algorithm to find z (z<0 for hyperbola, =0 for parabola,
% z>0 for ellipses).
z = fsolve(@(z) NewtRaphLambertProblem(z,r_init_norm,r_final_norm,temp, ...
    time_Flight,mu),1); % Initial guess 1 (maybe find a better one)

C_z              = (1-cos(sqrt(z)))/z;
S_z              = (sqrt(z)-sin(sqrt(z)))/(sqrt(z))^3;
Y_z              = r_init_norm + r_final_norm + temp * (z*S_z-1) / sqrt(C_z);
%(Eq-5.38 Curtis)

% Lagrange coefficients.
f                = 1 - Y_z / r_init_norm;  % (Eq-5.46a Curtis)
g                = temp * sqrt(Y_z/mu);    % (Eq-5.46b Curtis) [s]
gdot             = 1 - Y_z / r_final_norm; % (Eq-5.46d Curtis)

% Departure velocity (Eq-5.28 Curtis).
v_init           = (r_final - f * r_init) / g;

% Arrival velocity (Eq-5.29 Curtis).
v_final          = (gdot * r_final - r_init) / g;

% Keplerian elements of the orbit (it could be also be computed with
% r_final, v_final).
[a, e, incl, Omega, omega, phi] = cart2Kepl(r_init, v_init, mu);

end
```

C.4.1 Newton-Raphson function

```
%_____________________________________________________________________
% Author: PICHA Thibault
%
% Academic year: 2017-2018
%
% DESCRIPTION : this function describes the nonlinear function F in the
% variable z. This function is used with fsolve of Matlab in the
% function LambertProblem.m.
%
%
% Reference: Curtis p183-184 (universal variable), p267-269  (Lambert's
% problem)
%
% FUNCTION CALLED : \
%
```

```
%_____________________________________________________________________________

function F= NewtRaphLambertProblem(z,r_init_norm,r_final_norm,temp, ...
            time_Flight,mu)

% Stumpff functions
C_z  = (1-cos(sqrt(z)))/z;
S_z  = (sqrt(z)-sin(sqrt(z)))/(sqrt(z))^3;

% Y function (part of the function of interest F)
Y_z = r_init_norm + r_final_norm + temp * (z*S_z-1) / sqrt(C_z);
    %(Eq-5.38 Curtis)

% The function F is a nonlinear function of the variable z. z is found with
% the function fsolve of MATLAB

F=(Y_z/C_z)^(3/2) * S_z + temp * sqrt(Y_z)-sqrt(mu)*time_Flight;
 %(Eq-5.40 Curtis)

end
```

C.4.2 Conversion Cartesian position and velocity vectors to Keplerian elements

```
%_____________________________________________________________________________
% Author: PICHA Thibault
%
%
% Academic year: 2017-2018
%
% DESCRIPTION : this function transforms the position and velocity vectors
% given in Cartesian position and velocity vectors into Keplerian/orbital
% elements.
%
%
% INPUTS :
%
%
% - r         Position matrix.
%             Size: 3 x n [km]
%             where n is the number of position vectors.
%
%
% - rdot      Velocity matrix.
%             Size: 3 x n [km/s]
%
% - mu        Gravitational parameter.
%             Size: 1 x 1 [km^3/s^2]
%
% OUTPUTS:
%
%
```

```
%  - a         Semi-major axis .
%              Size: n x 1 [km].
%
%  - e         Eccentricity.
%              Size: n x 1 [-]
%
%  - incl      Inclination.
%              Size: n x 1 [deg]
%
%  - Omega     Longitude of the ascending node.
%              Size: n x 1 [deg]
%
%  - omega     Argument of the periapsis .
%              Size: n x 1 [deg]
%
%  - Phi       True anomaly .
%              Size: n x 1 [deg]
%
%
% FUNCTION CALLED: \
%
% Reference: \

%% Validation 1 : p272 Curtis r1, v1, mu = 398600 (elliptic case)

%% Validation 2 : p212 Curtis Example 4.3 (elliptic case)
% mu   =  398600
% r    = [-6045;-3490;2500]; % [km]
% rdot = [-3.457;6.618;2.533] % [km/s]

%% Validation 3 : Curtis p240 (elliptic case)

% mu   =  398600
% r    = [-3670;-3870;4400]; % [km]
% rdot = [4.7;-7.4;1] % [km/s]

%% Validation 4:  p252 Curtis Example 4.15 (hyperbolic case)

% mu   =  398600
% r = [-1984;-5348;3471] % [km/s]
% rdot = [10.36;-5.763;-2.961]; % [km]

%% Validation 5:  p252 Curtis Example 4.18 (hyperbolic case)

% mu   =  398600
% r = [-3726;2181;4962] % [km/s]
% rdot = [-4.188;-10.65;1.536]; % [km]

%_____________________________________________________________________________

function [a, e, incl, Omega, omega, phi] = cart2Kepl(r, rdot, mu)

r             =    transpose(r);
rdot          =    transpose(rdot);

% Specific angular momentum [km^2/s].
```

```
h             =   cross(r, rdot);
h_norm        =   sqrt(h(:, 1) .^2 + h(:, 2) .^2 + h(:, 3) .^2);

% Eccentricity [-] (orbit in space, slide 56).
r_norm        =   sqrt(r(:, 1) .^2 + r(:, 2) .^2 + r(:, 3) .^2);
e_vec(:,1)    = - r(:,1) ./ r_norm;
e_vec(:,2)    = - r(:,2) ./ r_norm;
e_vec(:,3)    = - r(:,3) ./ r_norm;
e_vec         =   e_vec - cross(h, rdot) / mu;
e             =   sqrt(e_vec(:, 1) .^2 + e_vec(:, 2) .^2 + e_vec(:, 3) .^2);

% Specific energy [J/kg].
en            =   0.5 * (rdot(:, 1) .^2 + rdot(:, 2) .^2 + rdot(:, 3) .^2) ...
                  - mu ./ r_norm;

% Semi-major axis [km].
a             = - 0.5 * mu ./ en;

% Inclination [rad].
incl          =   acos(h(:,3) ./ h_norm);

% Longitude of the ascending node [rad].
twoPi         =   2 * pi;
Omega         =   atan2(h(:, 1), - h(:, 2));
index1        =   find(Omega<0);
Omega(index1) =   twoPi + Omega(index1);

% Argument of the periapsis [rad].
n             =   [cos(Omega) sin(Omega) zeros(length(Omega),1)];
omega         =   acos(dot(e_vec, n, 2) ./ e);
index2        =   find(e_vec(:,3) < 0);
omega(index2) =   twoPi - omega(index2);

% True anomaly [rad].
phi           =   acos(dot(e_vec, r, 2) ./ (e .* r_norm));
index3        =   find(dot(r, rdot, 2) < 0);
phi(index3)   =   twoPi - phi(index3);

% Conversion radian to degree.
rad2deg       =   180   /  pi;
incl          =   incl  *  rad2deg;
Omega         =   Omega *  rad2deg;
omega         =   omega *  rad2deg;
phi           =   phi   *  rad2deg;
end
```

C.5 Main algorithm

```
%_____________________________________________________________________________
% Author: PICHA Thibault
%
% Academic year: 2017-2018
%
% DESCRIPTION : main function of the interplanetary orbital propagator.
%
% INPUTS :
%
% - a                       Initial semi-major axis.
%                           Size: 1x1 [km]
%
% - e                       Initial eccentricity. e is positive or equals to
%                           0.
%                           Size: 1x1 [-]
%
% - incl                    Initial inclination.
%                           Size: 1x1 [deg]
%
% - Omega                   Initial longitude of the ascending node.
%                           Size: 1x1 [deg]
%
% - omega                   Initial argument of periapsis.
%                           Size: 1x1 [deg]
%
% - phi                     Initial true anomaly.
%                           Size: 1x1 [deg]
%
%
% - number                  is the index of the coordinate system
%                           in which the initial orbital elements are
%                           expressed.
%                           Size: 1x1 [-]
%
%                           => 1: Mercury inertial coordinate system.
%                           => 2: Venus inertial coordinate system.
%                           => 3: Earth inertial coordinate system.
%                           => 4: Mars inertial coordinate system.
%                           => 5: Jupiter inertial coordinate system.
%                           => 6: Saturn inertial coordinate system.
%                           => 7: Uranus inertial coordinate system.
%                           => 8: Neptune inertial coordinate system.
%                           =>10: Heliocentric inertial coordinate system.
%
% - (Year, Month, Day,      Departure date in terrestrial time.
%   Hour, Minute, Second)
%
%
% - (m, A_sun, c_r)         There are the ballistic properties used
%                           for the solar radiation pressure perturbation:
%                            - Reflectivity coefficient    c_r.
%                              Size: 1x1 [-]
```

```
%                               - Surface area facing the Sun A_sun.
%                                 Size: 1x1 [km^2]
%                               - Mass of the spacecraft       m.
%                                 Size: 1x1 [kg]
%
% - onOffJ2                     = 1 if the J2 perturbation is activated.
%                               = 0 if the J2 perturbation is not activated.
%                               Size: 1x1 [-]
%
% - onOffSPR                    = 1 if the solar radiation pressure
%                               perturbation is activated.
%                               = 0 if the solar radiation pressure
%                               perturbation is not activated.
%                               Size: 1x1 [-]
%
% - onOffPMG                    = 1 if the point mass gravity perturbation
%                               is activated.
%                               = 0 if the point mass gravity perturbation
%                               is not activated.
%                               Size: 1x1 [-]
%
% - duration                    Duration of the propagation.
%                               Size: 1x1 [s]
%
% - dt                          Time step at which the user wishes to know the
%                               position and the velocity vectors of the
%                               spacecraft.
%                               Size: 1x1 [s]
%
% - number_target               indicates a planetocentric coordinate system
%                               in which the positions and velocities vectors
%                               of the spacecraft wish to be known: [1,8]
%                               Size: 1x1 [-]
%
%                               => 1: Mercury inertial coordinate system.
%                               => 2: Venus inertial coordinate system.
%                               => 3: Earth inertial coordinate system.
%                               => 4: Mars inertial coordinate system.
%                               => 5: Jupiter inertial coordinate system.
%                               => 6: Saturn inertial coordinate system.
%                               => 7: Uranus inertial coordinate system.
%                               => 8: Neptune inertial coordinate system.
%
% OUTPUTS:
%
% - t_vector                    contains the time in terrestrial time at the
%                               desired time steps.
%                               Size: nx1 [s]
%
% - r_helio                     Position vectors in the heliocentric inertial
%                               coordinate system at the desired time steps.
%                               Size: 3 x n [km]
%
% - rdot_helio                  Velocity vectors in the heliocentric inertial
%                               coordinate system at the desired time steps.
%                               Size: 3 x n  [km/s]
```

```
%
% - r_planet                  Position vectors in the planetocentric inertial
%                             coordinate system specified by number_planet at
%                             the desired time steps.
%                             Size: 3xn [km].
%
% - rdot_planet               Velocity vectors in the planetocentric inertial
%                             coordinate system specified by number_planet at
%                             the desired time steps.
%                             Size: 3xn [km/s].
%
% - te_vector                 contains the time at which the spacecraft
%                             entered or leaved a sphere of influence.
%                             [s]
%
% - location                  contains the regions in which the spacecraft
%                             has gone though.
%                             [-]
% _____________________________________________________________________________

function [t_vector,r_helio,rdot_helio,r_planet,rdot_planet,te_vector,location] ...
= IOP(a, e, incl, omega, Omega, phi, number, Year, Month, Day, Hour, Minute, ...
Second,  m, A_sun, c_r, onOffJ2, onOffSPR, onOffPMG, duration, dt,number_target)

% Importation of the constants.
Constants;

%------------------------ Initialization ---------------------------------

% Dimensional initial conditions.
[r_init, rdot_init] = kepl2cart(a, e, incl, Omega, omega, phi, ...
                      mu_bodies(number));

% Initial Julian date.
jd                  = juliandate([Year, Month, Day, Hour, Minute, Second]);
                    % [days]
jd_init             = jd; % [days]


% Time vector.
t_vector            = 0 : dt : duration; % [s]

% Positions and velocities in the heliocentric inertial coordinate system.
r_helio             = zeros(3,length(t_vector));   % [km]
rdot_helio          = zeros(3,length(t_vector));   % [km/s]

% Current time.
t_current           = 0;                           % [s]
index               = 1;                           % [-]

% Event time.
te_vector           = 0;                           % [s]
index_Event         = 1;                           % [-]

% Location of the spacecraft.
location            = number;                      % [-]
```

```
%------------------------------- Propagation -----------------------------
while t_current < duration


 %--- Motion within the SOI.
 if number ~= 10

  % Characteristic variables in function of the sphere of influence in
  % which the spacecraft is located (number).
  LU                  = Re_bodies(number);               % [km]
  TU                  = sqrt(LU^3 / mu_bodies(number));  % [s]

  % Dimensionless initial conditions.
  r_initTilde         = r_init / LU;                     % [-]
  rdot_initTilde      = rdot_init * TU / LU;             % [-]
  y0                  = [r_initTilde; rdot_initTilde];   % [-]

  % Time interval during which we search the condition: leave a sphere of
  % influence.
  tspan               = 0 : dt/TU : round(duration-t_current) / TU; % [s]

  % Numerical integration.
  options             = odeset('RelTol', 1e-12, 'AbsTol', 1e-12,'Events' ...
                        ,@(t, u) LeaveSOIEvents(t,u,TU,LU,number,jd_init));

  [t,y,te,ye,ie]      = ode113(@(t, u) odeWithinSphereOfInfluence(t, u, ...
                        J2_bodies(number), c_r,A_sun,m,jd_init,number,TU,LU, ...
                        onOffJ2,onOffSPR,onOffPMG), tspan, y0, options);

  % The condition below tests if the spacecraft has crossed or not the sphere
  % of influence. If no, the final position and velocity must be kept.
  % Otherwise, final = -1 due to the fact that the user has specificed the
  % time steps. Often, the event time does not match with one of these time
  % steps. Therefore, the final position and velocity are not taken into
  % account. The code comes back to the previous time step with final = -1.

  if isempty(te)==1
     final = 0;
  else
    final = -1;
    % Save event time.
    te_vector(index_Event) = te*TU;
    location(index_Event+1)  = 10;
    index_Event = index_Event +1;
  end

  % Conversion into dimensional variables.
  t                   = t*TU;                          % [s]
  y(:,1:3)            = LU * y(:, 1 : 3);              % [km]
  y(:,4:6)            = y(:, 4 : 6) * LU / TU;         % [km/s]
  r                   = y(:,[1 2 3]);                  % [km]
  rdot                = y(:,[4 5 6]);                  % [km/s]

  % Conversion in the heliocentric inertial coordinate system.
  for i = 1 : length(t) + final
```

```
  [r_helio(1:3,index+i-1), rdot_helio(1:3,index+i-1)] =  ...
  BodyInertial2Suninertial(transpose(r(i,1:3)),transpose(rdot(i,1:3)), ...
  jd_init+t(i)/86400,number);
 end

 % Updating.
 index                = index     + length(t) + final - 1;
 t_current            = t_current + round(t(end +final));
 jd_init              = jd_init   + round(t(end +final))/86400;
 [r_init,rdot_init]   = BodyInertial2Suninertial(transpose(r(end+final,1:3)), ...
                        transpose(rdot(end+final,1:3)),jd_init,number);
 number               = 10;


%--- Motion outside the spheres of influence.
else

 % Characteristic variables: sun equatorial radius and gravitational
 % parameter.
 LU                   = Re_bodies(10);                  % [km]
 TU                   = sqrt(LU^3 / mu_bodies(10));     % [s]

 % Dimensionless initial conditions.
 r_initTilde          = r_init / LU;                    % [-]
 rdot_initTilde       = rdot_init * TU / LU;            % [-]
 y0                   = [r_initTilde; rdot_initTilde]; % [-]

 % Time interval during which we search the condition: enter a sphere of
 % influence.
 tspan                = 0 : dt/TU : round(duration-t_current) / TU; % [s]

 % Numerical integration.
 options              = odeset('RelTol', 1e-12, 'AbsTol', 1e-12,'Events', ...
                         @(t, u) EnterAnySOIEvents(t,u,TU,LU,jd_init));


 [t,y_SR,te,ye,ie]    = ode113(@(t, u) odeOutsideSphereOfInfluence(t, u,c_r,...
                         A_sun,m,jd_init,onOffSPR,onOffPMG), tspan, ...
                         y0, options);

 if isempty(te)==1
   final = 0;
   ie    = 1;
 else
   final = -1;
   % Save event time.
   te_vector(index_Event) = te*TU;
   location(index_Event+1)  = ie;
   index_Event = index_Event +1;

 end

 % Conversion into dimensional variables.
 t                    = TU *t;                          % [s]
 y_SR(:,1:3)          = LU * y_SR(:, 1 : 3);            % [km]
 y_SR(:,4:6)          = y_SR(:, 4 : 6) * LU / TU;       % [km/s]
```

```
  r_helio(1:3,index:index + length(t) + final-1) = transpose( ...
                                                    y_SR(1:end+final,[1 2 3]));

  rdot_helio(1:3,index:index + length(t) + final-1) = transpose( ...
                                                     y_SR(1:end+final,[4 5 6]));



  % Updating.
  [r_init,rdot_init]  = SunInertial2BodyInertial(r_helio(1:3,index + ...
                        length(t) + final-1),rdot_helio(1:3,index + ...
                        length(t) + final-1),jd_init+t(end+final)/86400,ie);
  index               = index     + length(t) + final-1;
  t_current           = t_current + round(t(end +final));
  jd_init             = jd_init   + t(end +final) /86400;
  number              = ie;

 end

end

%---------------  Conversion in the planetocentric inertial ---------------
%---------------  coordinate system specified by number_target. -----------
r_planet              = zeros(3,length(t_vector));   % [km]
rdot_planet           = zeros(3,length(t_vector));   % [km/s]

for i = 1 : length(t_vector)
[r_pla,rdot_pla]      = SunInertial2BodyInertial(r_helio(1:3,i), ...
                        rdot_helio(1:3,i),jd+t_vector(i)/86400,number_target);
r_planet(1:3,i)       = r_pla;                       % [km]
rdot_planet (1:3,i)   = rdot_pla;                    % [km/s]
end

end
```

C.5.1 Initialization: conversion Keplerian elements to Cartesian position and velocity vectors

```
%_____________________________________________________________________________
% Author: PICHA Thibault
%
%
% Academic year: 2017-2018
%
% DESCRIPTION : this function transforms Keplerian/orbital elements to
% Cartesian position and velocity vectors.
%
% INPUTS :
%
% - a         Semi-major axis.
%             Size: 1x1 [km]
```

```
%
% - e          Eccentricity.
%              Size: 1x1 [-]
%
% - incl       Inclination.
%              Size: 1x1 [deg]
%
% - Omega      Longitude of the ascending node.
%              Size: 1x1 [deg]
%
% - omega      Argument of periapsis.
%              Size: 1x1 [deg]
%
% - phi        True anomaly.
%              Size: 1x1 [deg]
%
% - mu         Gravitational parameter.
%              Size: 1x1 [km^3/s^2]
%
% OUTPUTS:
%
%  - r         Position vector
%              Size: 3x1 [km]
%
%  - rdot      Velocity vector
%              Size: 3x1 [km/s]
%
%
% Reference:  p125 Vallado
% FUNCTION CALLED : \
%_____________________________________________________________________________

function [r,rdot] = kepl2cart(a,e,incl,Omega,omega,phi,mu)

%% Validation 1 : Curtis p272 (to retrieve r1 and v1)

% a             = 2.000291348609851e+04; %[km]
% e             = 0.433488296836517;     %[-]
% Omega         = 44.600196970157789     %[deg]
% incl          = 30.191044621582325     %[deg]
% omega         = 30.706214930417396;    %[deg]
% phi           = 3.508297481831328e+02  %[deg]
% mu            = 398600;                %[km^3/s^2]

%% Validation 2: example 5.3 p274 Curtis (hyperbolic case)

% a             = -1.290895132688327e+05; %[km]
% e             = 1.050648918934465;     %[-]
% Omega         = 0;      %[deg]
% incl          = 0;      %[deg]
% omega         = 1.548384635923532e+02;    %[deg]
% phi           =  2.051615364076468e+02;  %[deg]
% mu            = 398600;                %[km^3/s^2]

%% Validation 3:  p212 Curtis Example 4.3 (Elliptic case)
```

```
% a            = 8.788095117377654e+03; %[km]
% e            = 0.171212346284454;     %[-]
% Omega        = 2.552792853343962e+02;     %[deg]
% incl         = 1.532492285182475e+02;     %[deg]
% omega        = 20.068316650582524;    %[deg]
% phi          = 28.445628306614928;  %[deg]
% mu           = 398600;                %[km^3/s^2]

%% Validation 4:  p252 Curtis Example 4.15 (hyperbolic case)

% a            = -1.332299506025064e+04; %[km]
% e            = 1.501179721631599;     %[-]
% Omega        = 1.300118293714135e+02;     %[deg]
% incl         = 34.994890375126126;     %[deg]
% omega        = 1.149998180694285e+02;    %[deg]
% phi          = 3.599867236981295e+02;  %[deg]
% mu           = 398600;                %[km^3/s^2]

%% Validation 5:  p252 Curtis Example 4.18 (hyperbolic case)

% a            = -3.289604354408824e+04; %[km]
% e            =  1.199942915030137;     %[-]
% Omega        = 74.999780767957333;     %[deg]
% incl         = 50.000569412284598;     %[deg]
% omega        = 80.000638872143597;    %[deg]
% phi          = 3.599978837565484e+02;  %[deg]
% mu           = 398600;                %[km^3/s^2]
%_____________________________________________________________________________

% Semiparameter (describes the size of the conic section) [p104 Vallado]
p                   = a * (1 - e^2); % [km]


% Position in the perifocal coordinate system.
cos_phi             = cosd(phi);
sin_phi             = sind(phi);
r_norm              = p / (1 + e * cos_phi);
r_perifocal         = [cos_phi; sin_phi; 0] * r_norm;

% Velocity in the perifocal coordinate system
rdot_perifocal      = sqrt(mu / p) * [- sin_phi; e + cos_phi; 0];

% Transformation matrix R (p 125 Vallado)
cOmega              = cosd(Omega);
sOmega              = sind(Omega);
comega              = cosd(omega);
somega              = sind(omega);
cInc                = cosd(incl);
sInc                = sind(incl);

R11                 =   cOmega * comega - sOmega * somega * cInc;
R12                 = - cOmega * somega - sOmega * comega * cInc;
R13                 =   sOmega * sInc;
R21                 =   sOmega * comega + cOmega * somega * cInc;
R22                 = - sOmega * somega + cOmega * comega * cInc;
R23                 = - cOmega * sInc;
```

```
R31                     =   somega * sInc;
R32                     =   comega * sInc;
R33                     =   cInc;
R                       =   [R11, R12, R13; R21, R22, R23; R31, R32, R33];

% Position and velocity in the inertial coordinate system.
r                       = R * r_perifocal;
rdot                    = R * rdot_perifocal;

end
```

C.5.2 Motion within the spheres of influence

Ordinary differential equation

```
%_____________________________________________________________________________
% Author: PICHA Thibault
%
%
% Academic year: 2017-2018
%
% DESCRIPTION : it is the function called by ode113 to integrate the
% equations of motion within spheres of influence.
%
% INPUTS :
%
% - t                           Dimensionless time
%                               [-]
%
% - u                           u(1:3) dimensionless position vector in the
%                               planetocentric inertial coordinate system.
%                               [-]
%                               u(4:6) dimensionless velocity vector in the
%                               planetocentric inertial coordinate system.
%                               [-]
%
% - J2                          J2 coefficient. It takes into account the
%                               flattening of the poles of the considered
%                               planet.
%                               [-]
%
% - (c_r,A_sun,m)               There are the ballistic properties used
%                               for the solar radiation pressure perturbation:
%                               - Reflectivity coefficient    c_r.   [-]
%                               - Surface area facing the Sun A_sun. [km^2]
%                               - Mass of the spacecraft      m.     [kg]
%
% - jd_init                     Julian date at the beginning of the
%                               propagation expressed in terrestrial time.
%                               [days]
%
% - number                      [1,8] is the index of the sphere of influence
%                               in which the motion of the spacecraft occurs.
```

```
%                               [-]
%
%
%                               => 1 : Mercury
%                               => 2 : Venus
%                               => 3 : Earth
%                               => 4 : Mars
%                               => 5 : Jupiter
%                               => 6 : Saturn
%                               => 7 : Uranus
%                               => 8 : Neptune
%
%
% - TU                          Charasteristic time unit variable in the
%                               sphere of influence.
%                               [s]
%
% - LU                          Charasteristic length unit variable in the
%                               sphere of influence.
%                               [km]
%
% - onOffJ2                     = 1 if the J2 perturbation is activated.
%                               = 0 if the J2 perturbation is not activated.
%                               [-]
%
% - onOffSPR                    = 1 if the solar radiation pressure
%                               perturbation is activated.
%                               = 0 if the solar radiation pressure
%                               perturbation is not activated.
%                               [-]
%
% - onOffPMG                    = 1 if the point mass gravity attraction
%                               perturbation is activated.
%                               = 0 if the point mass gravity attraction
%                               perturbation is not activated.
%                               It takes into account the Sun and the seven
%                               planets other than the central body.
%                               [-]
%_______________________________________________________________________________


function dudt = odeWithinSphereOfInfluence(t, u, J2, c_r,A_sun,m,jd_init,...
                number,TU,LU,onOffJ2,onOffSPR,onOffPMG)

% Importation of the constants.
Constants;

% Current Julian day.
jd_current                  = jd_init+t*TU/86400;

% Position and norm of the position in the planetocentric inertial
% coordinate system (dimensionless and nondimensionless are needed).
r                           = u(1 : 3);                         % [-]
r_norm                      = norm(r);                          % [-]
r_dimen                     = r*LU;                             % [km]
rdot_dimen                  = [u(4);u(5);u(6)]* LU / TU;        % [km/s]
```

```
% All the perturbations are initialized to 0.
J2_pert                     = 0;
SRP_pert                    = 0;
PMG_tot                     = 0;
PMG_Moon                    = 0;



%-----------------------------J2 perturbation-------------------------------
% If the J2 perturbation is activated

if onOffJ2 == 1

J2_pert                     = 1.5 * J2 / r_norm^5 * r .* (5 * (r(3) ...
                              / r_norm)^2 - [1;1;3]);

end

%------------- Solar radiation pressure perturbation ----------------------
% If the solar radiation perturbation is activated

if onOffSPR ==1

% The first step is to compute the distance between the spacecraft and the
% Sun in the heliocentric coordinate system. The position and velocity of
% the spacecraft in the heliocentric inertial coordinate system are given
% by
[r_SunSpacecraft,rdot_SunSpacecraft] = BodyInertial2Suninertial(r_dimen,...
                                       rdot_dimen,jd_current,number); %[km]

% Solar radiation pressure at a distance R from the sun's center
S0                          = 5.67*10^-8 * 5777^4; % [W/m^2]
S                           = S0 * (Re_bodies(10) / norm(r_SunSpacecraft))^2;
P_SR                        = S / 2.998 / 10^8 * 1000; % [kiloNewton/km^2]

%----- Eclise model: Curtis

% Position of the Sun in the planetocentric inertial coordinate system.
% The Sun is at the center of the heliocentric coordinate system [0;0;0].
% This position is transformed in the planetocentric coordinate system.
[r_Sun,rdot_Sun]            = SunInertial2BodyInertial([0;0;0],[0;0;0],...
                                                       jd_current,number);

% Distance from centre of the planet to the Sun.
r_Sun_norm                  = norm(r_Sun) ; % [km]

% Angle between the spacecraft and Sun position vectors.
theta                       = acos(r' * r_Sun / r_norm  / r_Sun_norm);%[rad]

% Angle between the spacecraft and the tangent point.
theta1                      = acos(1 / r_norm); % [rad]

% Angle between the Sun and the tangent point.
theta2                      = acos(Re_bodies(number) / r_Sun_norm); % [rad]
```

```
% Shadow coefficient is initialised in full illumination.
v                           = 1; % [-]

% Shadow condition.
if theta1 + theta2 < theta
    v                       = 0;
end

%----- Expression of the solar radiation pressure perturbation

SRP_pert                    = v* Re_bodies(number)^2 * P_SR * c_r * ...
                              A_sun / m / mu_bodies(number) .* ...
                              (r_dimen-r_Sun)/norm(r_dimen-r_Sun);


end
%------------------------Point mass gravity perturbation ------------------
% If the point mass gravity perturbation is activated

if onOffPMG ==1

%----- Moon point mass gravity perturbation

    % Moon is taken into account if the spacecraft is within the Earth
    % sphere of influence.
    if number ==3
    [r_k_Moon]              = EphemerideMoon(jd_current);
    r_k_Moon                = r_k_Moon / LU;

    % Point mass gravity of Moon (PMG = Point Mass Gravity).
    PMG_Moon                =  4902.8005821478/ mu_bodies(number) * ...
       ( (r_k_Moon - r)/norm(r_k_Moon - r)^3 - r_k_Moon /norm(r_k_Moon)^3);


    end

%----- Sun point mass gravity perturbation

% Dimensionless position vector of the Sun in the planetocentric inertial
% coordinate system.
[r_k_Sun,rdot_k_Sun]        = SunInertial2BodyInertial([0;0;0],[0;0;0],...
                              jd_current,number);
r_k_Sun                     = r_k_Sun / LU;

% Point mass gravity of the Sun (PMG = Point Mass Gravity).
PMG_Sun                     = mu_bodies(10) / mu_bodies(number) * ...
           ( (r_k_Sun - r)/norm(r_k_Sun - r)^3 - r_k_Sun /norm(r_k_Sun)^3);

%----- Planetary point mass gravity perturbations

z                           =1;
PMG                         = zeros(3,7);

for i =1 :8

if i ~= number % i = number is the attraction of the central body
```

```
% Position vector between the Sun and the planet in the planetocentric
% inertial coordinate system.
[r_SP,rdot_SP]              = ephemerideVSOP87(jd_current,i);
[r_k,rdot_k]                = SunInertial2BodyInertial(r_SP,rdot_SP, ...
                               jd_current,number);

% Dimensionless quantities.
r_k                         = r_k /LU;
PMG(1:3,z)                  = mu_bodies(i) / mu_bodies(number) * ...
                             ((r_k - r)/norm(r_k - r)^3 - r_k /norm(r_k)^3);
z                           = z+1;

end

end

%----- Expression of the total point mass gravity perturbation


PMG_tot                     = PMG_Moon + PMG_Sun + PMG(1:3,1) +  ...
                              PMG(1:3,2) + PMG(1:3,3) + PMG(1:3,4) ...
                             +PMG(1:3,5) + PMG(1:3,6) + PMG(1:3,7);


end

%-------------------  Final set of equations -------------------------------

% The x,y and z components of the velocity vector are the derivates of the
% x,y and z components of the position vector.
dudt                          = zeros(6, 1);
dudt(1 : 3)                   = u(4 : 6, 1);
dudt(4 : 6)                   = - r / r_norm^3 + J2_pert + SRP_pert + PMG_tot;

end
```

Event: leave a sphere of influence

```
%_____________________________________________________________________________
% Author: PICHA Thibault
%
%
% Academic year: 2017-2018
%
% DESCRIPTION : this function detects the condition: leave sphere of
% influence i.e when the spacecraft crosses the sphere of influence of a
% planet from inside the sphere of influence to outside the sphere of
% influence (Event).
%
%
% INPUTS :
%
```

```
% - LU                       Charasteristic length unit variable in the
%                           sphere of influence.
%                           [km]
%
% - TU                       Charasteristic time unit variable in the
%                           sphere of influence.
%                           [s]
%
% - number                   [1,8] is the index of the celestial elements
%                           we want to leave.
%
%                           => 1 : Mercury
%                           => 2 : Venus
%                           => 3 : Earth
%                           => 4 : Mars
%                           => 5 : Jupiter
%                           => 6 : Saturn
%                           => 7 : Uranus
%                           => 8 : Neptune
%
%
%
% - t                        Dimensionless time
%                           [-]
%
% - u                        u(1:3) dimensionless position vector in the
%                           planetocentric inertial coordinate system.
%                           [-]
%                           u(4:6) dimensionless velocity vector in the
%                           planetocentric inertial coordinate system.
%                           [-]
%
% - jd_init                  Julian date corresponding to the beginning of
%                           of the propagation in terrestrial time.
%
%
% OUTPUTS:
%
% - value                    is a mathematical expression describing the
%                           event.  An event occurs when value is equal
%                           to 0 or positive. This is the equation of a
%                           sphere: x^2 + y^2 + z^2 = R^2.
%
%
%
% - isterminal               = 1. It means that the integration is to
%                           terminate when the event occurs.
%
%
% - direction                = 1. Positive direction only because we go
%                           from inside to outside the sphere of influence.
%                           At the beginning, value is negative. When we
%                           cross the sphere of influence, value is
%                           positive.
%
%
```

```
%
% FUNCTION CALLED : ephemerideVSOP87.m
%_____________________________________________________________________________

function [value,isterminal,direction] = LeaveSOIEvents(t,u,TU,LU,number, ...
                                         jd_init)

% Importation of the constants
Constants;

% Dimensional time
t_dimensional   = t * TU;

% Fraction of the day
frac_day        = t_dimensional / 86400;

% Current Julian date
jd              = jd_init + frac_day;

% Position of planets at current time [km] for which the spacecraft is
% within its sphere of influence.
[PositionPlanets,VelocityPlanets] = ephemerideVSOP87(jd, number);

% Radius at the sphere of influence at current time
R_SOI           = (m_bodies(number)/m_bodies(10))^(2/5)* ...
                  sqrt(PositionPlanets(1)^2+ PositionPlanets(2)^2+ ...
                  PositionPlanets(3)^2);

% Definition of the event
value           = sqrt((u(1)*LU)^2 + (u(2)*LU)^2 + (u(3)*LU)^2) - R_SOI;
isterminal      = 1;
direction       = 1;

end
```

C.5.3 Motion outside the spheres of influence

Ordinary differential equation

```
%_____________________________________________________________________________
% Author: PICHA Thibault
%
%
% Academic year: 2017-2018
%
% DESCRIPTION : it is the function called by ode113 to integrate the
% equations of motion outside spheres of influence.
%
% INPUTS :
%
% - t                         Dimensionless time
%                             [-]
%
```

```
% - u                          u(1:3) dimensionless position vector in the
%                             heliocentric inertial coordinate system.
%                             [-]
%                             u(4:6) dimensionless velocity vector in the
%                             heliocentric inertial coordinate system.
%                             [-]
%
%
% - (c_r,A_sun,m)             There are the ballistic properties used
%                             for the solar radiation pressure perturbation:
%                             - Reflectivity coefficient    c_r.   [-]
%                             - Surface area facing the Sun A_sun. [km^2]
%                             - Mass of the spacecraft       m.    [kg]
%
% - jd_init                   Julian date at the beginning of the
%                             propagation expressed in terrestrial time.
%                             [days]
%
% - TU                        Charasteristic time unit variable obtained
%                             with the gravitational parameter of the Sun
%                             and the radius of its photosphere.
%                             [s]
%
% - LU                        Charasteristic length unit variable obtained
%                             with the radius of the photosphere of the Sun.
%                             [km]
%
%
% - onOffSPR                  = 1 if the solar radiation pressure
%                             perturbation is activated.
%                             = 0 if the solar radiation pressure
%                             perturbation is not activated.
%                             [-]
%
% - onOffPMG                  = 1 if the point mass gravity attraction
%                             perturbation is activated.
%                             = 0 if the point mass gravity attraction
%                             perturbation is not activated.
%                             It takes into account the eight planets
%                             [-]
%_____________________________________________________________________________

function dudt = odeOutsideSphereOfInfluence(t, u,c_r,A_sun,m,jd_init, ...
                                            onOffSPR,onOffPMG)

% Importation of the constants
Constants;

% Current Julian date
jd_current          = jd_init+t*sqrt(Re_bodies(10)^3 / mu_bodies(10))/86400;


% Dimensionless position  and norm of the dimensionless position in the
% heliocentric coordinate system.
r                   = u(1 : 3); % [-]
r_norm              = norm(r);  % [-]
```

```
% All the perturbations are initialised to 0
SRP_perturb         = 0;
PMG_tot             = 0;


%---------------------Solar radiation pressure perturbation---------------
% If the solar radiation perturbation is activated

if onOffSPR == 1

% Solar radiation intensity S at a distance R from the sun's center
S0                  = 5.67*10^-8*5777^4;
S                   = S0 * (1/ r_norm)^2; % W/ m^2
P_SR                = S / 2.998 / 10^8 * 1000; % [kiloNewton/km^2]

SRP_perturb         = Re_bodies(10)^2 * P_SR * c_r * A_sun / m / mu_bodies(10)...
                  .* r/r_norm;

end

%----------------------N- bodies point mass interaction--------------------
% If the point mass gravity perturbation is activated

if onOffPMG == 1

PMG                 = zeros(3,8);


for i =1:8

[r_SC,rdot_SC]      = ephemerideVSOP87(jd_current,i);
r_k                 = r_SC / Re_bodies(10);
PMG(1:3,i)          = mu_bodies(i) / mu_bodies(10) *((r_k - r) ...
                      /norm(r_k - r)^3 - r_k /norm(r_k)^3);

end

PMG_tot             = PMG(1:3,1)+PMG(1:3,2)+PMG(1:3,3)+PMG(1:3,4)+PMG(1:3,5)...
                    + PMG(1:3,6) + PMG(1:3,7) + PMG(1:3,8);



end

%-----------------------------General equation-----------------------------
dudt           = zeros(6, 1);
dudt(1 : 3)    = u(4 : 6, 1);
dudt(4 : 6)    = - r / r_norm^3 + SRP_perturb + PMG_tot;

end
```

Event: enter a sphere of influence

```
%_____________________________________________________________________________
% Author: PICHA Thibault
%
%
% Academic year: 2017-2018
%
% DESCRIPTION : this file defines the event to detect if the spacecraft
% enters a sphere of influence.
%
% INPUTS :
%
% - t                           Dimensionless time
%                               [-]
%
% - u                           u(1:3) dimensionless position vector in the
%                               heliocentric inertial coordinate system.
%                               [-]
%                               u(4:6) dimensionless velocity vector in the
%                               heliocentric inertial coordinate system.
%                               [-]
%
% - jd_init                     Julian date at the beginning of the
%                               propagation expressed in terrestrial time.
%                               [days]
%
% - TU                          Charasteristic time unit variable obtained
%                               with the gravitational parameter of the Sun
%                               and the radius of its photosphere.
%                               [s]
%
% - LU                          Charasteristic length unit variable obtained
%                               with the radius of the photosphere of the Sun.
%                               [km]
%_____________________________________________________________________________

function [value,isterminal,direction] = EnterAnySOIEvents(t,u,TU,LU,jd_init)

% Importation of the constants
Constants;

%% Current Julian date

% Dimensional time
t_dimensional   = t * TU;

% Current Julian date
jd              = jd_init + t_dimensional / 86400;

value = zeros(8,1);
for i = 1 : 8

% Current position of the planet i
[PositionPlanets,VelocityPlanets] = ephemerideVSOP87(jd,i);

% Current Radius of the sphere of influence for the planet i
```

```
SOI  =(m_bodies(i)/Sun.m)^(2/5)*sqrt(PositionPlanets(1)^2+ ...
      PositionPlanets(2)^2+PositionPlanets(3)^2);

% Condition cross the sphere of influence of the planet i
value(i,1) = sqrt((u(1)*LU-PositionPlanets(1))^2 + (u(2)* ...
            LU-PositionPlanets(2))^2 + (u(3)*LU-PositionPlanets(3))^2 ) ...
            - SOI;

end

% isterminane is equal to 1 for all the planet because the integration
% stops if the spacecraft enters into any sphere of influence. It means
% that the integration is to terminate when one of the eights events occur
isterminal = [1;1;1;1;1;1;1;1];   % Stop the integration

% Negative direction only because we go from outside to
% inside the sphere of influence
direction = [-1;-1;-1;-1;-1;-1;-1;-1];

end
```

Bibliography

[1] BATE R., MUELLER D., WHITE J., *Fundamentals of Astrodynamics (Dover Books on Aeronautical Engineering)*, Dover Publications, 1971, ISBN 0486600610.

[2] BATTIN R., *An introduction to the mathematics and methods of astrodynamics*, American Institute of Aeronautics and Astronautics, 1999.

[3] BLITZER L., *Handbook of orbital perturbations*, astronautics 453, university of Arizona.

[4] CAPDEROU M., *Handbook of Satellite Orbits: from Kepler to GPS*, Springer International Publishing, 2014.

[5] BRETAGNON P., *Theory for the motion of all the planets-The VSOP82 solution*, Astronomy and Astrophysics, vol. 114, no. 2, Oct. 1982, pp.278-288.

[6] CURTIS H., *Orbital Mechanics for Engineering Students*, Second Edition, Butterworth-Heinemann, 2009.

[7] CURTIS H., *Chapter 12: Introduction to orbital perturbations*, in, *Orbital Mechanics for Engineering Students*, 3rd Edition, 2014, pp.651-720.

[8] DENG X., FAN M., XIE Y., *Comparisons and Evaluations of JPL Ephemerides*, Chinese Astronomy and Astrophysics 38, 2014.

[9] FRANZ M., HARPER D., *Heliospheric coordinate systems*, Planetary and Space Science, Vol.50(2),2002, pp.217-233.

[10] Gurfil P., *Modern Astrodynamics, Volume 1 Elsevier Astrodynamics Series*, Butterworth-Heinemann, 2006, ISBN 0123735629.

[11] HINTZ G., *Orbital Mechanics and Astrodynamics: Techniques and Tools for Space Missions*, Springer, 2015, ISBN 9783319094434.

[12] KERSCHEN G., *Interplanetary Trajectories*, Astrodynamics course, University of Liège, academic year 2017-2018.

[13] KERSCHEN G., *The Orbit in Space*, Astrodynamics course, University of Liège, academic year 2017-2018.

[14] PRUSSING J., CONWAY B., *Orbital Mechanics*, Oxford University Press, 2012.

[15] MEEUS J., *Astronomical Algorithms*, Willmann-Bell, 1991.

[16] MOISSON X. and BRETAGNON P. , *Analytical planetary solution VSOP2000*, institut de mécanique céleste, UMR8028, Observatoire de Paris, 77, avenue Denfert-Rochereau 75014, Paris, France.

[17] MONTENBRUCK O., GILL E., *Satellite Orbits : Models, Methods and Applications*, Springer Berlin Heidelberg, 2000.

[18] NASA Goddard Space Flight Center, *General Mission Analysis Tool (GMAT) Mathematical Specifications DRAFT*, Greenbelt RD, May 5, 2017.

[19] RAUW G., *Celestial mechanics and space trajectories*, Lecture notes, University of Liège, academic year 2017-2018.

[20] SIMON J.L, BRETAGNON P., CHAPRONT J., CHAPRONT-TOUZE M., FRANSCOU G., and LASKAR J., *Numerical expressions for precession formulae and mean elements for the Moon and the planets*, Astronomy and astrophysics, 1993.

[21] SIMPSON G., *Order of Convergence of Adaptive Step Algorithms for Ordinary: Differential Equations*, Cornell University, 2003.

[22] STANDISH E., *The observational basis for JPL's DE 200, the planetary ephemerides of the Astronamical Almanac*, Jet Propulsion Laboratory, 1990, pp.252-271.

[23] Standish E., *An approximation to the errors in the planetary ephemerides of the Astronomical Almanac*, CalTech/Jet Propulsion Laboratory, 301-150, Pasadena, CA 91109, USA.

[24] VALLADO D., *Fundamentals of astrodynamics and applications*, 2nd Edition, El segundo, 2001.

[25] `https://fr.wikipedia.org/wiki/Assistance_gravitationnelle`. [Image; accessed 14-May-2018]. The data was from JPL Horizons Ephemeris System.

[26] `https://en.wikipedia.org/wiki/Orbital_elements#/media/File:Orbit1.svg`. [Image; accessed 5-May-2018]

[27] `https://saturn.jpl.nasa.gov/` [Image; accessed 14-May-2018]

[28] `https://solarsystem.nasa.gov/` [accessed 26-May-2018]

[29] `https://www.nasa.gov/` [accessed 31-May-2018]

[30] `https://www.math.ksu.edu/~dbski/writings/shell.pdf`.[accessed 3-June-2018]